Final_thesis (17).pdf

Delhi Technological University

Document Details

Submission ID

trn:oid:::27535:121852727

Submission Date

Nov 18, 2025, 2:30 PM GMT+5:30

Download Date

Nov 18, 2025, 3:08 PM GMT+5:30

File Name

Final_thesis (17).pdf

File Size

3.8 MB

172 Pages

38,012 Words

184,210 Characters

9% Overall Similarity

The combined total of all matches, including overlapping sources, for each database.

Filtered from the Report

- ▸ Bibliography
- ▸ Quoted Text
- ▸ Cited Text
- ▸ Small Matches (less than 10 words)

Exclusions

- ▸ 1 Excluded Source

Match Groups

233 Not Cited or Quoted 9%
Matches with neither in-text citation nor quotation marks

0 Missing Quotations 0%
Matches that are still very similar to source material

0 Missing Citation 0%
Matches that have quotation marks, but no in-text citation

0 Cited and Quoted 0%
Matches with in-text citation present, but no quotation marks

Top Sources

5%	🌐	Internet sources
6%	📖	Publications
4%	👤	Submitted works (Student Papers)

Integrity Flags

1 Integrity Flag for Review

🚩 **Replaced Characters**
1595 suspect characters on 92 pages
Letters are swapped with similar characters from another alphabet.

Our system's algorithms look deeply at a document for any inconsistencies that would set it apart from a normal submission. If we notice something strange, we flag it for you to review.

A Flag is not necessarily an indicator of a problem. However, we'd recommend you focus your attention there for further review.

Match Groups

🔖 **233** Not Cited or Quoted 9%
Matches with neither in-text citation nor quotation marks

💬 **0** Missing Quotations 0%
Matches that are still very similar to source material

📄 **0** Missing Citation 0%
Matches that have quotation marks, but no in-text citation

📑 **0** Cited and Quoted 0%
Matches with in-text citation present, but no quotation marks

Top Sources

5%	🌐 Internet sources
6%	📖 Publications
4%	👤 Submitted works (Student Papers)

Top Sources

The sources with the highest number of matches within the submission. Overlapping sources will not be displayed.

1 Publication

M. M. Rayguru, I. N. Kar. "Contraction Theory Approach to Disturbance Observer ... **2%**

2 Internet

export.arxiv.org **<1%**

3 Publication

M. M. Rayguru, I. N. Kar. "High Gain Observer-Based Saturated Controller for Fee... **<1%**

4 Submitted works

Delhi Technological University on 2024-05-23 **<1%**

5 Submitted works

National Institute of Technology, Rourkela on 2016-11-11 **<1%**

6 Publication

Jinzhu Peng, Shuai Ding, Rickey Dubay. "Adaptive composite neural network distu... **<1%**

7 Internet

dspace.dtu.ac.in:8080 **<1%**

8 Internet

cires1.colorado.edu **<1%**

9 Publication

M. M. Rayguru, I. N. Kar. "Convergence analysis of high gain disturbance observe... **<1%**

10 Publication

Vincent Cocquempot. "Fault tolerant control for a class of hybrid impulsive syste... **<1%**

11	Internet		
core.ac.uk			<1%

12	Publication		
Ferdose Ahammad Shaik, Shubhi Purwar, Bhanu Pratap. "Real-time implementati...			<1%

13	Publication		
Madan Mohan Rayguru, Spandan Roy, Lim Yi, Mohan Rajesh Elara, Simone Baldi. ...			<1%

14	Submitted works		
Delhi Technological University on 2025-05-06			<1%

15	Submitted works		
Trinity College Dublin on 2016-09-15			<1%

16	Submitted works		
National Institute of Technology, Hamirpur on 2018-10-24			<1%

17	Publication		
Chimmula Kishore, Indra Narayan Kar. "Tracking Control of a Single Link Manipul...			<1%

18	Internet		
pastel.archives-ouvertes.fr			<1%

19	Publication		
"Proceedings of 2021 5th Chinese Conference on Swarm Intelligence and Coopera...			<1%

20	Submitted works		
IIT Delhi on 2017-11-07			<1%

21	Submitted works		
Sant Longowal Institute of Engineering & Technlogy on 2025-08-06			<1%

22	Internet		
etd.lib.metu.edu.tr			<1%

23	Internet		
etda.libraries.psu.edu			<1%

24	Submitted works		
Delhi Technological University on 2017-05-28			<1%

25	Internet	
www.iet.ntnu.no		<1%

26	Internet	
arxiv.org		<1%

27	Publication	
Ming Zeng, Yunling Li, Hongwei Xia, Changhong Wang. "Tracking Control with Pr...		<1%

28	Submitted works	
National Institute of Technology, Hamirpur on 2020-06-10		<1%

29	Internet	
thesai.org		<1%

30	Publication	
Madan Mohan Rayguru, Bhabani Shankar Dey, Indra Narayan Kar. "Output feedb...		<1%

31	Internet	
upcommons.upc.edu		<1%

32	Internet	
www.mdpi.com		<1%

33	Publication	
Gibbons, Francis John George. "A Hydrodynamic Flood Routing Model for One Di...		<1%

34	Publication	
S. Purwar. "ADAPTIVE FUZZY LOGIC BASED CONTROL OF INDUCTION MOTORS", C...		<1%

35	Internet	
dr.iiserpune.ac.in:8080		<1%

36	Internet	
ualberta.scholaris.ca		<1%

37	Internet	
mdpi-res.com		<1%

38	Publication	
M. M. Rayguru, I. N. Kar. "Contraction-based stabilisation of nonlinear singularly ...		<1%

53	Publication	
An-Min Zou. "Adaptive Control of a Class of Nonlinear Pure-Feedback Systems Usi...		<1%

54	Submitted works	
Glasgow Caledonian University on 2013-12-06		<1%

55	Publication	
Liu, Tianchi. "Advances in Robust and Practical Speaker Verification", National Un...		<1%

56	Publication	
M.M. Rayguru, I.N. Kar. "Design of Contractive Output Feedback Controllers For Fi...		<1%

57	Publication	
Mengyi Li, Zhong Liu, Lanfeng Hua, Oh-Min Kwon, Kaibo Shi. "Sliding Mode Contr...		<1%

58	Submitted works	
TU Delft on 2025-06-17		<1%

59	Submitted works	
University of Stellenbosch, South Africa on 2023-01-19		<1%

60	Publication	
Wendell de Queiróz Lamas. "A Comprehensive Approach to Lagrange's Equations ...		<1%

61	Internet	
kclpure.kcl.ac.uk		<1%

62	Internet	
library2.smu.ca		<1%

63	Internet	
pdfs.semanticscholar.org		<1%

64	Internet	
repository.enp.edu.dz		<1%

65	Publication	
Houssemeddine Gouta, Salim Hadj Said, Nabil Barhoumi, Faouzi M'Sahli. "Observ...		<1%

66	Publication	
M. M. Rayguru, I. N. Kar. "A singular perturbation approach to saturated controll...		<1%

67	Submitted works

National Institute of Technology, Hamirpur on 2017-10-26   <1%

68	Publication

Radial Basis Function (RBF) Neural Network Control for Mechanical Systems, 2013.   <1%

69	Submitted works

SASTRA University on 2017-02-27   <1%

70	Publication

Shigen Gao, Hairong Dong, Bin Ning. "Neural adaptive dynamic surface control fo...   <1%

71	Publication

Svetlana N. Yanushkevich, Vlad P. Shmerko. "Introduction to Logic Design", CRC P...   <1%

72	Publication

Xianyan Li, Dongdong Zheng, Kai Guo, Xuemei Ren. "Identification and Control of
...   <1%

73	Publication

Xinjun Wang, Ben Niu, Yahui Gao, Zihao Shang. "Adaptive Finite Time Output Fee...   <1%

74	Internet

coek.info   <1%

75	Internet

db.nzsee.org.nz   <1%

76	Internet

escholarship.org   <1%

77	Internet

nozdr.ru   <1%

78	Internet

paperhost.org   <1%

79	Internet

pdffox.com   <1%

80	Internet

spectrum.library.concordia.ca   <1%

81 Internet

theses.hal.science <1%

82 Internet

www.researchgate.net <1%

83 Publication

"Book of abstracts", 2012 IEEE 51st IEEE Conference on Decision and Control (CDC... <1%

84 Internet

9dok.org <1%

85 Publication

A. Raza, F. M. Malik, N. Mazhar, R. Khan. "Output Feedback Control of a Class of T... <1%

86 Publication

Aditya Kumar, Prodromos Daoutidis. "Control of nonlinear differential algebraic e... <1%

87 Publication

Chun Kiat Tan, Jianliang Wang, Yew Chai Paw, Teng Yong Ng. "Tracking of a movi... <1%

88 Publication

Harold Klee. "Simulation of Dynamic Systems with MATLAB and Simulink", CRC Pr... <1%

89 Submitted works

IIT Delhi on 2023-10-20 <1%

90 Submitted works

Indian Institute of Technology Roorkee on 2013-01-16 <1%

91 Submitted works

Indian Institute of Technology, Kharagpure on 2015-07-23 <1%

92 Publication

Jianquan Lu. "Exponential stabilization of switched stochastic dynamical network... <1%

93 Publication

Liu, Y.J.. "Adaptive fuzzy control for a class of uncertain nonaffine nonlinear   sys... <1%

94 Publication

M. Corless, F. Garofalo, L. Glielmo. "New results on composite control of singularl... <1%

95 Publication

Mohamed Kharrat, Moez Krichen, Hadil Alhazmi, Paolo Mercorelli. "Neural netwo... <1%

96 Submitted works

Phuket Rajabhat University on 2022-01-14 <1%

97 Publication

Tairen Sun, Xuexin Zhang, Hongjun Yang, Yongping Pan. "Singular perturbation-b... <1%

98 Submitted works

University of Macau on 2022-10-20 <1%

99 Submitted works

University of Sheffield on 2025-09-09 <1%

100 Submitted works

University of Sydney on 2024-05-24 <1%

101 Publication

Yan He, Defu Zhu, Chao Chen, Yang Wang. "Data-driven control of singularly pert... <1%

102 Publication

Yanli Liu, HongJun Ma, Hui Ma. "Adaptive Fuzzy Fault-Tolerant Control for Uncert... <1%

103 Publication

Yinsheng Song, Ziwei Li, Feng Li, Rongsheng Xia, Hao Shen. "H $$ {\mathcal{H}}_{... <1%

104 Publication

Yongling Xia, Yanbin Liu, Weichao Sun. "Disturbance observer-based full-state co... <1%

105 Publication

Zachary I. Bell, Runhan Sun, Kyle Volle, Prashant Ganesh, Scott A. Nivison, Warren... <1%

106 Internet

discovery.researcher.life <1%

107 Internet

downloads.hindawi.com <1%

108 Internet

scholar.afit.edu <1%

109   Internet

unsworks.unsw.edu.au   <1%

110   Internet

vdoc.pub   <1%

111   Internet

vtechworks.lib.vt.edu   <1%

112   Internet

www.searchanddiscovery.com   <1%

INVESTIGATIONS ON DYNAMICAL SYSTEMS WITH TIME SCALE SEPARATION

A Thesis Submitted In Partial Fulfillment of the Requirements

for the Degree of

DOCTOR OF PHILOSOPHY

by

DIPAK PRASAD

(Roll No. 2K21/PHDEE/16)

Under the Supervision of

Prof. SUDARSHAN K. VALLURU (Supervisor)

Department of Electrical Engineering

Delhi Technological University, Delhi - 110042, India

Dr. M. M. RAYGURU (Co-Supervisor)

University of Louisville, Kentucky, USA

Department of Electrical Engineering

DELHI TECHNOLOGICAL UNIVERSITY

(Formerly Delhi College of Engineering)

Shahbad Daulatpur, Main Bawana Road, Delhi - 110042. INDIA

November, 2025

DELHI TECHNOLOGICAL UNIVERSITY
(Formerly Delhi College of Engineering)
Shahbad Daulatpur, Main Bawana Road, Delhi-42

CANDIDATE'S DECLARATION

I hereby certify that the work which is being presented in the thesis entitled **INVESTIGATIONS ON DYNAMICAL SYSTEMS WITH TIME SCALE SEPARATION** in partial fulfillment of the requirements for the award of the Degree of Doctor of Philosophy and submitted in the Department of Electrical Engineering of the Delhi Technological University is an authentic record of my own work carried out during the period from July, 2021 to July, 2025 under the supervision of Prof. Sudarshan K. Valluru, Department of Electrical Engineering and Dr. Madan Mohan Rayguru, Assistant Professor, University of Louisville, Kentucky, USA.

The matter presented in this thesis has not been submitted by me for the award of any other degree of this or any other Institute.

(Dipak Prasad)

This is to certify that the student has incorporated at the corrections suggested by the examiners in the thesis and the statement made by the candidate is correct to the best of our knowledge.

Signature of Supervisors

Signature of External Examiner

DELHI TECHNOLOGICAL UNIVERSITY
(Formerly Delhi College of Engineering)
Shahbad Daulatpur, Main Bawana Road, Delhi-42

CERTIFICATE

Certify that **Dipak Prasad** (2K21/PHDEE/16) has carried out their work presented in this thesis entitled "**INVESTIGATIONS ON DYNAMICAL SYSTEMS WITH TIME SCALE SEPARATION**" for the award of **Doctor of Philosophy** from Department of Electrical Engineering, Delhi Technological University, Delhi, under our supervision. The thesis embodies results of original work, and studies are carried out by the student himself and the content of the thesis do not form the basis for the award of any other degree to the candidate or to anybody else from this or any other University/Institute.

(Prof. Sudarshan K. Valluru)   (Dr. Madan Mohan Rayguru)

Supervisor   Co-Supervisor

Date:

v

Abstract

The control of nonlinear dynamical systems exhibiting multi-time scale behaviors and discontinuities remains a significant challenge in the field of control theory. This thesis addresses two such classes of complex systems, singularly perturbed systems (SPS) and singularly perturbed switched systems (SPSS) and proposes advanced nonlinear control strategies to enhance their stability and robustness in the presence of uncertainties and external disturbances.

A novel saturated controller is developed for singularly perturbed systems that exhibit a time-scale separation between the slow and fast dynamics. These systems often suffer performance degradation due to inherent uncertainties and external disturbances. To mitigate these effects, a nonlinear saturated controller is proposed by leveraging the singular perturbation technique. The control scheme incorporates a filter to manage fast dynamics and a high-gain disturbance observer (HGDO) to estimate and reject unknown disturbances effectively. A contraction-theoretic framework is employed to establish the convergence of all closed-loop system states, thereby ensuring robust performance even under singular perturbations and model uncertainties. The proposed method is validated through the pitch angle control of a Twin Rotor MIMO System (TRMS), which serves as a practical benchmark for demonstrating the effectiveness of the controller in replicating real-time operational conditions.

Hereafter, the focus shifts to switched nonlinear systems, where discontinuities arise due to switching among subsystems, as commonly encountered in chemical processes, robotic systems, and multi-agent networks. A time-scale redesign-based robust filter backstepping controller is introduced for a class of uncertain switched nonlinear systems expressed in strict feedback form. Here, the singular perturbation technique plays a dual role: first, in the design of high-gain filters to address the "explosion of complexity" typically associated with backstepping methods; second, in the construction of high-gain disturbance observers to counteract unknown disturbances and unmodeled

vi

dynamics.   The interplay between system discontinuities, high-gain design elements, and disturbance rejection results in a three-time scale switched nonlinear closed-loop system. The stability of this system is rigorously analyzed using a Lyapunov-based average dwell time approach.   To demonstrate real-world applicability, the proposed control strategy is implemented on a single-link robotic manipulator, and the results confirm its efficacy in achieving robust performance and tracking accuracy under switching and uncertain conditions.

A filtered backstepping controller integrated with HGDO is specifically designed for SPSSs with frequent mode transitions.   Contraction theory is employed to guarantee stability and convergence within a bounded domain. The approach is applied to a robotic manipulator, showing strong robustness against switching and external disturbances.

A neural network-based disturbance observer (NNDO) within the filtered backstepping framework. Exploiting the approximation capabilities of neural networks, the NNDO enables real-time estimation and compensation of unknown disturbances.   Combined with a high-gain filter, this structure improves robustness while reducing computational burden. Stability is ensured using average dwell-time analysis, and simulations on a robotic manipulator confirm the approach's practical viability.

A neural backstepping controller is developed for singularly perturbed switched systems to effectively handle system nonlinearities and unknown disturbances.   The design incorporates a high-gain filter to manage the complexity typically associated with recursive backstepping, while a high-gain disturbance observer (HGDO) is employed for real-time disturbance rejection. The proposed control scheme is tested on a single-link robotic manipulator that includes actuator dynamics, demonstrating its strong robustness and practical applicability in dynamic and uncertain environments.

Overall, this thesis presents a unified framework for robust control of singularly perturbed and switched nonlinear systems by incorporating backstepping, high-gain observers, and rigorous stability tools.

vii

Acknowledgements

I sincerely thank the Almighty for blessing me with the strength, patience, and determination to complete my Ph.D. journey.

I am deeply grateful to my supervisor, Prof. Sudarshan K. Valluru, for his continuous support, expert guidance, and valuable encouragement throughout the course of my research. Prof. Valluru welcomed me to university with open arms despite the COVID pandemic. I have learned a great deal under his supervision, and I feel truly fortunate to have worked with him.

I would also like to express my sincere thanks to my co-supervisor, Dr. Madan Mohan Rayguru, for his guidance and suggestions. I would like to thank all my co-researchers who are part of the Control of Dynamical and Computation Laboratory. I extend my thanks to all the faculty members and staff of the Department of Electrical Engineering, Delhi Technological University, for creating a supportive research environment and for their help during the course of my Ph.D. I also appreciate the administrative support provided throughout this period. I would like to express my heartfelt gratitude to my parents, Elder brother, and family for their endless love, blessings, and sacrifices. Their belief in me has been a source of strength in both good and challenging times. I am especially thankful to my wife, whose patience, understanding, and constant support have meant the world to me during this journey. Her encouragement helped me stay focused and balanced. A very special mention goes to my son, whose arrival has brought immense joy and inspiration into my life. His presence has filled my heart with renewed energy and hope during the final phase of this thesis. Finally, I would like to thank all my friends, fellow research scholars, and labmates for their friendship, discussions, support, and for making this journey memorable. I am grateful to everyone who contributed in any way to the successful completion of my research.

Date: Dipak Prasad

Contents

x

90

List of Figures

xiv

XV

List of Tables

List of Abbreviations

SPS	Singularly Perturbed System
SPSS	Singularly Perturbed Switched System
ADT	Average Dwell Time
FJR	Flexible Joint Robot
$H\infty$	H-infinity (robust) control
DC	Direct Current (as in DC motor or converter)
LMI	Linear Matrix Inequality
PDT	Persistent Dwell-Time
SPP	Singular Perturbation Parameter
TS	Takagi-Sugeno (fuzzy model)
MDADT	Mode-Dependent Average Dwell Time
PI	Proportional-Integral
RBF	Radial Basis Function
NN	Neural Network
CLF	Common Lyapunov Function
NDO	Neural Disturbance Observer
UELS	Underactuated Euler–Lagrange Systems
MIMO	Multiple Input Multiple Output
TRMS	Twin Rotor MIMO System
HGDO	High-Gain Disturbance Observer
NNDO	Neural Network Disturbance Observer
SISO	Single Input Single Output

xxi

List of Symbols

$\|\cdot\|$	Euclidean distance between two trajectories at time t.
$\sigma(t)$	Switching signal that selects the active subsystem at time t.
$N_\sigma(t, t_0)$	Number of switchings in the interval $[t_0, t)$.
τ_a	Average dwell time; minimum average time the system remains in one mode.
N_0	Chatter bound; allows a finite number of fast switchings.
u	Control input to the system.
α_i	Virtual control law for the i-th subsystem.
α_{if}	First order Filtered paramerer.
μ	Perturbed parameter, $\mu \in (0, 1)$.
ω_d	Desired reference signal for the first state.
ν	Control input used in dynamic saturation law.
j_g	Jacobian of the fast dynamics $g(.)$ with respect to ν.
D_ν	Domain of the auxiliary variable ν.
ω_r	Reduced slow system state vector, $\omega_r \in \Re^n$.
D_ω	Domain of system state vector ω.
D_ν	Domain of auxiliary control variable ν.
P	Finite index set of subsystems.
$d_{i\sigma}(.)$	Unknown disturbance/uncertainty in the i-th subsystem under mode σ.
$\Theta_{\sigma i}(.)$	Unknown function governing the dynamics of the disturbance $d_{i\sigma}$.
ξ_i, η_i	Intermediate observer state for disturbance estimation.
$\hat{d}_{i\sigma}$	Estimated disturbance in the ith subsystem.
$d_{i\sigma}$	Actual disturbance in the ith subsystem.

xxii

$\tilde{d}_i$	Disturbance estimation error ($d_{i\sigma} - \hat{d}_{i\sigma}$).
u_σ	Control input under switching signal σ.
$\Delta_{i\sigma}(\cdot)$	Uncertain/disturbance term for i-th subsystem
$\hat{\Delta}_{i\sigma}$	Estimate of the uncertain/disturbance term
$\tilde{\Delta}_i$	Estimation error for i-th disturbance
ϕ_i	Basis function of the neural network
$\chi_{i\sigma}(z_i)$	User defined tuning function.

Chapter 1

Introduction and Motivation

1.1   Background

Modern engineering systems, such as robotics [1], power systems [2], aerospace vehicles [3], and industrial automation processes, often involve components that operate over multiple time scales [4]. These systems typically consist of fast and slow subsystems interacting dynamically. The modeling and analysis of such systems require mathematical frameworks that can distinctly capture this dual-time-scale behavior. Singular perturbation theory provides an effective analytical tool for such systems, where the presence of a small positive parameter multiplies the derivatives of certain state variables, thereby separating the dynamics into fast and slow subsystems [5]. These systems are formally known as Singularly Perturbed Systems (SPSs). A general class of SPSs can be expressed as a set of differential equations where the small parameter $\epsilon \ll 1$ determines the time-scale separation. The reduction of system complexity, simplification of control design, and improved numerical simulation are among the main advantages of singular perturbation techniques. In recent years, increasing attention has been devoted to switched systems, which consist of multiple subsystems and a switching signal that governs transitions among them. Such systems are common in networked control systems [6], fault-tolerant systems [7], and systems with mode-dependent behavior [8]. When the features of both singular perturbation and switching are present in a system, it leads to a more complex but realistic model known as a Singularly Perturbed Switched System (SPSS). SPSSs pose unique challenges in terms of modeling, stability analysis, and controller design due to the coexistence of multiple time scales and

Chapter 1. Introduction and Motivation

the discrete switching behavior. The interaction between fast–slow dynamics and switching logic significantly complicates the overall system behavior. Traditional control techniques, when applied directly, often fail to guarantee stability or desired performance in such systems. Thus, there is a strong need for advanced control frameworks capable of handling both the singular perturbation structure and the switching nature of the dynamics.

The motivation for studying Singularly Perturbed Systems and their switched counterparts arises from both theoretical and practical considerations. Theoretically, SPSs serve as an ideal platform for exploring reduced-order modeling, time-scale decomposition, and hierarchical control. The framework allows one to independently analyze and design controllers for fast and slow subsystems and then synthesize the results to achieve overall system stability. Extending these ideas to switched systems where the dynamics and time-scale structure may change with each switching signal opens new avenues in switched system theory and control design. In practical scenarios, numerous applications naturally exhibit singular perturbation characteristics along with switching behavior. Examples include, Control of robotic manipulators [9, 10], DC-DC converters in control systems [11], Process control systems [12], and Networked control systems [13]. Despite the rich applicability of SPSSs, designing controllers that guarantee stability and robustness remains a challenging task. Switching may introduce instability even if individual subsystems are stable, and fast-slow interactions can lead to unpredicted transient behaviors. Moreover, uncertainties, nonlinearities, and external disturbances further complicate control synthesis. This motivates the development of novel control techniques that:

- Exploit the time-scale separation of singularly perturbed systems.

- Handle the mode of transitions gracefully without compromising stability.

- Compensate for modeling uncertainties and external disturbances.

1.2 Contraction Theory for Nonlinear System Stability

Contraction theory provides a differential framework to analyze the stability of nonlinear systems. It examines whether all trajectories of the system converge towards each other, independent of their initial conditions. If this property holds, the system is said to be contracting, which guarantees global exponential stability [14]. The key idea is that if the distance between any two trajectories decreases over time, then the system "forgets" its initial condition and all solutions converge to a unique behavior. This makes contraction theory a useful tool for analyzing complex nonlinear systems, as it provides guarantees of stability that are independent of initial states. Contraction theory has been widely applied in nonlinear control [15], observer design [16], robotics [17], and biological systems [18], as it ensures robustness, synchronization, and global stability in a straightforward and systematic way.

Consider a generalised nonlinear system:

$$\dot{x} = f(x,t), \quad x \in \mathbb{R}^n \tag{1.1}$$

Let $J(x,t) = \frac{\partial f}{\partial x}$ be the Jacobian matrix of the system. The system is said to be contracting if the symmetric part of the Jacobian satisfies. Where x is the state of the system, t is time, λ is the contraction rate, and I is the identity matrix.

$$\frac{1}{2}\left(J(x,t) + J^\top(x,t)\right) \leq -\lambda I, \quad \lambda > 0 \tag{1.2}$$

This condition ensures that the Euclidean distance between any two trajectories decreases exponentially:

$$\|x_1(t) - x_2(t)\| \leq \|x_1(0) - x_2(0)\|e^{-\lambda t} \tag{1.3}$$

Hence, contraction theory guarantees that all system trajectories converge to each other, thereby ensuring global exponential stability.

1.3   Average Dwell Time

In switched systems, stability depends critically on the switching signal. To avoid destabilization caused by rapid switching, the concept of dwell time is used, which requires the system to remain in one mode for a minimum interval before switching [19, 20]. Since strict dwell time can be overly conservative, the notion of average dwell time (ADT) was introduced. Formally, let $N_\sigma(t, t_0)$ denote the number of switchings on the interval $[t_0, t)$. The switching signal $\sigma(t)$ is said to have an average dwell time $\tau_a > 0$ with chatter bound $N_0 \geq 0$ if

$$N_\sigma(t, t_0) \leq N_0 + \frac{t - t_0}{\tau_a}, \quad \forall t \geq t_0. \tag{1.4}$$

Here, N_0 allows a finite number of fast switchings, while τ_a governs the long-term switching frequency. If τ_a is chosen sufficiently large, system stability can be ensured, even when some subsystems are unstable, typically through multiple Lyapunov functions [21]. The ADT framework is less conservative than fixed dwell time and has become a fundamental tool in the analysis of nonlinear, uncertain, and singularly perturbed switched systems.

1.4   Literature Review

Singular perturbation theory is a powerful tool for analyzing systems with multiple time scales, where a small parameter significantly influences the system's dynamics. This approach is particularly useful for systems where the perturbation parameter is either constant or state-dependent, allowing for a broad range of applications in control and optimization problems. The theory's versatility is demonstrated through various methods and applications, including stability analysis, numerical simulations, and control design.

Liu and Jiang introduced a framework where the perturbation parameter is a state-dependent function, enhancing the robustness and stability analysis of nonlinear singularly perturbed systems. This approach is particularly beneficial for integral control and feedback optimization problems, providing solutions beyond traditional methods [22]. Cheng et al. applied sliding mode control to semi-Markov jumping systems with singular perturbations, incorporating neural

networks for weight estimation. This method ensures mean-square exponential stability and reduces triggering rates, demonstrating the practical applicability of singular perturbation theory in dynamic systems [13]. Liu et al. developed a continuous-discrete time observer for slow state estimation in singularly perturbed systems with discrete measurements. This approach addresses the challenges of high dimensionality and stiffness, providing a method to estimate observation errors and improve control algorithms based on slow dynamics [23]. Cardin and Teixeira explored the impact of singular perturbations on symmetric vector fields, using geometric singular perturbation theory to analyze the persistence of symmetry properties. This approach is crucial for understanding the behavior of fast-slow dynamical systems under perturbations [24]. Gunti and Movva applied singular perturbation methods to power factor correction converters, demonstrating the method's utility in managing fast and slow states in power systems. This application highlights the method's effectiveness in handling switching ripple effects and improving system performance [25].

In the Robotics field, singular perturbation is used to model flexible joint robots (FJRs) into fast and slow subsystems, which helps in handling underactuation and reducing noise amplification. This modeling facilitates the design of adaptive integral sliding mode controllers that achieve high tracking performance and robustness against disturbances [9]. Voltage control strategies for FJRs also benefit from singular perturbation by simplifying the control law and ensuring stability across different subsystems. This approach allows for practical implementation with reduced complexity compared to traditional methods [26]. In underactuated Euler-Lagrange systems, singular perturbation aids in designing saturated adaptive controllers that ensure semiglobal asymptotic stability without violating control input constraints. This method does not require high-order derivatives, making it efficient for practical applications [27]. For cable-driven systems, singular perturbation helps in decomposing the system into subsystems, allowing for effective damping compensation and tension stability. This method enhances the system's bandwidth and suppresses high-frequency resonances, outperforming conventional adaptive control methods [28]. In series elastic actuators, singular perturbation combined with time-delay estimation techniques allows for robust impedance control. This combination broadens the operational bandwidth and

6   *Chapter 1. Introduction and Motivation*

reduces driving-point impedance, improving safety and compliance during human-robot interactions [29].

Although singular perturbation theory has greatly advanced the study and control of multi-time-scale systems, challenges persist in dealing with state-dependent parameters and maintaining stability in complex dynamics. In robotic applications, these methods are extensively applied to handle systems with distinct time scales, such as flexible-joint manipulators and underactuated vehicles. By decomposing the overall dynamics into reduced-order subsystems, singular perturbation techniques streamline controller design, enhance stability, suppress noise, and improve robustness against disturbances. Nevertheless, their success relies heavily on precise subsystem modeling and the careful formulation of controllers that address the unique demands of each application, ensuring that performance benefits are not diminished by modeling errors or unmodeled constraints.

Controller design for singularly perturbed systems involves addressing the challenges posed by the multi-time-scale dynamics inherent in these systems. Singularly perturbed systems are characterized by a small parameter that causes the system to exhibit both fast and slow dynamics, necessitating specialized control strategies to ensure stability and performance. Various approaches have been proposed to tackle these challenges, each with unique methodologies and applications. A multi-rate sampling controller can be designed to stabilize singularly perturbed hybrid systems. This involves establishing a hybrid model and using the Lyapunov approach to ensure uniform global exponential stability. The relationship between the singular perturbation parameter and the fast sampling interval is crucial, as demonstrated in a DC motor model example [30]. For continuous-time Markov jump singularly perturbed systems, a decomposition into fast and slow subsystems is employed. Reinforcement learning algorithms, both offline and online, are used to design suboptimal controllers, with the suboptimality of these controllers being a key focus. An electric circuit model illustrates the method's applicability [31]. A fuzzy integral controller with an event-triggered strategy is proposed for nonlinear singularly perturbed systems. This approach uses the Takagi Sugeno fuzzy model and integral feedback to manage the effects of the singular perturbation parameter, achieving performance comparable to conventional controllers with reduced

communication events [32]. The design of $H\infty$ output feedback controllers for fuzzy nonlinear singularly perturbed systems involves linear matrix inequalities to ensure asymptotic stability. This method reduces conservatism and expands the application scope of the singular perturbation parameter [33]. Synchronization control for networked two-timescale dynamic agents is addressed by designing distributed controllers that guarantee synchronization within a specified stability bound. Techniques such as particle swarm optimization are used to enlarge this stability bound [34].

While these approaches provide robust solutions for controller design in singularly perturbed systems, challenges remain, such as dealing with input constraints and ensuring finite-time stability. These issues are addressed through finite-time fuzzy control, which ensures state boundedness within a fixed time interval [35]. The diversity of methods highlights the complexity and adaptability required in controller design for singularly perturbed systems.

The design of controllers for singularly perturbed switched systems is a complex task that involves addressing the challenges posed by the multi-time-scale dynamics inherent in these systems. Singular perturbations introduce fast and slow dynamics, requiring specialized control strategies to ensure system stability and performance. Various approaches have been proposed to tackle these challenges, each focusing on different aspects of controller design, such as stability, robustness, and fault tolerance.

Composite control strategies involve designing controllers for individual slow and fast subsystems, which are then synthesized to stabilize the overall system under specific switching rules. This approach is effective when the perturbation parameter is small, allowing for the stabilization of switched singularly perturbed systems through state transformation techniques [36]. Asynchronous control designs address the practical scenario where system and controller modes may not be synchronized. Non-fragile control mechanisms enhance reliability by accounting for uncertainties in controller implementation, ensuring mean-square stability and dissipative performance through linear matrix inequalities (LMIs) [37]. Fault-tolerant control strategies are crucial for maintaining system stability in the presence of actuator faults. Techniques such as the Takagi-Sugeno fuzzy model and Lyapunov function approaches are employed to design controllers that ensure exponential stability and robust

Chapter 1. Introduction and Motivation

performance under time-varying delays [38].   The paper [39] presents a quantized fuzzy controller design for singularly perturbed switched nonlinear systems, utilizing persistent dwell-time switching, singular perturbation techniques, and interval type-2 Takagi-Sugeno (TS) fuzzy models to ensure stability and $H\infty$ performance through SPP-dependent Lyapunov-like functions. The paper [40] proposes a slow-state feedback control method to design controllers for singularly perturbed switched systems (SPSSs) with persistent dwell-time (PDT) switching, ensuring global uniform exponential stability and deriving mode-dependent controller gains for improved performance.

While these methodologies provide robust solutions for controller design in singularly perturbed switched systems, challenges remain in terms of scalability and real-time implementation. Future research could focus on integrating these approaches with advanced computational techniques to enhance their applicability in complex, real-world systems.

The concept of average dwell time (ADT) in singularly perturbed switched systems is a critical aspect in ensuring system stability and performance. ADT refers to the minimum average time that the system remains in a particular mode before switching to another, which is crucial for maintaining stability in systems with fast and slow dynamics. This mechanism is particularly relevant in systems where switching between both modes can lead to instability if not properly managed. The papers [41, 42] explore various control strategies and stability criteria for singularly perturbed switched systems under ADT and related mechanisms. Mode-dependent average dwell time (MDADT) is a refined approach that considers the specific characteristics of each mode in a switched system, allowing for more precise control and stability analysis. It is particularly useful in systems where different modes have varying stability properties and perturbation parameters. This approach has been applied to ensure exponential stability and weighted $H\infty$ performance in singularly perturbed switched systems by constructing Lyapunov functions that depend on the singular perturbation parameter.   The use of MDADT in stability analysis involves constructing Lyapunov functions that account for the singular perturbation parameters, ensuring that the system remains stable despite the presence of fast and slow dynamics [41, 43]. In the context of fuzzy control systems, MDADT helps in designing controllers that can handle nonlinearities and mode

mismatches during switching, thereby maintaining system stability [42, 44]. The inverted pendulum system has been used to demonstrate the effectiveness of MDADT in ensuring stability and performance in singularly perturbed switched systems [42, 45]. Numerical simulations and practical models, like tunnel diode circuits, further validate the applicability of MDADT in real-world scenarios, highlighting its potential in complex dynamic networks [40, 46]. While MDADT provides a robust framework for stability and control in singularly perturbed switched systems, it is important to consider the limitations and challenges associated with its implementation. The complexity of designing mode-dependent controllers and the need for precise parameter estimation can pose significant challenges. Additionally, the approach may require extensive computational resources, especially in systems with a large number of modes or highly nonlinear dynamics. Nonetheless, MDADT remains a valuable tool in the analysis and control of such systems, offering a balance between stability and performance.

Contraction theory has emerged as a powerful tool for analyzing and stabilizing singularly perturbed systems (SPS) and switched systems. This approach focuses on ensuring that the trajectories of these systems converge towards a desired state, thereby enhancing stability and performance. Contraction theory has been applied to singularly perturbed systems to design feedback controllers that achieve bounded tracking errors without the need for interconnection conditions, unlike traditional Lyapunov-based methods. This approach is robust to additive bounded uncertainties and does not rely on the smallness of the singular perturbation parameter [47]. The concept of k-contraction extends the classical notion of contraction to higher dimensions, allowing for a richer characterization of system behavior. For singularly perturbed systems, k-contraction properties can be derived from the boundary-layer (fast) system and the reduced order (slow) model, especially when there is a large time-scale separation [48]. Contraction theory also provides explicit bounds on the convergence rate of trajectories to the slow manifold and the asymptotic error between the trajectories of the singularly perturbed system and those of the reduced system [49]. For switched systems, contraction theory has been used to suppress harmonics in mechanical systems by ensuring that the output frequency matches the input perturbation, thus reducing unintended

Chapter 1. Introduction and Motivation

vibrations [50].   In the context of singularly perturbed switched systems, contraction theory aids in designing controllers that stabilize the system despite the numerical stiffness introduced by small parameters. This is achieved through ϵ-dependent and ϵ-independent controllers that do not suffer from ill-conditioning linked to the small parameter (ϵ) [51]. The use of persistent dwell-time switching laws in singularly perturbed switched systems ensures global uniform exponential stability and improved dissipative performance, verified through numerical examples [40]. While contraction theory offers significant advantages in stabilizing singularly perturbed and switched systems, it is important to consider the limitations and challenges associated with its application. For instance, the design of contraction-based controllers may require precise knowledge of system parameters and conditions, which can be difficult to obtain in practice. Additionally, the extension of contraction theory to more complex systems, such as those with non-linear dynamics or time-varying parameters, remains an area of active research.

The development of neural backstepping controllers for switched systems is a significant advancement in control theory, particularly for managing nonlinear and uncertain systems.   These controllers leverage neural networks to approximate unknown system dynamics and employ backstepping techniques to ensure stability and performance under arbitrary switching conditions. The integration of neural networks with backstepping provides a robust framework for handling the complexities and uncertainties inherent in switched systems. This approach is particularly beneficial in applications where system parameters are not easily measurable or subject to rapid changes. A multilayer neural network pre-observer is utilized to reconstruct system states that cannot be directly measured, effectively neutralizing abrupt state changes due to switching parameters, and the observer error compensation mechanism further refines state estimation, reducing approximation errors and enhancing tracking performance [52].   The backstepping technique is embedded within a discontinuous controller design, incorporating proportional-integral (PI) compensation to address tracking control challenges in uncertain switched systems and Filippov's theory and nonsmooth Lyapunov functions are employed to construct a robust controller capable of handling approximation errors from neural networks [53]. Radial basis function (RBF) neural networks

approximate unknown functions in discrete-time switched systems, simplifying the controller design process and ensuring stability [54].   Adaptive neural controllers are developed using actor-critic architectures, optimizing control strategies within the backstepping framework to meet predefined performance criteria [55]. Predefined-time adaptive neural tracking control ensures that all signals in the switched system remain bounded, with tracking errors converging to zero within a specified time frame and The use of common Lyapunov functions and finite-time differentiators enhances the robustness and efficiency of the control strategy [56].   Event-triggered adaptive neural network backstepping control reduces the frequency of control signal updates, maintaining system stability without Zeno behavior [57].   Observer-based adaptive neural network backstepping sliding mode control addresses stability in fractional order systems with unmeasured states, ensuring robust performance under switching conditions [58].

systems with unmeasured states, ensuring robust performance under switching conditions(Chen et al., 2021). While neural backstepping controllers offer significant advantages in managing switched systems, challenges remain in terms of computational complexity and real-time implementation.   The integration of neural networks requires careful tuning and training to ensure accurate approximation of system dynamics.   Additionally, the design of backstepping controllers must consider the trade-off between robustness and computational efficiency, particularly in systems with high switching frequencies or complex dynamics. Despite these challenges, the continued development of neural backstepping techniques holds promise for advancing control strategies in a wide range of applications.

Neural disturbance observers (NDOs) are advanced control mechanisms that integrate neural networks to estimate and compensate for disturbances in dynamic systems.   These observers are particularly useful in systems with unknown or time-varying disturbances, providing robust control solutions across various applications.   The integration of neural networks allows for real-time adaptation and learning, enhancing the system's ability to maintain stability and performance under uncertain conditions. A neural-network-based disturbance observer is used in MEMS gyroscopes to estimate unknown gyro parameters and integrate with sliding mode control to reduce chattering and

Chapter 1. Introduction and Motivation

ensure system stability. This approach leverages Lyapunov stability theory to validate the control system's stability, demonstrating effectiveness through simulation results [59]. In quadrotor UAVs, a neural controller with a disturbance observer compensates for aerodynamic disturbances. The system uses feedforward neural networks to handle internal disturbances, while external disturbances are estimated by the observer. Composite learning enhances performance by updating the controller and observer in real-time, proving robust trajectory tracking in challenging conditions [60]. An adaptive neural network control scheme with a disturbance observer is applied to robotic manipulators for trajectory tracking under external disturbances and model uncertainties. The observer estimates approximation errors and disturbances, providing compensation to reduce tracking errors. The system's stability is confirmed using Lyapunov theory [61]. A neural network disturbance observer is integrated into a fault detection scheme for electro-mechanical flight actuators. This observer efficiently estimates nonlinear factors and disturbances, aiding in fault detection by analyzing estimation errors. The approach ensures stability and convergence of observer errors [62]. In uncertain nonlinear systems, a disturbance observer-based adaptive neural network control compensates for approximation errors and disturbances. This method eliminates the need for an exact system model, enhancing control effectiveness through online compensation and simulation validation [63]. For multi-degree-of-freedom robots, a robust control method using a neural network disturbance observer addresses time-varying parameters and external disturbances. The observer tracks total disturbances, significantly reducing angular displacement and velocity errors compared to traditional methods [64]. An extreme learning machine neural network disturbance observer is used in hypersonic vehicles to manage disturbances and ensure precise tracking control. The system converts nonlinear dynamics into a linear model, simplifying control law design and enhancing performance through direct feedback compensation [65].

While neural disturbance observers offer significant advantages in handling disturbances and uncertainties, they also present challenges such as computational complexity and the need for accurate neural network training. These systems require careful design to ensure stability and performance, particularly in real-time applications. Despite these challenges, the integration of

neural networks with disturbance observers continues to advance, providing robust solutions across diverse fields.

The design of saturated controllers for singularly perturbed systems (SPS) is a complex task due to the inherent fast and slow dynamics of these systems. These dynamics allow for the decomposition of the system into distinct timescales, which can complicate control strategies, especially when actuator saturation and nonlinear perturbations are present. Various approaches have been proposed to address these challenges, each leveraging different techniques to ensure stability and performance under saturation constraints. A saturated smooth adaptive controller is proposed for underactuated Euler-Lagrange systems (UELS) with modeling uncertainties and control saturations. This controller ensures semiglobal asymptotic stability without violating control input constraints. The use of Hoppensteadt's Theorem demonstrates the controller's ability to maintain stability and track desired positions effectively, validated through simulations on a two-link robot arm [27]. For discrete-time semi-Markov jump singularly perturbed systems, a stabilization strategy is developed considering actuator saturation and partially known semi-Markov kernel information. The convex hull approach and Lyapunov stability theory are employed to derive conditions for mean-square stability, with numerical examples validating the control strategy [66]. In coal-fired power generation systems, a fuzzy controller design is proposed using singular perturbation theory to address nonlinearity and input saturation. An event-triggered observer-based controller structure is used to ensure asymptotic stability, avoiding ill-conditioned numerical problems and the Zeno phenomenon [67]. An adaptive fuzzy control approach is developed for singular systems with nonlinear perturbation and actuator saturation. This method uses a backstepping technique and an auxiliary system to manage saturation effects. The approach ensures that the closed-loop system remains impulse-free and regular, with bounded signals and adjustable tracking errors [68]. A time-scale redesign-based saturated tracking controller is introduced for MIMO nonlinear systems, focusing on reducing the vulnerability to actuator saturation and noise. This method allows for tuning controller performance without arbitrary reduction of singular perturbation parameters, demonstrated through experiments with a wheeled mobile robot [69].

While these approaches offer robust solutions for handling saturation in

Chapter 1. Introduction and Motivation

singularly perturbed systems, they also highlight the complexity and diversity of methods required to address different system characteristics and constraints. Each method's effectiveness is often validated through simulations or experimental setups, underscoring the importance of practical applicability in real-world scenarios.

1.5   Research gaps

Despite significant progress in the control of nonlinear systems, several gaps remain in the literature, particularly for singularly perturbed and switched systems:

- Rigorous quantitative analysis of controller performance for uncertain singularly perturbed systems is missing.

- The existing timescale-based controller designs do not consider discontinuities in the system dynamics.

- Further, most of the techniques assume full state measurement, which is costly due to multiple sensors.

1.6   Research objectives

Based on the research gap identified from the comprehensive literature review, the following research objectives are proposed.

- Develop robust controllers for singularly perturbed systems with uncertainties.

- Extend the robust controllers for singularly perturbed systems to handle switching in dynamics.

- Develop an output feedback controller for singularly perturbed systems with uncertainties and switching.

- Apply the developed controllers to benchmarked dynamical systems like the robotic manipulator, inverted pendulum and Twin Rotor MIMO System, etc.

1.7   Research contributions

Following are the contributions:

- Designed a saturated controller for SPS using contraction theory.

- Introduced switching into SPS and designed a filtered backstepping controller using average dwell time (ADT).

- Developed a filtered backstepping controller for SPSS using contraction analysis.

- Proposed a Neural Disturbance Observer-based Backstepping Controller for SPSS.

- Developed a neural backstepping controller for SPSS.

1.8   Organization of the thesis

Chapter 1: This chapter introduces the control challenges in singularly perturbed and switched nonlinear systems, emphasizing the difficulties arising from multi-time-scale dynamics, switching mechanisms, and external disturbances. These complexities necessitate the development of robust control strategies. To address these issues, advanced methods such as backstepping, high-gain filters, and disturbance observers are discussed, highlighting their effectiveness in stabilizing nonlinear switched systems. In addition to motivating the research problem, the chapter also presents important preliminaries that provide the theoretical foundation of the study. These include contraction theory, which ensures incremental stability of nonlinear systems; Lyapunov theory, which provides the basic framework for analyzing system stability; and Lyapunov-based average dwell time (ADT), which offers a stability criterion for switched systems by regulating the switching frequency. Finally, the chapter sets the stage for the subsequent research gaps, objectives, and contributions also concludes by outlining the overall structure of the thesis, followed by concluding remarks.

Chapter 2: This chapter begins with a brief introduction to singularly perturbed systems (SPS), highlighting their inherent time-scale separation and control challenges under uncertainties. It then presents the motivation behind designing a saturated controller using singular perturbation techniques. The proposed method integrates a filter and disturbance observer, and leverages contraction theory to ensure stability and convergence of the closed-loop system. Finally, the chapter outlines the validation of the proposed control strategy using the Twin Rotor MIMO System (TRMS) for pitch angle control.

Chapter 3: This chapter introduces switched nonlinear systems and their relevance in modeling real-world systems such as chemical processes, robotic systems, and multi-agent networks. It outlines the motivation for designing a robust filter backstepping controller using time-scale redesign for uncertain switched systems in strict feedback form. The use of singular perturbation theory is emphasized for designing high-gain filters and disturbance observers to address complexity and uncertainties. The chapter also describes how the resulting three-time-scale switched closed-loop system is stabilized using an average dwell time-based Lyapunov approach. Lastly, the controller's effectiveness is validated through numerical simulations on a single-link manipulator.

Chapter 4: This chapter presents an overview of singularly perturbed switched systems and the challenges posed by frequent mode transitions and system uncertainties. It introduces the motivation for designing a filtered backstepping controller augmented with a high-gain disturbance observer (HGDO) to handle such complexities. The chapter outlines how contraction theory is employed to ensure closed-loop convergence and robust performance across switching modes. Finally, the practical applicability of the proposed controller is demonstrated through its implementation on a robotic manipulator, highlighting its effectiveness under real-time disturbances.

Chapter 5: This chapter introduces the control challenges associated with nonlinear singularly perturbed switched systems (SPSSs), particularly under mode transitions and external disturbances. It presents the motivation for using

a filtered backstepping controller combined with a high-gain filter to manage system complexity.   To enhance robustness, a neural network disturbance observer (NNDO) is integrated to estimate and compensate for unknown disturbances in real-time.   The chapter also discusses how Lyapunov-based analysis with average dwell time is employed to ensure closed-loop stability during switching. Finally, the proposed control strategy is validated through simulations on a robotic manipulator, demonstrating its effectiveness and practical applicability.

Chapter 6:   This chapter introduces singularly perturbed switched systems (SPSSs), emphasizing the coexistence of fast and slow dynamics along with the challenges introduced by switching among multiple subsystems. It motivates the need for a robust control strategy capable of handling system uncertainties and complexity.   To address this, a neural backstepping controller is proposed, integrated with a high-gain filter to manage design complexity and a high-gain disturbance observer (HGDO) to counteract external disturbances. This chapter concludes with the validation of the proposed approach on a single-link manipulator with actuator dynamics, demonstrating its practical effectiveness and feasibility.

Chapter 7:   This chapter summarises the key findings of the research by emphasising the effectiveness of the proposed control strategies for singularly perturbed and nonlinear switched systems. It highlights the main outcomes from simulations in terms of stability, robustness, and tracking performance. This chapter also outlines the limitations of the research work and concludes with possible future research directions, such as extending the methodology to MIMO systems, implementing hardware validation, and exploring adaptive or learning-based control techniques.

1.9   Concluding Remarks

In this chapter, the fundamental challenges associated with singularly perturbed and switched nonlinear systems have been introduced.   The discussion highlighted the complexities arising from multi-time-scale dynamics, abrupt

Chapter 1. Introduction and Motivation

switching, and the presence of external disturbances, all of which significantly influence the stability and performance of such systems. The necessity for advanced and robust control strategies was emphasized, with particular attention to approaches such as backstepping, high-gain filtering, and disturbance observer-based methods. These techniques provide a foundation for addressing the limitations of conventional controllers and form the motivation for the investigations presented in this thesis. Finally, the chapter outlined the overall structure of the thesis, thereby preparing the ground for the detailed analysis, controller design methodologies, and applications that follow in subsequent chapters.

Chapter 2

Saturated controller design for singularly perturbed systems

2.1   Background

Singularly perturbed systems (SPS) are nonlinear dynamical systems characterised by fast and slow dynamics evolving on different time scales [70]. Such systems appear in various engineering applications including robotics [71], aerospace [72, 73], and power electronics [74], where time-scale separation introduces analytical and design challenges.   In addition, uncertainties, nonlinearities, and actuator limitations such as saturation further complicate control design. To overcome these issues, a nonlinear saturated controller is proposed in this chapter. A filter and a disturbance observer are integrated into the design to handle uncertainties and external disturbances while maintaining actuator limitations. The analysis relies on contraction theory, which provides a rigorous mathematical framework to guarantee convergence of closed-loop trajectories irrespective of initial conditions. This property makes contraction theory particularly suitable for SPS where disturbances and fast-slow interactions can destabilize the system. The effectiveness of the proposed method is validated through simulations on the Twin Rotor MIMO System (TRMS) for pitch angle control. The obtained results demonstrate that the designed controller effectively stabilizes the system and achieves accurate pitch

20   *Chapter 2. Saturated controller design for singularly perturbed systems*

angle tracking even in the presence of singular perturbations, parameter uncertainties, and actuator saturation constraints. The control input remains within permissible limits, ensuring practical feasibility of the design. Moreover, the convergence of all system states to their desired trajectories highlights the robustness and reliability of the proposed approach. These findings further indicate that the developed control strategy can be extended to other nonlinear and high-order systems with similar characteristics.

2.2   System description

We consider the class of nonlinear systems which is in strict feedback form described as:

$$
\begin{aligned}
\dot{x}_1 &= g_1 x_2 + f_1(x_1) \\
\dot{x}_2 &= g_2 x_3 + f_2(x_1, x_2) \\
&\vdots \\
\dot{x}_n &= g_n u + f_n(x_1, x_2, \ldots, x_n)
\end{aligned}
\tag{2.1}
$$

Equation (2.1) can be represented in the following form:

$$
\dot{x}_n = G(x)u + F(x)
\tag{2.2}
$$

$f_i(.)$ are sufficiently smooth function and $g_i \neq 0$. The equation (2.2) can be converted into equation (2.4) by choosing z_i, α_i and α_{if} as (2.3): Where,

$$
\begin{aligned}
z_i &= x_i - \alpha_{if}, i = 1, 2, 3...n \\
\mu \dot{\alpha}_{if} &= -\alpha_{if} + \alpha_i \\
\alpha_{1f} &= \omega_d \\
\alpha_i &= \frac{1}{g_{(i-1)}} \big[-f_{(i-1)}(x_1, ..x_{(i-1)}) \\
&\quad - g_{(i-2)} z_{(i-2)} + \dot{\alpha}_{(i-1)f} \big], i = 2, 3, 4...n
\end{aligned}
\tag{2.3}
$$

Where, $\mu \in (0, 1)$, ω_d is desire signal and α_{if} are obtained through the first order filter [75, 76]. The initial conditions are $\alpha_{if}(0) = \alpha_i(0)$, $g_0 = 0$. As we can see in

equation (2.1) and (2.3) a nonlinear system in strict feedback form and a controller structure have been defined respectively. After applying the controller in the equation (2.1), equation (2.4) can be derived as

$$
\begin{aligned}
\dot{z}_1 &= g_1 z_2 \\
\dot{z}_i &= -g_{(i-1)} z_{(i-1)} + g_i z_{(i+1)} \\
\dot{z}_n &= -g_{(n-1)} z_{(n-1)}
\end{aligned}
\tag{2.4}
$$

This equation (2.4) can be written in compact form as $\dot{z} = Az$, which can be seen in equation (2.5).

$$
A = \begin{pmatrix}
0 & g_1 & 0 & \cdots & 0 \\
-g_1 & 0 & g_2 & \cdots & 0 \\
\ddots & \ddots & \ddots & \cdots & \ddots \\
0 & \cdots & 0 & -g_{(n-1)} & 0
\end{pmatrix}
$$

Where A is a skew-symmetric matrix. For a skew-symmetric matrix A, the inequality $A + A^T \leq 0$ always holds true, and the closed loop dynamics described by A is therefore stable even though marginally stable. Additionally, we have added robustifying terms to make the closed-loop dynamics uniformly ultimately bounded.

$$
\dot{z} = f(z) = Az
\tag{2.5}
$$

By using equation (2.3), equation (2.1) can be converted into the following form:

$$
\dot{z}_n = G(z)u + F(z)
\tag{2.6}
$$

Assumption:2.1 A transformation $\omega = T(x)$ exists for which the equation (2.2) can be expressed as in the following form:

$$
\dot{\omega} = A\omega + B(f(\omega) + h(\omega)u)
\tag{2.7}
$$

Where, A and B are in Brunovsky canonical form. $\omega \in D_\omega \subset \Re^n$. $f(\omega) : D_\omega \to \Re, h(\omega) : D_\omega \to \Re$ and $h(\omega) \neq 0, \forall \omega \in \Re^n$.
Assumption:2.2 The function $f(\omega)$ and $h(\omega)$ are locally Lipschitz.
Assumption:2.3 A smooth saturation function with the following properties

22   *Chapter 2. Saturated controller design for singularly perturbed systems*

$(\sigma(.) : \mathfrak{R} \to \mathfrak{R})$ exists -

(a) $\sigma(0) = 0$ and $s\sigma(s) > 0 \forall s \neq 0$

(b) $\lim_{s \to \infty} \sigma(s) = 1$, $\lim_{s \to -\infty} \sigma(s) = -1$

(c) For a finite set $D_s \subset \mathfrak{R}$, $\frac{\partial \sigma(s)}{\partial s} > 0 \forall s \in D_s$

Assumption 2.1 can transform the system (2.1) into a fully linearizable form. Assumption 2.2 gives information about existence of solution and uniqueness of solution for equation (2.2). And finally Assumption 2.3 implies that the saturation function $\sigma(s)$ is continuously differentiable and it will be an odd function such as sigmoid function, the hyperbolic tangent function, etc.

The aim is find an input u that ensures the closed loop trajectories of the system $w(t)$ closely match the states $\omega_d(t)$ of a stable system, as mentioned below:

$$\dot{\omega}_d = A_d \omega_d + B_d r \tag{2.8}$$

Where, $\omega_d = [\omega_{d1}, \omega_{d2}, ..., \omega_{dn}]' \in \mathfrak{R}^n$, r represents bounded reference input.

$$A_d = \begin{pmatrix} 0 & 1 & \cdots & 0 \\ \vdots & \vdots & \ddots & \vdots \\ 0 & 0 & \cdots & 1 \\ -a_{d1} & -a_{d2} & \cdots & -a_{dn} \end{pmatrix}$$

$$B_d = \begin{pmatrix} 0 \\ \vdots \\ 0 \\ b_d \end{pmatrix}$$

Where A_d is Hurwitz for suitable a_{di}, $i = (1, 2, 3...n)$.

2.3   Controller Design

Here, the objective is to solve the tracking problem of a non-affine system by using a saturated control rule $u = \beta\sigma(\frac{v}{\beta})$, where v is a new control input.

Error dynamics can be denoted as:

$$\dot{e} = A\omega + BF(\omega, v) - A_d\omega_d - B_d r \tag{2.9}$$

$$\mu\dot{v} = -sign(j_g)[F(z) + G(z)\sigma(v) - \dot{\omega}_d + \sum_{i=1}^{n} tanh(z_i)] \tag{2.10}$$

Where, $e = \omega - \omega_d$ and $F(\omega, v) = f(\omega) + \beta h(\omega)\sigma(\frac{v}{\beta}), h(\omega) > 0$. Equation (2.7) and Equation (2.10) can be represented in the following forms:

$$\dot{\omega} = A\omega + BF(\omega, v)$$
$$\mu\dot{v} = g(v, z, \omega_d, r) \tag{2.11}$$

Where,

$$g(.) = -sign(j_g)[F(z) + G(z)\sigma(v) - \dot{\omega}_d + \sum_{i=1}^{n} tanh(z_i)] \tag{2.12}$$

Equation (2.11) represents the time scale form of the system and the system's dynamics are in a standard singularly perturbed form (The fast dynamics consist of an isolated and unique root). This fact can be observed in Theorem 2.1.

Theorem 2.1: The ensuing closed-loop dynamics may be described in the standard singularly perturbed form if the pre-stated assumptions (2.1-2.3) continue to hold true and the dynamic controller is chosen as $u = \beta\sigma(\frac{v}{\beta})$. In this situation, $v = p(z, \omega_d, r)$ of the equation $g(v, z, \omega_d, r) = 0$ will be the unique root.

proof: Reference [49, 77] presents findings that prove the existence of a distinct root for a vector field that is partially contracting. The Jacobian matrix of the vector field $g(.)$ with respect to the variable v is designated as:

$$j_g = -\alpha(h(\omega)\frac{\partial(\sigma(v/\beta))}{\partial(v/\beta)})$$
$$= -a_v||((h(\omega)\frac{\partial(\sigma(v/\beta))}{\partial(v/\beta)}))|| \tag{2.13}$$

24   *Chapter 2. Saturated controller design for singularly perturbed systems*

The expression j_g exhibits negative definiteness within a specific bounded region of D_ω and D_v, as indicated by equation (2.13). So, the equation $\mu \dot{v} = g(v, z, \omega_d, r)$ will be partially contracting in v and there will be a unique and isolated solution of $g(v, z, \omega_d, r) = 0$ [14, 49]. In other words, we can say that a mapping between the variables z, ω_d, r, and control input v exists inside the domain D_ω and D_v. That's why equation (2.11) is in the typical form of a singularly perturbed equation.

Corollary: The error dynamics involving the slow reduced system of equations (2.11) is contracting in e and $(\omega_r - \omega_d) \to 0$.

Proof: Consider the root of the equation $g(v, z, \omega_d, r) = 0$ is denoted by $v = p(z, \omega_d, r)$. Hence, the reduced slow system of equations (2.11) will be as:

$$\dot{\omega}_r = A\omega + BF(\omega_r, p(z, \omega_d, r)) \tag{2.14}$$

Using $g(p(.), z, \omega_d, r) = 0$, we can write

$$
\begin{aligned}
u &= \beta\sigma\left(\frac{p(.)}{\beta}\right) \\
&= \frac{1}{G(z)}\left(-F(z) - \sum_{i=1}^{n} a_{di}\omega_{di} + \sum_{i=1}^{n} b_{di}r \right. \\
&\quad \left. - \sum_{i=1}^{n} tanh(z_i)\right)
\end{aligned}
\tag{2.15}
$$

The error dynamics can be expressed as:

$$\dot{e} = A\omega + F(\omega, p(.)) - A_d\omega_d - B_d r = A_e e \tag{2.16}$$

Where the A_e is a Hurwitz matrix and it has distinct real eigen values. A positive definite matrix M_{Ae} will exist in such a way that $\overline{A}_e = M_{Ae}A_e M_{Ae}^{-1}$ is negative definite. Here, M_{Ae} is an invertible matrix. So, equation (2.16) is contracting in M_{Ae} and $\omega(t)$ exponentially converge to ω_d i.e. $(\omega_r - \omega_d) \to 0$ and $e(t) \to 0$[78].

Feasible region: With a limited actuation power, any unstable system may not be globally or semi-globally stabilized. The tracking problem in this article can be solved inside a certain domain. From equation $u = \beta\sigma(\frac{v}{\beta})$, the dynamic inversion

with a limited actuation power β is feasible, provided

$$u = \beta\sigma(\frac{p(.)}{\beta})$$
$$= \frac{1}{G(z)}(-F(z) - \sum_{i=1}^{n} a_{di}\omega_{di} + \sum_{i=1}^{n} b_{di}r \qquad (2.17)$$
$$- \sum_{i=1}^{n} tanh(z_i))$$

The parameter, denoted as a_{di}, is adjustable, and $||\sigma(.)|| \leq 1$. Consequently, the region of attraction, represented by the finite region $(D_\omega \times D_v)$, can be approximated. Within this region, the vector fields satisfy the following condition.

$$||\frac{1}{h(\omega)}(-f(\omega) + \dot{\omega}_d)|| < \beta \qquad (2.18)$$

2.4   Convergence Analysis

Equation (2.11) is convergent in nature. This crucial information provides the boundedness of closed-loop system and is represented in the form of a lemma.

Lemma 2.1: Consider a system $\dot{\omega} = f(\omega)$ which is contracting in a transformation matrix M with rate λ and assume a perturbed system $\dot{\omega}_p = f(\omega_p) + w(\omega_p, \xi)$, ξ: An external signal.

(1) if $||w(\omega_p, \xi)|| \leq m_0$, $m_0 \in R^+$, then the following equation will be satisfied.

$$||\omega_p(t) - \omega(t)|| \leq \Gamma e^{-\lambda t}||\omega_p(0) - \omega(0)|| + \frac{\Gamma m_0}{\lambda} \qquad (2.19)$$

where Γ represents the supremum of the condition number for M.

(2) Let us consider two positive scalars m_{on}, m_{1n} such that $||w(\omega_p, \xi)|| \leq m_{on} + m_{1n}||\omega_p||$. Also consider that, a forward bounded solution ω_b exists for the system's dynamics, $\dot{\omega} = f(\omega)$, where the inequality $m_{1n} \leq \frac{\lambda}{\Gamma}$, then

$$\dot{\omega}_p = f(\omega_p) + w(\omega_p, \xi) \qquad (2.20)$$

Chapter 2. Saturated controller design for singularly perturbed systems

is partially contracting in ω_p and

$$||\omega_p(t) - \omega(t)|| \leq \Gamma e^{-(\lambda - \Gamma m_{1n})t}||\omega_p(0) - \omega(0)|| + m_{2n} \tag{2.21}$$

bound can be obtained. where, $m_{2n} = \frac{\Gamma(m_{on} + m_{1n}\omega_b)}{\lambda - \Gamma m_{1n}}$.

2.4.1 Convergence to Slow Manifold, $p(z, \omega_d, r)$

The above-mentioned controller in equation (2.10) is given in the form:

$$\mu\dot{v} = g(v, z, \omega_d, r) \tag{2.22}$$

Let us consider a virtual perturbed system of equations (2.10) in stretched time scale $\tau = \frac{t}{\mu}$,

$$\frac{dv_{ds}}{d\tau} = g(v_{ds} + p(.), z, \omega_d, r) + p'(v_{ds}, z, \omega_d, r, \mu) \tag{2.23}$$

where,

$$p'(v_{ds}, z, \omega_d, r, \mu) = -\mu\frac{d}{dt}(p(.))$$
$$v_{ds} = v(t) - p(z, \omega_d, r) \tag{2.24}$$

$p'(.)$ can be evaluated as:

$$p'(v_{ds}, z, \omega_d, r, \mu) = \mu(\frac{\partial p(.)}{\partial z}\dot{z} + \frac{\partial p(.)}{\partial \omega_d}\dot{\omega}_d + \frac{\partial p(.)}{\partial r}\dot{r}) \tag{2.25}$$

By using the Lipschitz properties of the function $f(\omega)$, u, and $p(z, \omega_d, r)$ it can be derived that[78]:

$$||p'|| \leq m_{2a}||v_{ds}|| + m_{2b}||\omega_d|| + m_{2c}||\dot{r}|| + m_{2d} \tag{2.26}$$

where, m_{2a}, m_{2b}, m_{2c}, m_{2d} are positive scalars. Let us consider $p'(.) = 0$ then $\frac{dv_{ds}}{d\tau}$ is partially contracting in v_{ds}. Let's assume contraction rate is $\frac{\overline{\lambda_v}}{\mu}$, M_v is transformation matrix and Ω_v is supremum of the condition number for M_v. Reference [79] ensures forward boundedness of trajectories inside the unperturbed system $\frac{dv_{ds}}{d\tau} = g(v_{ds} + p(.), z, \omega_d, r)$. It is stated in Lemma 2.2.

Lemma 2.2 [79]: Let us assume that $\dot{\omega} = f(\omega, t)$, $\omega \in R^n$, is contracting in ω for all $t > 0$. Suppose the contraction matrix is time invariant, finite, and also $||f(0,t)|| \leq a < \infty$ for all $t > 0$, then the trajectories $\omega(t)$ remain bounded and the solution $\omega(t)$ will be well defined for all $t > 0$.

If $v_{ds} = 0$ then $v = p(.)$ which implies that the function $g(v_{ds} + p(.), z, \omega_d, r)$ die out at $v_{ds} = 0$. By using Lemma 2.2 we can summarize that $v_{ds}(\tau)$ of the unperturbed system $\frac{dv_{ds}}{d\tau} = g(v_{ds} + p(.), z, \omega_d, r)$ are forward bounded for all $t > 0$ and a positive number a_0 exist for which $||v_{ds}(t)|| \leq a_0$ for all $t > 0$. For equation $g(0 + p(.), z, \omega_d, r) = 0$, $v_{ds} = 0$ can act as a particular solution of $\frac{dv_{ds}}{d\tau} = g(v_{ds} + p(.), z, \omega_d, r) + p'(v_{ds}, z, \omega_d, r, \mu)$ in the absence of perturbation term.

There exist a scalar μ_m such that $m_{2a} \leq \frac{\overline{\lambda_v}}{\mu^2 \Omega_v}$ for all $\mu < \mu_m$. That is why Lemma 2.1 can be used in equation $\frac{dv_{ds}}{d\tau} = g(v_{ds} + p(.), z, \omega_d, r) + p'(v_{ds}, z, \omega_d, r, \mu)$ to derive:

$$||v_{ds}(t) - 0|| \leq ||v(t) - p(z, \omega_d, r)||$$
$$\leq \Omega_v e^{-(\frac{\lambda_v}{\mu})t} ||v(0) - p(z(0), \omega_d(0), r)|| + \frac{\mu \Omega_v d_2}{\lambda_v} \tag{2.27}$$

Where, λ_v and d_2 can be evaluated from [79] as $\lambda_v = \overline{\lambda_v} - \mu \Omega_v m_{2a}$ and $d_2 = \mu(m_{2a} v_0 + m_{2c} ||r|| + m_{2d})$. By using [79], the following bound can be obtained.

$$\lim_{t \to \infty} ||v(t) - p(z, \omega_d, r)|| \leq \mu \Omega_v \frac{d_2}{\lambda_v} \tag{2.28}$$

2.4.2 Convergence analysis of trajectories

Equation (2.7) can be written in the following form with extra perturbation terms:

$$\dot{\omega} = A\omega + BF(\omega, p(z, \omega_d, r)) + BF(\omega, v)$$
$$- BF(\omega, p(z, \omega_d, r)) \tag{2.29}$$

The first two terms $A\omega + BF(\omega, p(z, \omega_d, r))$ is same as equation (2.11), and that's why it is partially contracting in ω with transformation matrix M_{Ae}. By employing the Lipschitz properties of the function $F(.)$ it can be determined that there exists a Lipschitz constant denoted as L_1. This constant ensures

$||BF(\omega, v) - BF(\omega, p(z, \omega_d, r))|| \leq L_1 ||v - p(z, \omega_d, r)||$. The bounds of equation (2.28) are finite inside the region of interest. That is why finite perturbation terms for all $t > 0$ in (2.29) can be derived. In (2.29) the nominal unperturbed dynamics are partially contracting, so Lemma 2.2 can be used to obtain forward boundedness of trajectories $\omega(t) \; \forall t \geq 0$. By using Lemma 2.1 on (2.14) and (2.29), the following bounded equation can be derived:

$$\lim_{t \to \infty} ||\omega(t) - \omega_r(t)|| \leq \frac{\Omega_{ae} L_1}{\lambda_{ae}} \left(\frac{\mu \Omega_v d_2}{\lambda_v} \right) \tag{2.30}$$

where λ_{ae} is the minimum eigen value of $\overline{A}_e$ and Ω_{ae} is the condition number of M_{Ae}. From equation (2.30), the bounded steady state tracking error can be derived by using triangle inequalities.

$$\lim_{t \to \infty} ||\omega(t) - \omega_d(t)|| \leq \frac{\Omega_{ae} L_1}{\lambda_{ae}} \left(\frac{\mu \Omega_v d_2}{\lambda_v} \right) \tag{2.31}$$

2.5   Filtered Saturated Controller With Disturbance Observer

A disturbance observer with a high gain is provided to estimate the uncertain dynamics of the systems. The system uncertainties can be eliminated through disturbance observer $\delta_i(.)$[80].

$$
\begin{aligned}
\dot{\xi}_i &= -k(\xi_i + kx_i + f_i(x_1, x_2, \ldots, x_i) + g_i x_{i+1}) \\
\dot{\xi}_n &= -k(\xi_n + kx_n + f_n(x_1, x_2, \ldots, x_n) + g_n u) \\
\hat{\delta}_i(.) &= \xi_i + kx_i \\
\hat{\delta}_n(.) &= \xi_n + kx_n
\end{aligned}
\tag{2.32}
$$

where the scalar $k > 0$ is a large positive constant, $\hat{\delta}_i(.)$ is the estimation of disturbance $\delta_i(.)$, and ξ_i is an intermediate variable. Using observer (2.32), the dynamics of the disturbance estimator $(\hat{\delta}_i)$ are given by:

$$\dot{\hat{\delta}}_i = h_i(\hat{\delta}_i, \delta_i) = -k(\hat{\delta}_i - \delta_i). \tag{2.33}$$

2.5. Filtered Saturated Controller With Disturbance Observer   29

Defining a disturbance error variable $\tilde{\delta}_i = \delta_i(.) - \hat{\delta}_i(.)$, the estimation error dynamics can be written as:

$$\epsilon \dot{\tilde{\delta}}_i(.) = -\tilde{\delta}_i - \epsilon \dot{\delta}_i(.). \tag{2.34}$$

where $0 \le \epsilon = 1/k \le 1$. The boundary layer dynamics resulting from (2.34) can be written as:

$$\frac{\delta}{\delta\tau}(\tilde{\delta}_i) = \tilde{\delta}_i. \tag{2.35}$$

2.5.1   Conversion to Singularly Perturbed form

The filter-based saturated control law u chosen for system (2.1) is based on a disturbance observer and filtering.

$$
\begin{aligned}
u &= \beta\sigma(\frac{v}{\beta}) \\
\mu\dot{v} &= -sign(j_g)[F(z) + G(z)\sigma(v) - \hat{\delta}_i \\
&\quad - \dot{w}_d + \sum_{i=1}^{n} tanh(z_i)] \\
z_i &= x_i - \alpha_{if}, (i = 1, 2......m) \\
\alpha_{1f} &= \omega_d, \ i \in [2, 3 \ldots m] \\
\alpha_i &= \frac{1}{g_{(i-1)}}[-f_{(i-1)}(x_1, ..x_{(i-1)}) \\
&\quad - g_{(i-2)}z_{(i-2)} + \dot{\alpha}_{(i-1)f} - \hat{\delta}_{(i-1)}], i = 2, 3, 4...n.
\end{aligned}
\tag{2.36}
$$

The closed-loop system described in equation (2.1) with the control law given in equation (2.36) can be represented as follows:

$$
\begin{aligned}
\dot{z}_1 &= g_1 z_2 + g_1 \tilde{\alpha}_{2f} + \tilde{\delta}_1 \\
\dot{z}_i &= g_{(i-1)} z_{i-1} \\
&\quad + g_{(i)} z_{i+1} + g_i \tilde{\alpha}_{(i+1)f} + \tilde{\delta}_i \\
\dot{z}_n &= -g_{(n-1)} z_{n-1} + \tilde{\delta}_{(n)}.
\end{aligned}
\tag{2.37}
$$

Rewriting (2.37) in a compact form as (2.38),(2.39), and (2.40)

Chapter 2.   Saturated controller design for singularly perturbed systems

$$\dot{z} = f(z, \tilde{\alpha}_f, \tilde{\delta}) \tag{2.38}$$

$$\mu \dot{\tilde{\alpha}}_f = g(\alpha_f, \alpha_i) = -\tilde{\alpha}_f + \mu \dot{\alpha}_i \tag{2.39}$$

$$\epsilon \dot{\tilde{\delta}} = h(\hat{\delta}, \delta_i) = -\tilde{\delta} + \epsilon \dot{\delta}_i \tag{2.40}$$

where $\hat{\delta} = [\hat{\delta}_1, \hat{\delta}_2, \ldots, \hat{\delta}_n]$, $\tilde{\delta} = [\tilde{\delta}_1, \tilde{\delta}_2, \ldots, \tilde{\delta}_n]$ $\delta_i = [\delta_1 \delta_2, \ldots, \delta_n]$. In equations (2.38)-(2.39), the system dynamics undergo a transformation, resulting in a singularly perturbed system with three distinct time scales. By employing the ratio $\frac{\epsilon}{\mu}$ this system can be further simplified into a two-time scale format. Assuming, without loss of generality, that $\epsilon < \mu$, indicating that the observer dynamics operates at a faster rate as compared to the filter dynamics. A suitable choice for ϵ is $\epsilon = \kappa \mu$, where $\kappa < 1$ is a small positive constant. Express the fast subsystem (2.39), (2.40) as:

$$\mu \dot{\tilde{v}} = W(\tilde{v}, \dot{v}, \kappa) = - \begin{bmatrix} 1 & 0 \\ 0 & \frac{1}{\kappa} \end{bmatrix} \tilde{v} + \mu \dot{v} \tag{2.41}$$

where $\tilde{v} = [\tilde{\alpha}_f^T, \tilde{\delta}^T]^T$, $\dot{v} = [\dot{\alpha}_i^T, \dot{\delta}_i^T]^T$ and $W(.) = [g^T(.), \frac{1}{\kappa} h^T(.)]^T$. By using Equation (2.41), the dynamics of the closed-loop system can be described using two distinct time scales in a singularly perturbed form. Convergence of system trajectories can be analysed by using the same reasoning.

2.6   Experimental outcomes

The TRMS serves as a benchmark in the field of aerodynamics and shares similarities with helicopter dynamics, featuring two inputs and two outputs. This system contains vertical and horizontal rotors, which are actuated by two DC motors. The vertical rotor gives vertical take off and landing momentum (pitch angle ψ) and the horizontal rotor gives the steering action (yaw angle ϕ) under strong coupling. The following momentum equations [81] for the vertical take off and landing of TRMS is considered to validate the boundedness and convergence of the proposed filter saturated controller:

$$I_1 \ddot{\psi} = M_1 - M_{FG} - M_{B\psi} - M_G \tag{2.42}$$

and

$$\tau_1 = \frac{k_1}{T_{11}s + T_{10}}u \tag{2.43}$$

Where,

$M_1 = a_1\tau_1^2 + b_1\tau$, nonlinear static characteristic

$M_{FG} = M_g sin(\psi)$, gravity momentum

$M_{B\psi} = B_{1\psi}\dot{\psi} + B_{2\psi}sign(\dot{\psi})$, friction forces momentum

$M_G = K_{gy}M_1\dot{\phi}cos(\psi)$, gyroscopic momentum

The parametric values of the experimental setup of TRMS [82] are given in Table 2.1. The actuated motor momentum is described by the equation (2.43). Here, u is a bounded control input.

Consider, $x_1 = \psi$, $x_2 = \dot{\psi}$ and $x_3 = \tau_1$.

TABLE 2.1: Parametric values of TRMS

TRMS Parameters	Values
I_1 (Moment of inertia of vertical rotor)	6.8×10^{-2} Kg m^2
T_{11} (Motor 1 denominator parameter)	1.1
T_{10} (Motor 1 denominator parameter)	1
M_g (Gravity momentum)	0.3 N·m
$B_{1\psi}$ (Friction momentum function parameter)	6×10^{-3} N·m·s/rad
$B_{2\psi}$ (Friction momentum function parameter)	1×10^{-3} N·m·s^2/rad
k_{gy} (Gyroscopic momentum parameter)	0.05 s/rad
a_1 (Static characteristic parameter)	0.0135
b_1 (Static characteristic parameter)	0.0924

$$\dot{x}_1 = g_1x_2 + f_1(x_1)$$
$$\dot{x}_2 = g_2x_3 + f_2(x_1, x_2) \tag{2.44}$$
$$\dot{x}_3 = g_3u + f_3(x_1, x_2, x_3)$$

Where, $g_1 = 1$, $f_1(x_1) = 0$, $g_2 = \frac{b_1}{I_1}$, $f_2(x_1, x_2) = -\frac{1}{I_1}[M_g sinx_1 + B_{1\psi}x_2 + B_{2\psi}signx_2]$, $g_3 = \frac{1}{T_{11}}$ and

32   *Chapter 2. Saturated controller design for singularly perturbed systems*

$$f_3(x_1, x_2, x_3) = -\frac{T_{10}}{T_{11}} x_3$$

The proposed controller was tested and validated on a TRMS under two different test cases. Additionally, in both cases, a nonlinearity term $\delta = 10^3 * tanh(2t)$ has been added to the state x_2.

For the first test case, the reference parameters a_{di} of the stochastic bounded signal has been taken as $a_{d1} = 20$, $a_{d2} = 21$ and $a_{d3} = 42$ with perturbed parameter $\mu = 0.01$. It is observed from the Figure 2.1 that the closed-loop state response x_1 of the TRMS tracks the stochastic bounded reference signal quickly and ensures stability during a disturbed environment. The required control law to track the reference, depicted in Figure 2.2, is designed to achieve quick stability.

The tracking performance of the designed controller has also been tested under second test case for different reference parameters such as $a_{d1} = 25$, $a_{d2} = 26$, $a_{d3} = 40$ with perturbed parameter $\mu = 0.01$. It is observed from Figure 2.3 that the trajectory of the closed-loop state x_1 of TRMS satisfactorily follows the reference signal. The required control law to track the reference is depicted in Figure 2.4. Finally, the results reveal that the nonlinear saturated controller satisfactorily meets control design objectives.
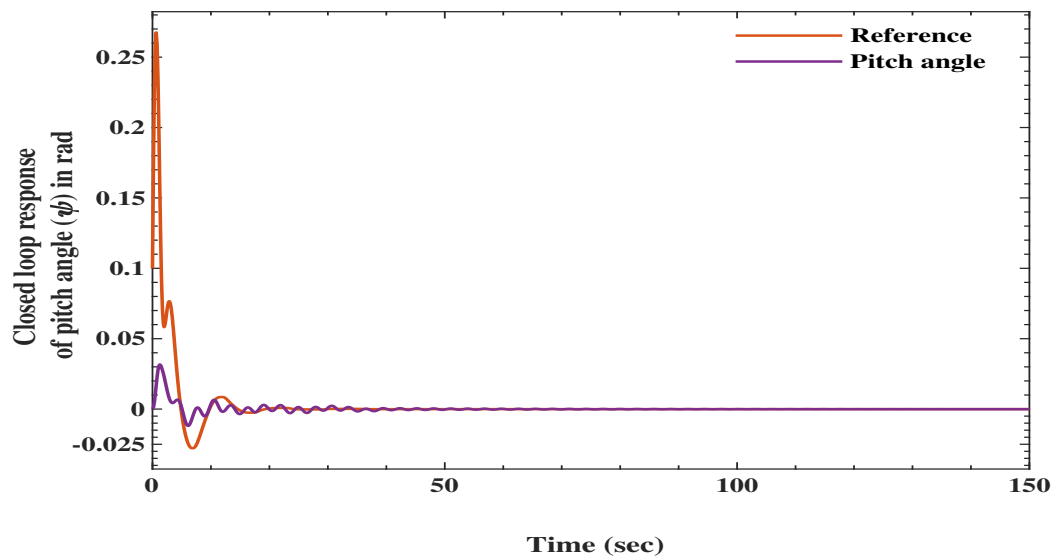
FIGURE 2.1: Closed loop response of pitch angle in rad and reference signal with parameters $a_{d1} = 20, a_{d2} = 22, a_{d3} = 42$ as first test case
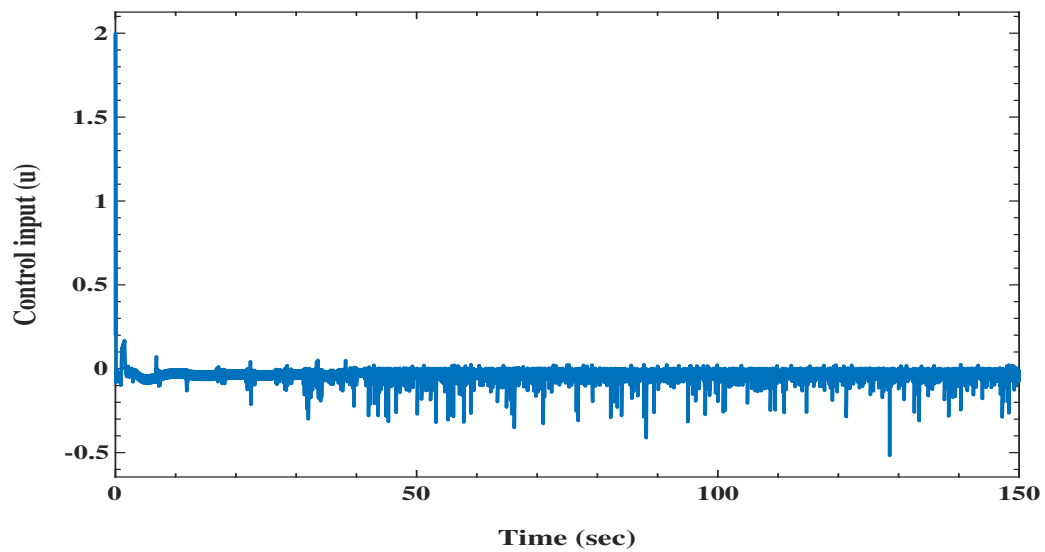
FIGURE 2.2: Closed loop control signal with parameters $a_{d1} = 20$, $a_{d2} = 22, a_{d3} = 42$ as first test case

Chapter 2. Saturated controller design for singularly perturbed systems
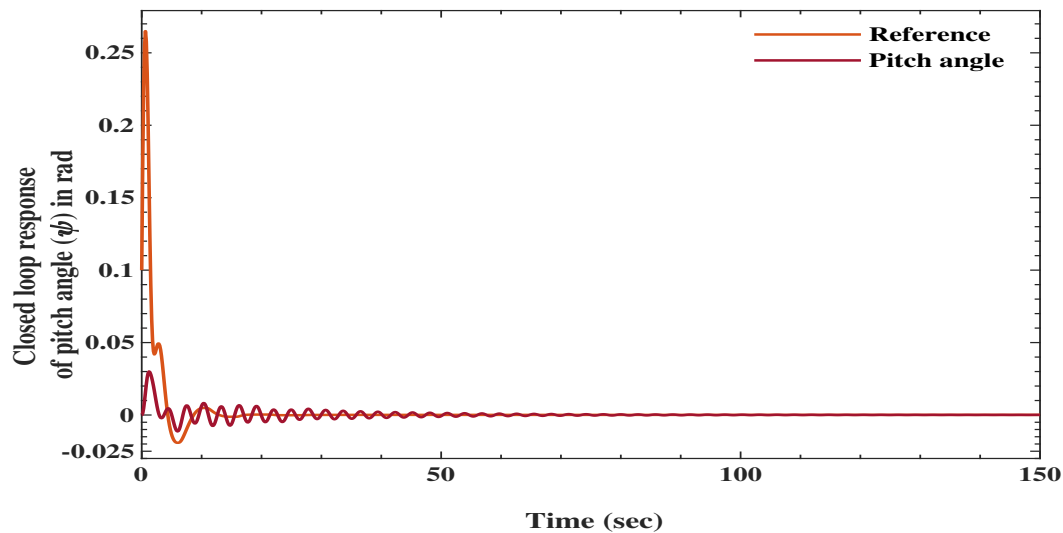
FIGURE 2.3: Closed loop response of pitch angle in rad and reference signal with parameters $a_{d1} = 25$, $a_{d2} = 26$, $a_{d3} = 40$ as second test case
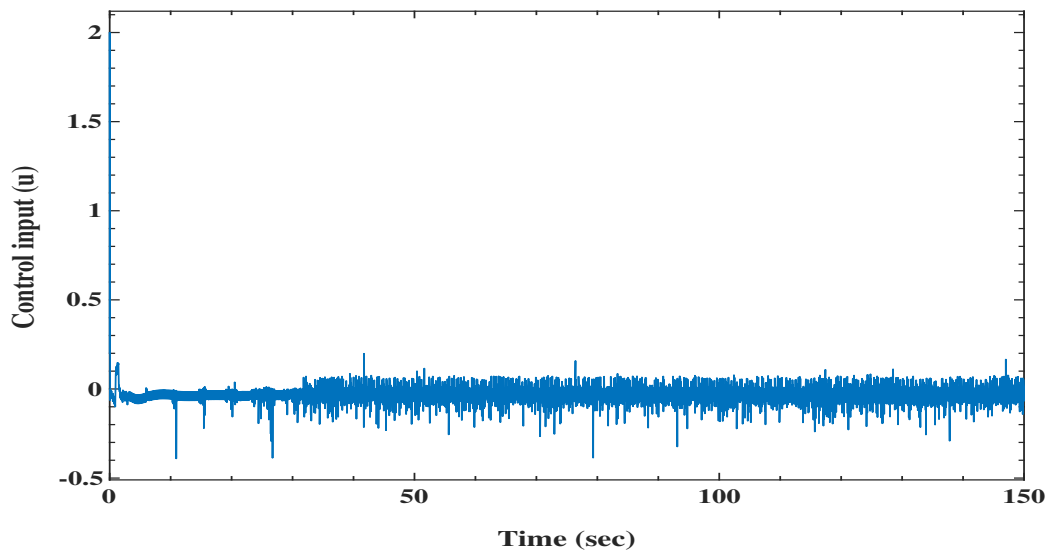
FIGURE 2.4: Closed loop control signal with parameters $a_{d1} = 25$, $a_{d2} = 26$, $a_{d3} = 40$ as second test case

2.7   Concluding remarks

In this chapter, a contraction theory-based nonlinear saturated controller has been designed specifically for singular perturbation systems. The effectiveness of the designed controller has been tested on a Twin rotor MIMO System (TRMS) for tracking of pitch angle at two different unknown dynamical scenarios. The obtained outcomes suggest that the controller has the capability to provide reliable and precise control under changing conditions. One of the notable versatile strengths of this novel controller is its boundedness and convergence under all closed loop states. Its effective application and performance analysis on TRMS show that it may be used to a variety of physical systems, such as robotics platforms, inverted pendulums, and single-link manipulators etc. In summary, the designed nonlinear saturated controller exhibits encouraging outcomes when applied to TRMS for pitch angle tracking. Also, It may have great potential to tackle control issues in diverse dynamic systems.

Chapter 3

Singular perturbation-based filtered backstepping controller for singularly perturbed switched systems

3.1 Background

Switched nonlinear systems represent a class of hybrid dynamical systems capable of describing discontinuous behaviors encountered in many real-world processes, such as robotics [83, 84], chemical plants [85, 86], and multi-agent networks [87, 88]. Their analysis and control are challenging due to the coexistence of nonlinearities, switching dynamics, and external disturbances. To address these challenges, this chapter develops a time-scale redesign-based robust filter backstepping controller for uncertain switched nonlinear systems in strict-feedback form. The proposed approach leverages singular perturbation techniques to design high-gain filters, which eliminate the explosion of complexity in backstepping, and high-gain disturbance observers, which compensate for uncertainties. The interaction between switching, disturbances, and high-gain filtering leads to a three-time-scale closed-loop system, whose stability is ensured using an average dwell-time Lyapunov framework. The

effectiveness of the proposed controller is validated through simulations on a single-link robotic manipulator. The results clearly demonstrate the controller's ability to achieve precise trajectory tracking despite the presence of system uncertainties and external disturbances. This confirms the robustness and stability of the designed control scheme. Furthermore, the successful performance on the single-link manipulator highlights the controller's adaptability and scalability, indicating its strong potential for extension to more complex, higher-order, and multi-link robotic systems.

3.2   System Description and Problem Statement

Consider a class of switched nonlinear systems described as:

$$
\begin{aligned}
\dot{x}_1 &= f_{1\sigma}(x_1) + b_{1\sigma}(x_1)x_2 + d_{1\sigma}(x_1, t) \\
\dot{x}_2 &= f_{2\sigma}(x_1, x_2) + b_{2\sigma}(x_1, x_2)x_3 + d_{2\sigma}(x_1, x_2, t) \\
&\vdots \\
\dot{x}_n &= f_{n\sigma}(x_1, x_2, x_3....x_n) + b_{n\sigma}(x_1, x_2, \ldots, x_n)u + d_{n\sigma}(x, t)
\end{aligned}
\tag{3.1}
$$

where $f_{i\sigma}(.), b_{i\sigma}(.)$ are known sufficiently smooth functions, $x = [x_1, x_2, ..., x_n]^T$, $b_{i\sigma}(.) \neq 0 \ \forall x \in R^n$ and $\sigma \in P = [1, 2, \cdots, N]$ is piece-wise constant signal with finite number of values and $u \in R$ is the control input. The terms $d_{i\sigma}(.)$ denote uncertain parts of system dynamics. To ensure that the output $x_1(t)$ follows a desired signal $x_d(t)$ while retaining stability in the closed loop, the goal is to design a control law utilizing the filter backstepping approach, represented as u. Generally, the filtered backstepping literature frequently contains assumptions 3.1 and 3.2 [76], [89], [90]. Assumption 3.2 is analogous to rate-bounded uncertainties which hold for many disturbances, including friction, saturation, smooth periodic uncertainty [91, 92].

Assumption 3.1: The desired signal $x_d(t)$ and its derivatives are continuous and bounded. $f_{i\sigma}(.)$, $b_{i\sigma}(.)$ and its partial derivative are continuous upto 2nd order.

Assumption 3.2: The unknown terms in the system dynamics including disturbances can be modeled as: $\dot{d}_{\sigma i} = \Theta_{\sigma i}(d_{\sigma i})$, where $i \in 1, 2..., n$ and $\Theta_{\sigma i}(d_{\sigma i})$ are unknown functions whose norms are bounded by a positive scalar c, which may be written as $||\Theta_{\sigma i}(d_{\sigma i})|| \leq c$, $\forall i, \sigma$.

3.3 Filtered Backstepping in the Absence of Disturbances

This section introduces a filtered backstepping (FB) controller design. The approach assumes that the system dynamics (3.1) do not include disturbance terms represented by $d_{i\sigma}(.)$. The control law is similar to the singularly perturbed systems without switching. In this section, a control law (u_σ) has been proposed for singularly perturbed switched systems. The standard FB control law in the absence of any uncertainties is expressed as:

$$u_\sigma = \frac{1}{b_{n\sigma}(x)}[-f_{n\sigma}(x) - b_{(n-1)\sigma}(x)z_{n-1} - \chi_{n\sigma}(z_n) + \dot{\alpha}_{nf}]$$

$$z_i = x_i - \alpha_{if}, (i = 1, 2......n)$$

$$\alpha_{1f} = \alpha_1 = x_d(t)$$

(3.2)

where $\chi_{n\sigma}(z_n)$ are user-defined scalar tuning functions, which are chosen as $k_{i\sigma}z_i$, where, $i \in 1, 2, 3...n$, $k_{i\sigma} > 0$. The terms α_{if} are obtained through the first order filter[75, 76]. It can be expressed expressed as:

$$\mu\dot{\alpha}_{if} = -\alpha_{if} + \alpha_{i\sigma} \quad i = 2, \cdots, n$$

$$\alpha_{i\sigma} = \frac{1}{b_{(i-1)\sigma}(x)}[-f_{(i-1)\sigma}(x_1,..x_{i-1}) - \chi_{(i-1)\sigma}(z_{i-1})$$

$$- b_{(i-2)\sigma}(x)z_{i-2} + \dot{\alpha}_{(i-1)f}], b_{0\sigma} = 0 \ i = 2, \cdots, n$$

(3.3)

where $\chi_{(i-1)\sigma}, i \in 1, 2, 3...n$ is scalar tuning function and $\mu \in (0, 1)$ is called perturbed parameter. The initial condition of (3.3) is chosen as $\alpha_{if}(0) = \alpha_i(0)$. Using (3.2) and (3.3), the closed-loop system can be expressed in the following

form.

$$\dot{z}_1 = -\chi_{1\sigma}(z_1) + b_{1\sigma}(x)z_2 + b_{1\sigma}(x)\tilde{\alpha}_{2\sigma}$$
$$\dot{z}_i = -b_{(i-1)\sigma}(x)z_{i-1} - \chi_{i\sigma}(z_i) + b_{i\sigma}(x)z_{i+1} + b_{i\sigma}(x)\tilde{\alpha}_{(i+1)\sigma} \qquad (3.4)$$
$$\dot{z}_n = -b_{(n-1)\sigma}(x)z_{n-1} - \chi_{n\sigma}(z_n), \;\; i = 2, \dots, n-1$$

where $\tilde{\alpha}_{if} = \alpha_{if} - \alpha_{i\sigma}$. The overall closed-loop system with the FB controller can be written as (3.5), (3.6) and (3.7).

$$\dot{z} = f_\sigma(z, \tilde{\alpha}_f) \qquad (3.5)$$

$$\mu\dot{\alpha}_f = g_\sigma(\alpha_f, \alpha_\sigma) = -\alpha_f + \alpha_\sigma \qquad (3.6)$$

where $\alpha_\sigma = [\alpha_{2\sigma}, \alpha_{3\sigma}, \alpha_{4\sigma}...\alpha_{n\sigma}]^T$, $\alpha_f = [\alpha_{2f}, \alpha_{3f}, \alpha_{4f}...\alpha_{nf}]^T$, $\tilde{\alpha}_f = [\tilde{\alpha}_{2f}, \tilde{\alpha}_{3f}, \tilde{\alpha}_{4f}...\tilde{\alpha}_{nf}]^T$ and $f_\sigma(.) = [\bar{f}_{1\sigma}, \bar{f}_{2\sigma}, \bar{f}_{3\sigma}...\bar{f}_{n\sigma}]^T$ with

$$\bar{f}_{1\sigma}(.) = -\chi_{1\sigma}(z_1) + b_{1\sigma}(x)z_2 + b_{1\sigma}(x)\tilde{\alpha}_{2\sigma}$$
$$\bar{f}_{i\sigma}(.) = -b_{(i-1)\sigma}(x)z_{i-1} - \chi_{i\sigma}(z_i) + b_{i\sigma}(x)z_{i+1} + b_{i\sigma}(x)\tilde{\alpha}_{(i+1)\sigma}, \;\; (i = 2, 3..., n-1)$$
$$\bar{f}_{n\sigma}(.) = -b_{(n-1)\sigma}(x)z_{n-1} - \chi_{n\sigma}(z_n)$$

$$(3.7)$$

3.4   Stability of the Closed Loop System

It should be noted that the closed loop dynamics (3.5)-(3.6) is a switched nonlinear singularly perturbed system [93]. Replacing the root of the fast subsystem α_σ in place of α_f in (3.7), the reduced slow subsystem can be obtained as:

$$\dot{z}_1 = -\chi_{1\sigma}(z_{1r}) + b_{1\sigma}(x)z_{2r}$$
$$\dot{z}_i = -b_{(i-1)\sigma}(x)z_{(i-1)r} - \chi_{i\sigma}(z_{ir}) + b_{i\sigma}(x)z_{(i+1)r} \qquad (3.8)$$
$$\dot{z}_n = -b_{(n-1)\sigma}(x)z_{(n-1)r} - \chi_{n\sigma}(z_{nr}), i = 2, ..., (n-1).$$

The reduced slow system in compact form can be written as:

$$\dot{z} = f_\sigma(z) \qquad (3.9)$$

Consider the fast filter dynamics, when

$$\mu \to 0 \Rightarrow g_\sigma(\alpha_f, \alpha_\sigma) \to 0 \Rightarrow \alpha_f \to \alpha_\sigma = \alpha_{sm\sigma}$$

where the slow manifold is represented as $(\alpha_{sm\sigma})$. Define a error variable $y = \alpha_f - \alpha_\sigma$, whose dynamics can be derived as:

$$\mu \dot{y} = -y - \mu \dot{\alpha}_\sigma. \tag{3.10}$$

The fast boundary layer dynamics of (3.10), which are expressed in a stretched timescale $\tau = \frac{t}{\mu}$, can be formulated as follows [93].

$$\frac{dy}{d\tau} = -y. \tag{3.11}$$

3.4.1 Stability of System Between Switching Instants

For a suitable choice of $\chi_{i\sigma}(z_i) = k_{i\sigma} z_i$ with $k_{i\sigma} > 0 \ \forall \sigma$, the reduced order dynamics (3.8) can be derived to be linear in z, and (3.9) takes the form of

$$\dot{z} = f_\sigma(z) = A_\sigma z \tag{3.12}$$

where

$$A_\sigma = \begin{bmatrix} -k_{1\sigma} & b_{1\sigma}(x) & 0 & \dots & 0 \\ -b_{1\sigma}(x) & -k_{2\sigma} & b_{2\sigma}(x) & \dots & 0 \\ \ddots & \ddots & \ddots & \ddots & \ddots \\ 0 & \dots & 0 & b_{(n-1)\sigma}(x) & -k_{n\sigma} \end{bmatrix}$$

is a skew symmetric matrix through the selections of k_i. Exploiting the properties of skew symmetric matrices:

$$\frac{A_\sigma^T + A_\sigma}{2} = \begin{bmatrix} -k_{1\sigma} & 0 & 0 & \dots & 0 \\ 0 & -k_{2\sigma} & 0 & \dots & 0 \\ \ddots & \ddots & \ddots & \ddots & \ddots \\ 0 & \dots & 0 & 0 & -k_{n\sigma} \end{bmatrix}.$$

Chapter 3.　Singular perturbation-based filtered backstepping controller for singularly perturbed switched systems

Hence, there exists a set of symmetric positive definite matrices M_σ, Q_σ such that

$$M_\sigma A_\sigma + A_\sigma^T M_\sigma \leq -Q_\sigma. \tag{3.13}$$

Let us define a Lyapunov function candidate

$$V_{r\sigma} = \frac{1}{2} z^T M_\sigma z \tag{3.14}$$

Then

$$\underline{m}_\sigma ||z||^2 \leq V_{r\sigma} \leq \overline{m}_\sigma ||z||^2 \tag{3.15}$$

where $\underline{m}_\sigma = \lambda_{\min}(M_\sigma), \overline{m}_\sigma = \lambda_{\max}(M_\sigma)$. Using (3.15) yields

$$\dot{V}_{r\sigma} \leq -\beta_\sigma ||z||^2 \leq -(\beta_\sigma/\overline{m}_\sigma)V_{r\sigma}, \tag{3.16}$$

where $\beta_\sigma = \lambda_{\min}(Q_\sigma)$.

Similarly, constructing a Lyapunov function $V_f = \frac{1}{2}y^T y$ and using (3.16), we can show

$$\dot{V}_f \leq -||y||^2 = -2V_f. \tag{3.17}$$

Once, the stability of the reduced order system has been established, it can be considered a scalar $(0 < p < 1)$ and set of composite Lyapunov functions

$$V_\sigma = (1-p)V_{r\sigma} + pV_f \tag{3.18}$$

whose derivative along the trajectories of all systems (3.5), (3.10) can be derived as

$$
\begin{aligned}
\dot{V}_\sigma(z,y) &= (1-p)\frac{\partial V_{r\sigma}}{\partial z}(f_\sigma(z,\tilde{\alpha}_f)) - \frac{p}{\mu}\frac{\partial V_f}{\partial y}y - p\frac{\partial V_f}{\partial y}\dot{\alpha}_\sigma \\
\implies \dot{V}_\sigma(z,y) &= (1-p)\frac{\partial V_{r\sigma}}{\partial z}(f_\sigma(z)) - \frac{p}{\mu}\frac{\partial V_f}{\partial y}y - p\frac{\partial V_f}{\partial y}\dot{\alpha}_\sigma \\
&+ (1-p)\frac{\partial V_{r\sigma}}{\partial z}\left(f_\sigma(z,\tilde{\alpha}_f) - f_\sigma(z)\right).
\end{aligned}
\tag{3.19}
$$

3.4. Stability of the Closed Loop System

43

The last term of (3.19) can be further simplified using the following Lemma.

Lemma 3.1: There exist positive constants $L_{1\sigma}$ such that

$$\frac{\partial V_{r\sigma}}{\partial z}\left(f_\sigma(z,\tilde{\alpha}_f) - f_\sigma(z)\right) \leq 2L_{1\sigma}||z||||y||. \tag{3.20}$$

Proof: Using Lipschitz inequality:

$$\Rightarrow \frac{\partial V_{r\sigma}}{\partial z}\left(f_\sigma(z,\tilde{\alpha}_f) - f_\sigma(z)\right) \leq \frac{\partial V_{r\sigma}}{\partial z}L_{1\sigma}||\tilde{\alpha}_f||.$$

From the structure of V_r, $||\frac{\partial V_{r\sigma}}{\partial z}|| \leq 2||M_\sigma||||z|| \leq 2\overline{m}_\sigma||z||$. Note that, $\tilde{\alpha} = y$ from the definition of y. Combining these two equations, R.H.S of (3.20) can be evaluated.

Assumption 3.3: There exist positive scalars $L_{2\sigma}, L_{3\sigma}$ such that.

$$||\dot{\alpha}_\sigma|| = ||\frac{\partial \alpha_\sigma}{\partial z}\dot{z}|| \leq 2L_{2\sigma}||z|| + L_{3\sigma}||y|| + L_{31\sigma}. \tag{3.21}$$

Assumption 3.3 is standard for singularly perturbed dynamics[93]. It implies the rate of change of the virtual control signal α_σ to be slower than the growth of the weighted combination of z and the fast variable y. Further, many practical systems like robotic manipulators, inverted pendulums, ships, chemical systems, synchronous machines, etc., shall satisfy Assumption 3.3 ([93, 94]).

Previously, it is defined that $V_f = \frac{1}{2}y^2y$. So, the value of $\frac{\partial V_f}{\partial y}$ can be evaluated. Also from the equations (3.16) and (3.20) $\frac{\partial V_{r\sigma}}{\partial z}$ and $\frac{\partial V_{r\sigma}}{\partial z}\left(f_\sigma(z,\tilde{\alpha}_f) - f_\sigma(z)\right)$ can be exploited in equation (3.19) respectively to obtain the following equation (3.22).

$$\dot{V}_\sigma \leq -\beta_\sigma(1-p)||z||^2 - \frac{p}{\mu}||y||^2 + 2pL_{2\sigma}||z||||y||$$
$$+ pL_{3\sigma}||y||^2 + 2(1-p)L_{1\sigma}||z||||y|| + pL_{31\sigma}||y||. \tag{3.22}$$

It can be written in a compact form as:

$$\dot{V}_\sigma = -Z^T S_\sigma Z + pL_{31\sigma}Z \tag{3.23}$$

where $Z = [z,y]^T$ and

Chapter 3. Singular perturbation-based filtered backstepping controller for singularly perturbed switched systems

$$S_\sigma = \begin{bmatrix} (1-p)\beta_\sigma & -(1-p)L_{1\sigma} - pL_{2\sigma} \\ -(1-p)L_{1\sigma} - pL_{2\sigma} & p(\frac{1}{\mu} - L_{3\sigma}) \end{bmatrix} \tag{3.24}$$

The overall system is asymptotically stable only when S_σ is positive definite [4]. By Schur's complement, it can be derived that S_σ is positive definite if

$$\mu_\sigma \le \mu_\sigma^* = \frac{\beta_\sigma}{\beta_\sigma L_{3\sigma} + \frac{1}{p(1-p)}((1-p)L_{1\sigma} + pL_{2\sigma})^2} \tag{3.25}$$

From the properties of M_σ, there exist two positive constants m_l, m_h such that

$$m_l I \le M_\sigma \le m_h I.$$

So, one can derive

$$\underline{\alpha}||Z||^2 \le V_\sigma \le \bar{\alpha}||Z||^2. \tag{3.26}$$

where

$$\underline{\alpha} = \min(\frac{(1-p)m_l}{2}, \frac{p}{2}), \; \bar{\alpha} = \max(\frac{(1-p)m_h}{2}, \frac{p}{2}).$$

Hence, it can be concluded that within any two consecutive switching instances, the dynamics of the overall singularly perturbed system is stable, if $\mu_\sigma \le \mu_\sigma^*$, i.e.

$$\dot{V}_\sigma \le -\beta_\sigma^o V_\sigma + pL_{31\sigma}||Z|| \tag{3.27}$$

where $\beta_\sigma^o = \frac{\lambda_{\min}(S_\sigma)}{\lambda_{\max}(S_\sigma)}$. Let

$$M_{p\sigma} = \begin{bmatrix} (1-p)M_{r\sigma} & 0 \\ 0 & pM_{v\sigma} \end{bmatrix}$$

then

$$\lambda_{\min}(M_{p\sigma})||Z||^2 \le V_\sigma \le \lambda_{\max}(M_{p\sigma})||Z||^2.$$

Therefore,

$$\frac{dV_\sigma}{dt} \le -\frac{\beta_\sigma^o}{2}V_\sigma - \frac{\beta_\sigma^o}{2}V_\sigma + \frac{pL_{3\sigma}}{\sqrt{\lambda_{\min}(M_{p\sigma})}}\sqrt{V_\sigma}$$

$$\frac{dV_\sigma}{dt} \le -\frac{\beta_\sigma^o}{2}V_\sigma + \frac{0.5(pL_{3\sigma})^2}{\beta_\sigma^o \lambda_{\min}(M_{p\sigma})}$$

For

$$V_\sigma > \frac{(pL_{3\sigma})^2}{\lambda_{\min}(M_{p\sigma})} \Rightarrow \frac{dV_\sigma}{dt} \leq 0$$

Once the trajectories Z enter the UUB (uniformly ultimately bounded) region, they might not stay within it because of switching, even if the average dwell time condition

$$\tau_a > \frac{\ln l_\mu}{\beta^o}.$$

Further discussed in section 3.4.2, equation (3.31) to satisfy (3.3.1). Therefore, further investigation is required to ensure that the trajectories remain within a maximum bound. To analyze this, consider a time instant T_1 and V_σ enters an ultimate bound defined as B_u. Let N^o represent the number of switchings between any initial time t_o and $t_o + T_1$. By using $V(t_{i+1}) \leq l_\mu V(t_{i+1}^-)$, $N_\sigma(0, T) \leq \frac{T-t}{\tau_a} + N_o$ & $\tau_a > \frac{\ln l_\mu}{\beta^o}$ (Also further discussed in section 4.3) it can be derived that

$$V_\sigma(t) \leq \exp(N^o \ln l_\mu) V_\sigma(t_o) \tag{3.28}$$

From $V(t_{i+1}) \leq l_\mu V(t_{i+1}^-)$ it can be derived that $V_\sigma(t_{N^o+1}) \leq l_\mu B_u$, where t_{N^o+1} is the first switching time after T_1. This indicates that V_σ may exceed the bound B_u. Let's denote T_2 as the time just before another switching happens. For all $t \in [t_{N^o+1}, t_o + T_2]$,

$$V_\sigma(t) \leq \exp(N^o \ln l_\mu) V_\sigma(t_{N^o+1}) \leq \exp(N^o \ln l_\mu) l_\mu B_u$$

However, $V_\sigma(t) \leq B_u$ and the Lyapunov function cannot exceed $l_\mu B_u$ after the next switching instant. So, by applying a similar recursive approach, it can be concluded that the Lyapunov function cannot grow beyond $\exp(N^o \ln l_\mu) l_\mu B_u$. So

$$V_\sigma(t) \leq \max\{\exp(N^o \ln l_\mu) l_\mu B_u, \exp(N^o \ln l_\mu) V_\sigma(t_o)\}.$$

3.4.2 Lyapunov Function at Switching Instants

Starting with any time stamp $t_i, i \in N$, let the subsystem $\sigma(t_{i+1}^-)$ is active in the time interval $t \in [t_i, t_{i+1})$, and $\sigma(t_{i+1})$ is active when $t \in [t_{i+1}, t_{i+2})$. From

Chapter 3. Singular perturbation-based filtered backstepping controller for singularly perturbed switched systems

(3.26),(3.27), and the structure of the Lyapunov function V_σ, one can derive:

$$V(t_{i+1}) - V(t_{i+1}^-) \leq \frac{\overline{\alpha} - \underline{\alpha}}{\underline{\alpha}} V(t_{i+1}^-)$$

at the switching instant t_{i+1}. Therefore,

$$V(t_{i+1}) \leq l_\mu V(t_{i+1}^-). \tag{3.29}$$

where $l_\mu = \frac{\overline{\alpha}}{\underline{\alpha}} \geq 1$. Consider a time (0, T), where the time of switchings is defined as $t_1, ..., t_{N_\sigma(0,T)}$. For a function

$$R(t) = \exp(\beta_\sigma^o t) V_\sigma, \ \beta^o = \min(\beta_\sigma^o) \forall \sigma \in P$$

it's time derivative in $t \in (t_i, t_{i+1})$ is given by

$$\dot{R}(t) = \beta^o R(t) + \exp(\beta^o t) \dot{V}_\sigma$$

which is non-positive in between two consecutive switching times. Exploiting (3.29), it can be derived that

$$R(T^-) \leq (l_\mu)^{N_\sigma(0,T)} R(t)$$

An average dwell time $\tau_a > 0$ in the interval (0, T) exists if there exists a positive scalar N_o such that

$$N_\sigma(0, T) \leq \frac{T - t}{\tau_a} + N_o \tag{3.30}$$

Using (3.29), it can be obtained

$$\Rightarrow \exp(\beta^o t) V_{\sigma(T^-)} Z(T) \leq (l_\mu)^{N_\sigma(0,T)} \exp(\beta_\sigma^o \times 0) V_{\sigma(0)} Z(0).$$

$$\Rightarrow \exp(\beta^o t) V_{\sigma(T^-)} Z(T) \leq (l_\mu)^{N_\sigma(0,T)} V_{\sigma(0)} Z(0).$$

$$\Rightarrow V_{\sigma(T^-)} Z(T) \leq \exp(-\beta^o t) (l_\mu)^{N_\sigma(0,T)} V_{\sigma(0)} Z(0).$$

$$\Rightarrow V_{\sigma(T^-)} Z(T) \leq \exp(\ln l_\mu^{N_\sigma(0,T)}) \exp(-\beta_\sigma^o t) V_{\sigma(0)} Z(0).$$

$$\Rightarrow V_{\sigma(T^-)} Z(T) \leq \exp(\ln l_\mu (N_\sigma(0, T))) - \beta_\sigma^o t) V_{\sigma(0)} Z(0).$$

For the time T and by using (3.30) it can be obtained that

$$\Rightarrow V_{\sigma(T^-)}Z(T) \leq \exp(\ln l_\mu(\frac{T}{\tau_a} + N_o) - \beta_\sigma^o T)V_{\sigma(0)}Z(0).$$

$$\Rightarrow V_{\sigma(T^-)}Z(T) \leq \exp(N_o\ln l_\mu)\exp(\frac{T}{\tau_a}\ln(l_\mu) - \beta_\sigma^o T)V_{\sigma(0)}Z(0).$$

$$\Rightarrow V_{\sigma(T^-)}Z(T) \leq \exp(N_o\ln l_\mu)\exp(\frac{\ln(l_\mu)}{\tau_a}T - \beta_\sigma^o T)V_{\sigma(0)}Z(0).$$

$$\Rightarrow V_{\sigma(T^-)}Z(T) \leq \exp(N_o\ln l_\mu)\exp((-\beta^o + \frac{\ln l_\mu}{\tau_a})T)V_{\sigma(0)}Z(0)$$

Therefore, the function $V_{\sigma(T^-)}Z(T)$ asymptotically converges to zero if the average dwell time satisfies

$$\tau_a > \frac{\ln l_\mu}{\beta^o}. \tag{3.31}$$

3.5 Robust Filtered Backstepping With Disturbance Observer

This section proposes a new time scale redesign based on robust filtered backstepping controller design for the uncertain system (3.1) by estimating the unknown parts of the dynamics and then canceling them with feedback. The proposed observer in [80] for each $d_i(.)$ is given by:

$$
\begin{aligned}
\dot{\xi}_i &= -k(\xi_i + kx_i + f_{i\sigma}(x_1, x_2, \ldots, x_i) + b_{i\sigma}x_{i+1}) \\
\dot{\xi}_n &= -k(\xi_n + kx_n + f_{n\sigma}(x_1, x_2, \ldots, x_n) + b_{n\sigma}u) \\
\hat{d}_{i\sigma}(.) &= \xi_i + kx_i \\
\hat{d}_{n\sigma}(.) &= \xi_n + kx_n
\end{aligned}
\tag{3.32}
$$

where the scalar $k > 0$ is a large positive constant, $\hat{d}_{i\sigma}(.)$ is the estimate of $d_{i\sigma}(.)$, and ξ_i is an intermediate variable. Using the observer structure in (3.32), the dynamics of the disturbance estimator $(\hat{d}_i)$ can be written as:

$$\dot{\hat{d}}_i = \dot{\xi}_i + k\dot{x}_i = -k(\hat{d}_i - d_{i\sigma}) = h_{i\sigma}(\hat{d}_i, d_{i\sigma}). \tag{3.33}$$

Chapter 3. Singular perturbation-based filtered backstepping controller for singularly perturbed switched systems

Defining a disturbance error variable $\tilde{d}_i = d_{i\sigma}(.) - \hat{d}_{i\sigma}(.)$, the estimation error dynamics can be written as:

$$\epsilon \dot{\tilde{d}}_i(.) = -\tilde{d}_i - \epsilon \dot{d}_{i\sigma}(.). \tag{3.34}$$

where $0 \leq \epsilon = 1/k \leq 1$. The boundary layer dynamics resulting from (3.34) can be written as:

$$\frac{d}{d\tau}(\tilde{d}_i) = -\tilde{d}_i. \tag{3.35}$$

3.5.1 Conversion to Singularly Perturbed form

The disturbance observer-based filtered backstepping control law for the system (3.1) is selected as:

$$
\begin{aligned}
u_\sigma &= \frac{1}{b_{n\sigma}(x)}\big[-f_{n\sigma}(x) - b_{(n-1)\sigma}(x)z_{n-1} \\
&\quad - \chi_{n\sigma}(z_n) + \dot{\alpha}_{nf} - \hat{d}_{n\sigma}\big] \\
z_i &= x_i - \alpha_{if}, (i = 1, 2 \ldots\ldots n) \\
\alpha_{1f} &= \alpha_{1\sigma} = x_d(t) \ \text{ and for } i \in [2 \ldots n] \\
\alpha_{i\sigma} &= \frac{1}{b_{(i-1)\sigma}(x)}\big[-f_{(i-1)\sigma}(x_1, ..x_{i-1}) - \chi_{(i-1)\sigma}(z_{i-1}) \\
&\quad - b_{(i-2)\sigma}(x)z_{i-2} + \dot{\alpha}_{(i-1)f} - \hat{d}_{(i-1)\sigma}\big].
\end{aligned}
\tag{3.36}
$$

where the tuning functions are chosen similarly to the case with no disturbances in the system dynamics, i.e. $\chi_{i\sigma}(z_i) = k_{i\sigma}z_i$. The closed loop system of (3.1) with the control law (3.36) can be expressed as:

$$
\begin{aligned}
\dot{z}_1 &= -\chi_{1\sigma}(z_1) + b_{1\sigma}(x)z_2 + b_{1\sigma}(x)\tilde{\alpha}_{2\sigma} + \tilde{d}_1 \\
\dot{z}_i &= b_{(i-1)\sigma}(x)z_{i-1} - \chi_{i\sigma}(z_i) \\
&\quad + b_{i\sigma}(x)z_{i+1} + b_{i\sigma}(x)\tilde{\alpha}_{(i+1)\sigma}, +\tilde{d}_i \\
\dot{z}_n &= -b_{(n-1)\sigma}(x)z_{n-1} - \chi_{n\sigma}(z_n) + \tilde{d}_n.
\end{aligned}
\tag{3.37}
$$

Rewriting (3.37) in a compact form, we can get

3.5. Robust Filtered Backstepping With Disturbance Observer   49

$$\dot{z} = f_\sigma(z, \tilde{\alpha}_f, \tilde{d}) \tag{3.38}$$

$$\mu \dot{\tilde{\alpha}}_f = g_\sigma(\alpha_f, \alpha_\sigma) = -\tilde{\alpha}_f + \mu \dot{\alpha}_\sigma \tag{3.39}$$

$$\epsilon \dot{\tilde{d}} = h(\hat{d}, d_\sigma) = -\tilde{d} + \epsilon \dot{d}_\sigma \tag{3.40}$$

where $\hat{d} = [\hat{d}_1, \hat{d}_2, \ldots, \hat{d}_n]$, $\tilde{d} = [\tilde{d}_1, \tilde{d}_2, \ldots, \tilde{d}_n]$ $d_\sigma = [d_{1\sigma} d_{2\sigma}, \ldots, d_{n\sigma}]$. The dynamics are transformed into a three-time scale singularly perturbed switched system. However, it can be transformed into a two-time scale form, using the ratio $\frac{\epsilon}{\mu}$. Without any loss of generality let's assume that $\epsilon < \mu$, so that the observer dynamics is faster than the filter dynamics. We can select $\epsilon = \kappa\mu$ where κ is a small positive constant less than one. Express the fast subsystem (3.39), (3.40) as:

$$\mu \dot{\tilde{v}} = W_\sigma(\tilde{v}, \dot{v}_\sigma, \kappa) = - \begin{bmatrix} 1 & 0 \\ 0 & \frac{1}{\kappa} \end{bmatrix} \tilde{v} + \mu \dot{v}_\sigma \tag{3.41}$$

where $\tilde{v} = [\tilde{\alpha}_f^T, \tilde{d}^T]^T$, $\dot{v}_\sigma = [\dot{\alpha}_\sigma^T, \dot{d}_\sigma^T]^T$ and $W_\sigma(.) = [g_\sigma^T(.), \frac{1}{\kappa}h_\sigma^T(.)]^T$. Using (3.41), the closed-loop dynamics can be written in two-time scale singularly perturbed form, and hence, the convergence of the system trajectories can also be derived with similar arguments as mentioned in Section 3.4.

3.5.2 Closed Loop Stability

The closed loop system comprises of (3.38) and (3.41). When,

$$\mu \to 0 \Rightarrow \tilde{d} \to 0, \text{ and } \tilde{\alpha}_f \to 0$$

$$\Rightarrow \hat{d} \to d_\sigma(.) \text{ and } \alpha_f \to \alpha_\sigma.$$

Hence the slow manifold is obtained as: $v_\sigma = [\alpha_\sigma{}^T, d_\sigma{}^T]^T$. The reduced slow system can be obtained by replacing the slow manifold in (3.38), i.e:

$$\dot{z}_r = f_\sigma(z_r, 0, 0)$$

This dynamics is the same as (3.9), which is the reduced slow system in the absence of uncertainties. Hence, a set of quadratic Lyapunov functions can be

Chapter 3.   Singular perturbation-based filtered backstepping controller for singularly perturbed switched systems

chosen as (3.14), which satisfies (3.15).

The boundary layer dynamics for (3.41) is obtained as:

$$\frac{d\tilde{v}}{d\tau} = -\begin{bmatrix} 1 & 0 \\ 0 & \frac{1}{\kappa} \end{bmatrix}\tilde{v} \tag{3.42}$$

Consider a Lyapunov function $V_v = \frac{1}{2}v^T v$, for which

$$\dot{V}_{v\sigma} \leq -\begin{bmatrix} 1 & 0 \\ 0 & \frac{1}{\kappa} \end{bmatrix}||v||^2 \leq -||v||^2 \leq -2V_{v\sigma}. \tag{3.43}$$

Consider a scalar $(0 < p < 1)$ and set of composite Lyapunov functions

$$V_{m\sigma} = (1-p)V_{r\sigma} + pV_v \tag{3.44}$$

whose derivative along the overall system (3.38), (3.41) can be derived as

$$\dot{V}_{m\sigma} = (1-p)\frac{\partial V_r}{\partial z}(f_\sigma(z)) + \frac{p}{\mu}\frac{\partial V_v}{\partial \tilde{v}}\dot{\tilde{v}} + p\frac{\partial V_v}{\partial v_\sigma}\dot{v}_\sigma$$
$$+ (1-p)\frac{\partial V_{r\sigma}}{\partial z}\left(f_\sigma(z, \tilde{\alpha}_f, \tilde{d}) - f_\sigma(z)\right). \tag{3.45}$$

The first and second terms of (3.45) are negative definite. As the structure of $V_{r\sigma}$ is the same as (3.14), the last term in (3.45) can be upper bounded similarly as Lemma 3.1. By exploiting Lipschitz continuity property of $f(.)$, and Lemma 3.1, it can be derived that

$$\frac{\partial V_{r\sigma}}{\partial z}\left(f_\sigma(z, \tilde{\alpha}_f, \tilde{d}) - f_\sigma(z_\sigma)\right) \leq 2L_{4\sigma}||z||||v||. \tag{3.46}$$

where $L_{4\sigma} \in R^+$. Expanding the third term:

$$||\frac{\partial V_v}{\partial v_\sigma}\dot{v}_\sigma|| \leq ||\frac{\partial V_v}{\partial v}||(||\dot{\alpha}_\sigma|| + ||\dot{d}_\sigma||) \leq ||v||(||\dot{\alpha}_\sigma|| + ||\dot{d}_\sigma||) \tag{3.47}$$

Here, the disturbance terms considered satisfy the following premise.

Assumption 3.4: There exist $L_{5\sigma}, L_{6\sigma}, L_{7\sigma} \in R^+$ s.t

$$||\dot{d}_\sigma|| \leq L_{5\sigma}||z|| + L_{6\sigma}||\tilde{d}|| + L_{7\sigma} \tag{3.48}$$

3.5. Robust Filtered Backstepping With Disturbance Observer 51

for any σ.

Using assumption 3.3 and assumption 3.4, the third term of (3.45) can be upper bounded as:

$$||p\frac{\partial V_v}{\partial v_\sigma}\dot{v}_\sigma|| \leq L_{8\sigma}||\tilde{v}||||z|| + L_{9\sigma}||\tilde{v}||^2 + L_{7\sigma}||\tilde{v}||$$

for some positive constants $L_{8\sigma}, L_{9\sigma}$.

The equation (3.45) can be simplified to:

$$\dot{V}_{m\sigma} \leq -\beta_{s\sigma}(1-p)||z||^2 - \frac{p}{\mu}||v||^2 + 2pL_{8\sigma}||z||||v||$$
$$+ pL_{9\sigma}||v||^2 + 2(1-p)L_{4\sigma}||z||||v|| + pL_{7\sigma}||v||. \quad (3.49)$$

It can be written in a compact form as:

$$\dot{V}_{m\sigma} \leq -Y^T S_{m\sigma} Y + pL_{7\sigma}||Y|| \quad (3.50)$$

where $Y = [z^T, \tilde{v}^T]^T$ and

$$S_{m\sigma} = \begin{bmatrix} (1-p)\beta_{s\sigma} & -(1-p)L_{4\sigma} - pL_{8\sigma} \\ -(1-p)L_{4\sigma} - pL_{8\sigma} & p(\frac{1}{\mu} - L_{8\sigma}) \end{bmatrix} \quad (3.51)$$

The overall system can be stable only when $S_{m\sigma}$ is positive definite. By using some basic matrix algebra, it can be derived that $S_{m\sigma}$ is positive definite if

$$\mu_\sigma \leq \mu_\sigma^* = \frac{\beta_{s\sigma}}{\beta_{s\sigma}L_{9\sigma} + \frac{1}{p(1-p)}((1-p)L_{4\sigma} + pL_{8\sigma})^2} \quad (3.52)$$

If $\mu_\sigma \leq \mu_\sigma^*$,

$$\dot{V}_{m\sigma} \leq -\beta_{m\sigma}V_{m\sigma} + pL_{7\sigma}||Y||$$

where $\beta_{m\sigma} = \frac{\lambda_{\min}(S_{m\sigma})}{\lambda_{\max}(S_{m\sigma})}$. Let

$$M_{t\sigma} = \begin{bmatrix} (1-p)M_{r\sigma} & 0 \\ 0 & pM_{v\sigma} \end{bmatrix}$$

then

$$\lambda_{\min}(M_{t\sigma})||Y||^2 \leq V_{m\sigma} \leq \lambda_{\max}(M_{t\sigma})||Y||^2.$$

Therefore,

$$\frac{dV_{m\sigma}}{dt} \leq -\frac{\beta_{m\sigma}}{2}V_{m\sigma} - \frac{\beta_{m\sigma}}{2}V_{m\sigma} + \frac{pL_{9\sigma}}{\sqrt{\lambda_{\min}(M_{t\sigma})}}\sqrt{V}_{m\sigma}$$

$$\frac{dV_{m\sigma}}{dt} \leq -\frac{\beta_{m\sigma}}{2}V_{m\sigma} + \frac{0.5(pL_{9\sigma})^2}{\beta_{m\sigma}\lambda_{\min}(M_{t\sigma})}$$

For

$$V_{m\sigma} > \frac{(pL_{9\sigma})^2}{\lambda_{\min}(M_{t\sigma})} \Rightarrow \frac{dV_{m\sigma}}{dt} \leq 0$$

Once the trajectories Y enters the UUB bound, they may not remain inside it due to switching even if the average dwell time condition derived in (3.31) holds. Therefore, further investigations are necessary to assure the trajectories to remain inside a maximum bound. To analyze more, assume a time instant T_1, when $V_{m\sigma}$ enters an ultimate bound defined as B_u. Define the number of switchings between any initial time t_o to $t_o + T_1$ as N^o. From (3.29), (3.30) and (3.31), it can be derived that

$$V_{m\sigma}(t) \leq \exp(N_o \ln l_\mu) V_{m\sigma}(t_o) \tag{3.53}$$

From (3.29), it can be derived that $V_{m\sigma}(t_{N^o+1}) \leq l_\mu B_u$, where t_{N^o+1} is the immediate switching time after T_1. So, it seems $V_{m\sigma}$ may breach the bound B_u. Let's denote T_2 as the time just before another switching happens. For all $t \in [t_{N^o+1}, t_o + T_2]$,

$$V_{m\sigma}(t) \leq \exp(N_o \ln l_\mu) V_{m\sigma}(t_{N^o+1}) \leq \exp(N_o \ln l_\mu) l_\mu B_u$$

However, $V_{m\sigma}(t) \leq B_u$, and the Lyapunov function can not be greater than $l_\mu B_u$ after next switching instant. A similar recursive approach can be followed to conclude that, the Lyapunov function can not grow beyond $\exp(N_o \ln l_\mu) l_\mu B_u$. So

$$V_{m\sigma}(t) \leq \max\{\exp(N_o \ln l_\mu) l_\mu B_u, \exp(N_o \ln l_\mu) V_{m\sigma}(t_o)\}.$$

The results of this research can be effectively summarized and formalized in the form of a theorem.

Theorem 3.1: Consider a singularly perturbed switched system described by Equation (3.1). Let the assumptions 3.1-3.4 hold true. Then under a switched control law (3.36), the states of the closed-loop dynamics will asymptotically converge to the bound (3.52) provided the average dwell time satisfies the inequality (3.31).

3.6   Implementation of FB controller on single link manipulator system with actuator dynamics

Here, an example of a single link manipulator system with actuator dynamics has been considered [95, 96]. The system dynamics is given by

$$
\begin{aligned}
D\ddot{q} + B\dot{q} + N\sin(q) &= \tau \\
M\dot{\tau} + H\tau + K_m\dot{q} &= u
\end{aligned}
\tag{3.54}
$$

The value of model parameters D, B, N, M, H, and K_m depend on the robot's and actuator's physical parameters. The scalars q and $\dot{q}$ represent the angular component of the position and velocity of the joint respectively. τ is the torque supplied at the joint using the motor. u represents the voltage supplied control input to the motor for generating the torque. The above equations can be represented in the following form by choosing,

$$
\begin{aligned}
x_1 &= q \\
x_2 &= \dot{q} \\
x_3 &= \tau
\end{aligned}
\tag{3.55}
$$

Equation (3.54) can be written as

$$
\begin{aligned}
\dot{x}_1 &= x_2 \\
\dot{x}_2 &= \frac{1}{D}(-N\sin(x_1) - Bx_2) + \frac{1}{D}x_3 \\
\dot{x}_3 &= -\frac{1}{M}(K_m x_2 + Hx_3) + \frac{1}{M}u
\end{aligned}
\tag{3.56}
$$

The controller aims to force the output q to converge to desired trajectories $x_d(t)$ with all other signals remaining bounded. The tracking error $e = q - x_d$ and select z_i as $z_i = x_i - \alpha_{if}$ where $i = 1, 2, 3...n$ and $\alpha_{1f} = \alpha_1 = x_d(t)$.

Here, the control input u_σ has been designed for the switching signals $\sigma = 1, 2, 3$. The values of system parameters i.e D,B,N,M,H and k$_m$ for switching signal $\sigma = 1, 2, 3$ are given in Table 3.1.

TABLE 3.1: The parameters of the system for three-time switching.

System Parameters	D	B	N	M	H	km
For $\sigma = 1$	1	1	10	0.01	0.5	100
For $\sigma = 2$	10	150	10	0.01	0.5	10
For $\sigma = 3$	10	1	10	0.01	0.5	100

TABLE 3.2: The parameters of the system for four-time switching.

System Parameters	D	B	N	M	H	km
For $\sigma = 1$	1	1	10	0.01	0.5	100
For $\sigma = 2$	10	150	10	0.01	0.5	10
For $\sigma = 3$	10	150	1	0.01	0.5	10
For $\sigma = 4$	10	1	10	0.01	0.5	100

Here, $\chi_{i\sigma}(z_i) = k_{i\sigma}z_i$ (select the suitable value of gain, $k_{i\sigma}$) and perturbed parameter $\mu = 0.001$ are given. Disturbances are $d1 = 0.1\tanh(2t)$ and $d2 = 0.1\tanh(2t)$ for $\sigma = 1$ and $d1 = 0.1\sin(2t)$, $d2 = 0.1\cos(2t)$ for $\sigma = 2, 3$. The average dwell time (τ_a) has been calculated in the interval 0 to 1.5 sec. ($\tau_a = \frac{\text{Time interval}}{\text{No. of switching}}$). For the switching signal $\sigma = 1$ at $t < 0.20$ sec, τ_a can be calculated as $\tau_a = \frac{1.5}{1} = 1.5$ sec which satisfies the equation $\tau_a > \frac{\ln l_\mu}{\beta^o}$, where $\frac{\ln l_\mu}{\beta^o} = 0.60$ sec. For switching $\sigma = 1$ at $t < 0.20$ sec and for $\sigma = 2$ in the interval 0.2 to 0.55 sec, average dwell time is $\tau_a = \frac{1.5}{2} = 0.75$ sec which also satisfies the condition $\tau_a > \frac{\ln l_\mu}{\beta^o}$. So, the state x_1 tracks the desired signal $\sin(5t)$, $\sin(10t)$ and $\pi\sin(-5t)$, which have been shown in Figure 3.1, Figure 3.5 and Figure 3.9,

3.6. Implementation of FB controller on single link manipulator system with actuator dynamics

55

respectively and the tracking error for state x_1 ($\sigma = 1, 2$) with reference signals $sin(5t)$, $sin(10t)$, $\pi sin(-5t)$ is shown in Figure 3.3, Figure 3.6 and Figure 3.10 respectively. For switching signal $\sigma = 1$ at $t < 0.20$ sec, for $\sigma = 2$ in interval 0.20 to 0.55 sec and for $\sigma = 3$ at $t > 0.55$ sec, τ_a can be calculated as $\tau_a = \frac{1.5}{3} = 0.50$ which do not satisfies the inequality $\tau_a > \frac{\ln l_\mu}{\beta^o}$ and that is why, the state x_1 is not able to track the reference signal $sin(5t)$, $sin(10t)$ and $\pi sin(-5t)$ which have been shown in Figure.3.4, Figure 3.8, and Figure 3.12, respectively.

Another example with four time switching for the same reference $sin(5t)$, $sin(10t)$, $\pi sin(-5t)$ signals has been shown in Figures 3.13 to 3.21. Based on the different values of $k_{i\sigma}$ and system parameters the value of $\frac{\ln l_\mu}{\beta^o} = 0.48$ sec can be obtained. The system parameters for $\sigma = 1, 2, 3, 4$ can be given in Table 3.2. Here, disturbances are $d1 = 0.1 \tanh(2t)$ and $d2 = 0.1 \tanh(2t)$ for $\sigma = 1$ and $d1 = 0.1 \sin(2t)$, $d2 = 0.1 \cos(2t)$ for $\sigma = 2, 3, 4$. Average dwell time for $\sigma = 1, 2$ at $t < 0.20$ sec and in interval 0.20 to 0.50 sec respectively, $\tau_a = \frac{1.5}{2} = 0.75$ s which satisfy $\tau_a > \frac{\ln l_\mu}{\beta^o}$, here $\frac{\ln l_\mu}{\beta^o} = 0.48$ sec. So the state x_1 tracks the reference signals as shown in Figure.3.13, Figure.3.16 and Figure.3.19. For $\sigma = 1, 2, 3$ at $t < 0.20$ sec and in intervals 0.20 to 0.55 sec and 0.50 to 1 sec respectively, average dwell time $\tau_a = \frac{1.5}{3} = 0.50$ sec which satisfy $\tau_a > \frac{\ln l_\mu}{\beta^o}$ so the state x_1 is still able to track the reference signals which have been shown in Figure.3.14, Figure.3.17 and Figure.3.20. Average dwell time for $\sigma = 1, 2, 3, 4$ at $t < 0.20$ sec and in the intervals 0.20 to 0.50 sec, 0.50 to 1 sec and at $t > 1$ sec respectively, $\tau_a = \frac{1.5}{4} = 0.37$ sec which do not satisfy $\tau_a > \frac{\ln l_\mu}{\beta^o}$ that is why state x_1 is not able to track the reference signals which have been shown in Figure.3.15, Figure.3.18 and Figure.3.21. The same control law without switching given in reference [80] is:

$$u = \frac{1}{b_n(x)}[-f_n(x) - b_{(n-1)}(x)z_{n-1} - \chi_n(z_n) + \dot{\alpha}_{nf}]$$
$$z_i = x_i - \alpha_{if}, (i = 1, 2......n) \tag{3.57}$$
$$\alpha_{1f} = \alpha_1 = x_d(t)$$

where $\chi_i(z_i) = k_i z_i$ are user-defined tuning functions for which $k_i > 0$. The terms α_{if} are obtained through the first order filter [75, 76]. By using this controller mentioned in (3.57) the performance of state x_1 during switching signal σ for

Chapter 3. Singular perturbation-based filtered backstepping controller for singularly perturbed switched systems

reference signals $\sin(5t)$, $\sin(10t)$, and $\pi \sin(-5t)$ have been shown in Figure 3.3, Figure 3.7, and Figure 3.11 respectively, and it can be observed that, the system tries to follow the reference signal with the switching signal $\sigma = 1, 2$. However, the state x_1 cannot follow the reference signal x_d properly because of changes in the system's parameters. So, to fix this issue, a filtered backstepping controller has been used.

3.6.1   Controller performance for three-time switching:

Initially, the manipulator starts moving when the switching signal is set to $\sigma = 1$. It then modifies its parameters as the switching signal changes to $\sigma = 2$ and continues its movement. When the switching signal shifts to $\sigma = 3$, the parameters are adjusted once more. However, after the switching signal reaches $\sigma = 3$, the manipulator does not meet the average dwell time criteria, leading to an inability to track the reference signal. Consequently, a divergence behavior is seen with each switching event. To check the performance of the proposed controller a comparison between standard backstepping and filtered backstepping technique for switching $\sigma = 1, 2$ have been shown in Figure 3.1 and Figure 3.3, Figure 3.5 and Figure 3.7, Figure 3.9 and Figure 3.11. In this chapter, a single-link manipulator has been taken as an example. The system parameters are given in Table 3.1. For three-time switching, this manipulator starts with compressed mode ($\sigma = 1$) at $t < 0.20$ sec and it changes its shape to $\sigma = 2$ during the interval 0.20 to 0.55 sec and again it changes its shape to $\sigma = 1$ at $t = 0.55$ sec. So, for this switching, i.e. $\sigma = 1, 2$ the condition of average dwell time is satisfied that is why the system can track the references as shown in Figure 3.1, Figure 3.5, and Figure 3.9. Again, the manipulator changes its configuration to $\sigma = 3$ at $t > 0.55$ sec. By this time, the average dwell time condition is not satisfied so the manipulator is not able to follow the references. The scenario of this phenomenon has been shown in Figure 3.4, Figure 3.8, and Figure 3.12.

3.6.2   Controller performance for four time switching:

For the four-time switching, this manipulator also starts with compressed mode ($\sigma = 1$) at $t < 0.20$ sec and changes its shape to $\sigma = 2$ during the interval 0.20 to

3.6. Implementation of FB controller on single link manipulator system with actuator dynamics

57

0.50 sec and again it changes its shape to $\sigma = 1$ at t=0.5 sec. Again, the manipulator again changes its configuration to $\sigma = 3$ during the interval 0.50 to 1 sec. So for this switching signals i.e $\sigma = 1, 2, 3$ the condition of average dwell time is satisfied that is why the manipulator is still able to track the references. This scenario has been shown in the Figure.3.14, Figure 3.17, and Figure 3.20. Again, the system changes its shape to $\sigma = 4$ at $t > 1$ sec and by this time the condition of average dwell time is not satisfied that is why, the manipulator is not able to track the references as shown in Figure 3.15, Figure 3.18, and Figure 3.21.

FIGURE 3.1: Closed loop response for x_1 with disturbances and reference $sin(5t)$ for $\sigma = 1, 2$
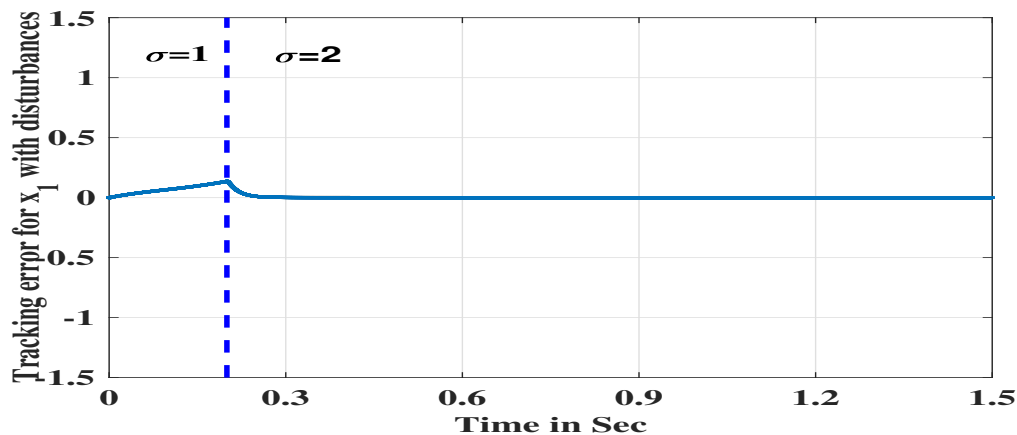
FIGURE 3.2: Tracking error for state x_1 ($\sigma = 1, 2$) for reference signal $sin(5t)$.

Chapter 3.   Singular perturbation-based filtered backstepping controller for singularly perturbed switched systems

Closed loop response for x1 at t<0.20 sec and in interval (0.20,0.55) sec for σ=1 and σ=2 respectively

FIGURE 3.3:   Tracking with a standard backstepping controller without switching for reference $sin(5t)$.

Closed loop response for x1 at t<0.20 sec and in interval (0.20,0.55) sec for σ=1 and σ=2 respectively and at t>0.55 sec for σ=3

FIGURE 3.4:   Closed loop response for Average dwell time not satisfying $\tau_a > \frac{ln l_\mu}{\beta^o}$ and doesn't track the reference signal $sin(5t)$

3.6. Implementation of FB controller on single link manipulator system with actuator dynamics

FIGURE 3.5: Closed loop response for x_1 with disturbances and reference $sin(10t)$ for $\sigma = 1, 2$

FIGURE 3.6: Tracking error for state x_1 ($\sigma = 1, 2$) for reference signal $sin(10t)$.

Chapter 3.   Singular perturbation-based filtered backstepping controller for singularly perturbed switched systems
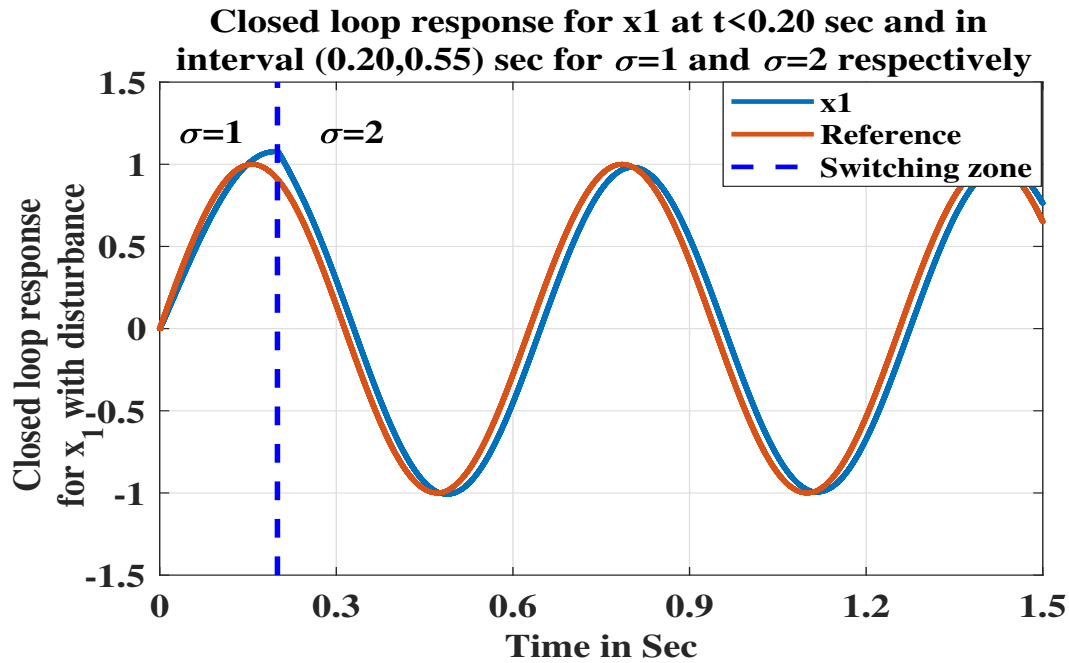
FIGURE 3.7:   Tracking with a standard backstepping controller without switching for reference $sin(10t)$.

FIGURE 3.8:   Closed loop response for Average dwell time not satisfying $\tau_a > \frac{lnl_\mu}{\beta^o}$ and doesn't track the reference signal $sin(10t)$

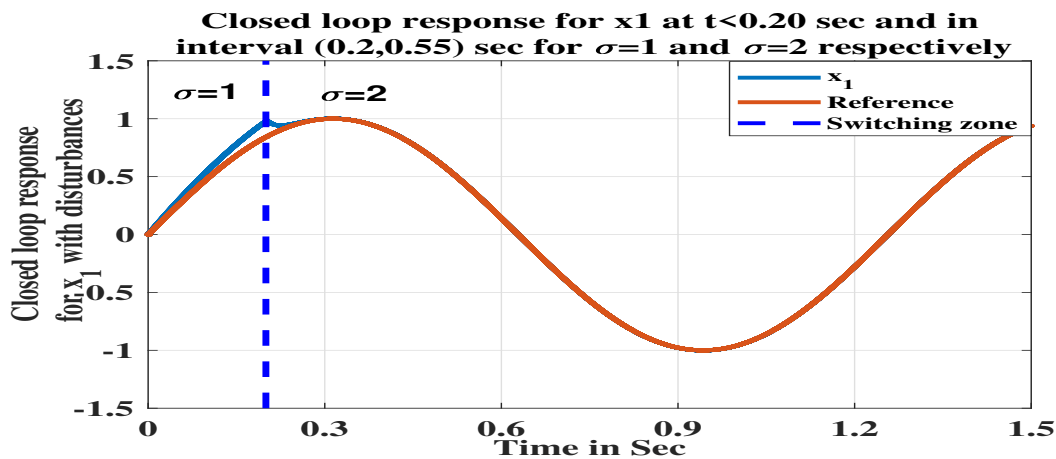### 3.6. Implementation of FB controller on single link manipulator system with actuator dynamics
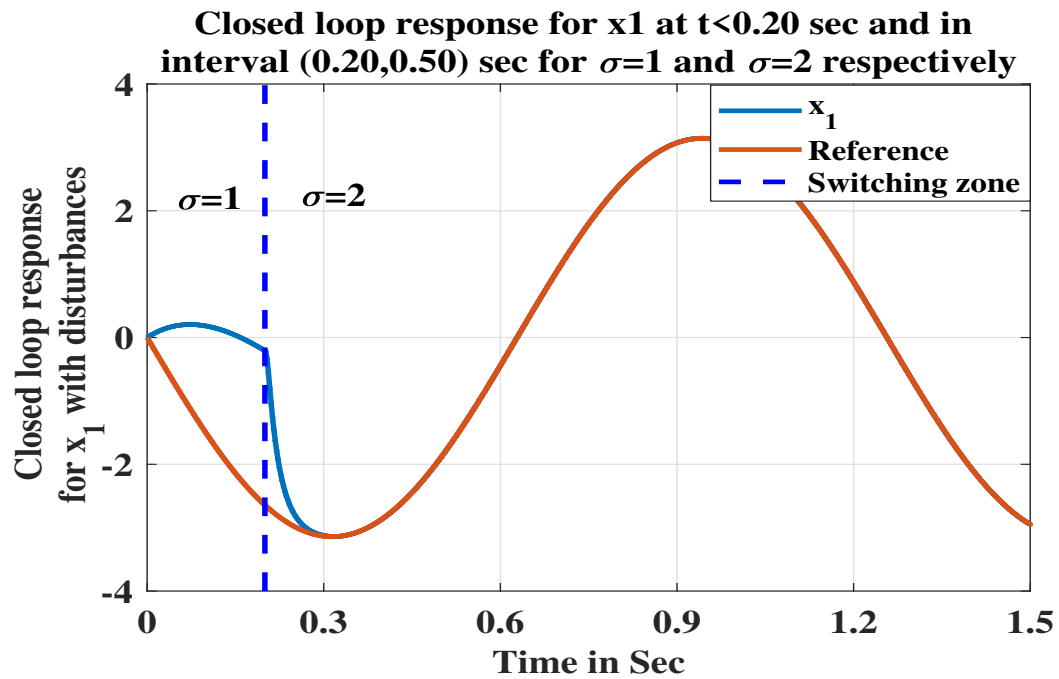
FIGURE 3.9: Closed loop response for x_1 with disturbances and reference $\pi sin(-5t)$ for $\sigma = 1, 2$

FIGURE 3.10: Tracking error for state x_1 ($\sigma = 1, 2$) for reference signal $\pi sin(-5t)$.

Chapter 3. Singular perturbation-based filtered backstepping controller for singularly perturbed switched systems
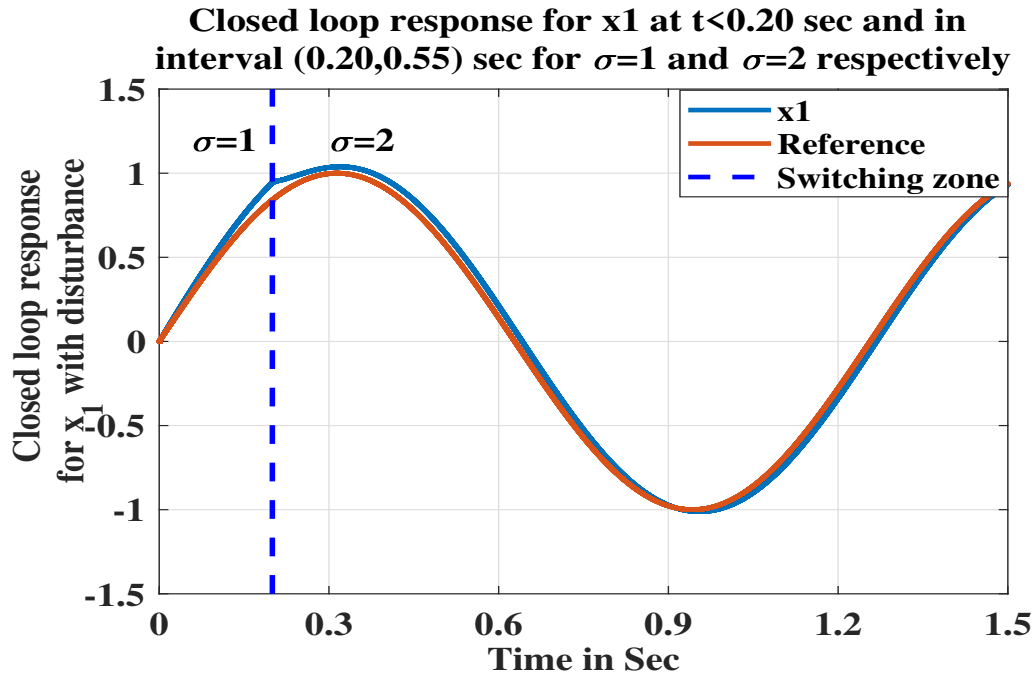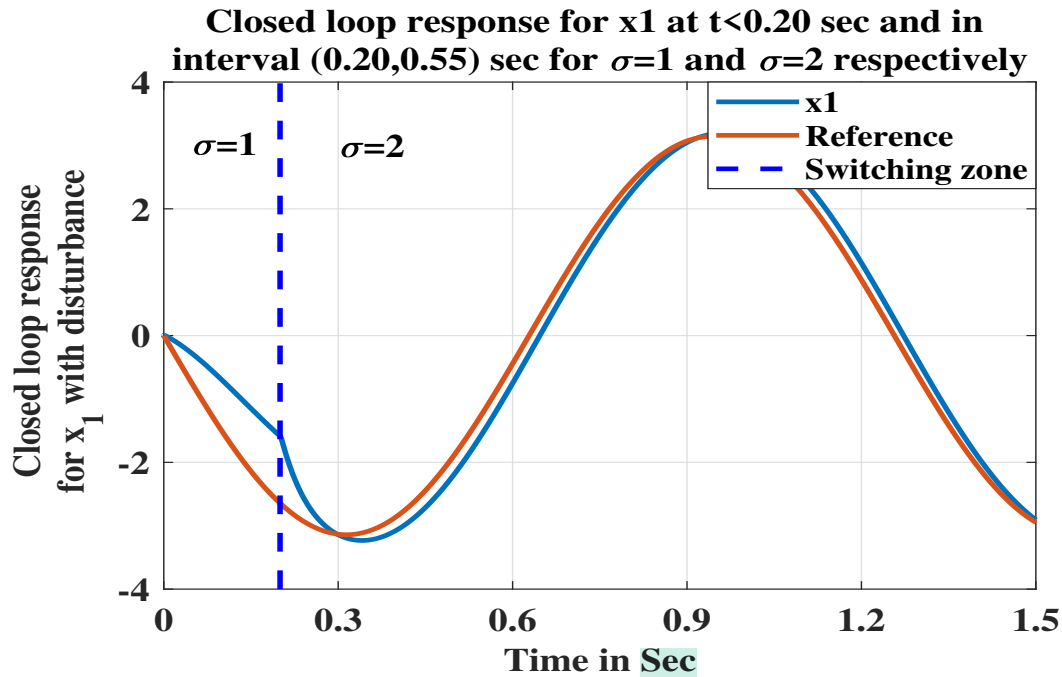

FIGURE 3.11:   Tracking with a standard backstepping controller without switching for reference $\pi sin(-5t)$.

FIGURE 3.12:   Closed loop response for Average dwell time not satisfying $\tau_a > \frac{lnl_\mu}{\beta^o}$ and doesn't track the reference signal $\pi sin(-5t)$

3.6. Implementation of FB controller on single link manipulator system with actuator dynamics

63

FIGURE 3.13: Closed loop response for x_1 with disturbances and reference $sin(5t)$ for $\sigma = 1, 2$

FIGURE 3.14: Closed loop response for x_1 with disturbances and reference $sin(5t)$ for $\sigma = 1, 2, 3$

Chapter 3.   Singular perturbation-based filtered backstepping controller for singularly perturbed switched systems

Closed loop response for x1 at t<0.20 sec for σ=1 and in the interval (0.2,0.5),(0.5,1) & at t>1 sec for σ=2,σ=3 & σ=4 respectively
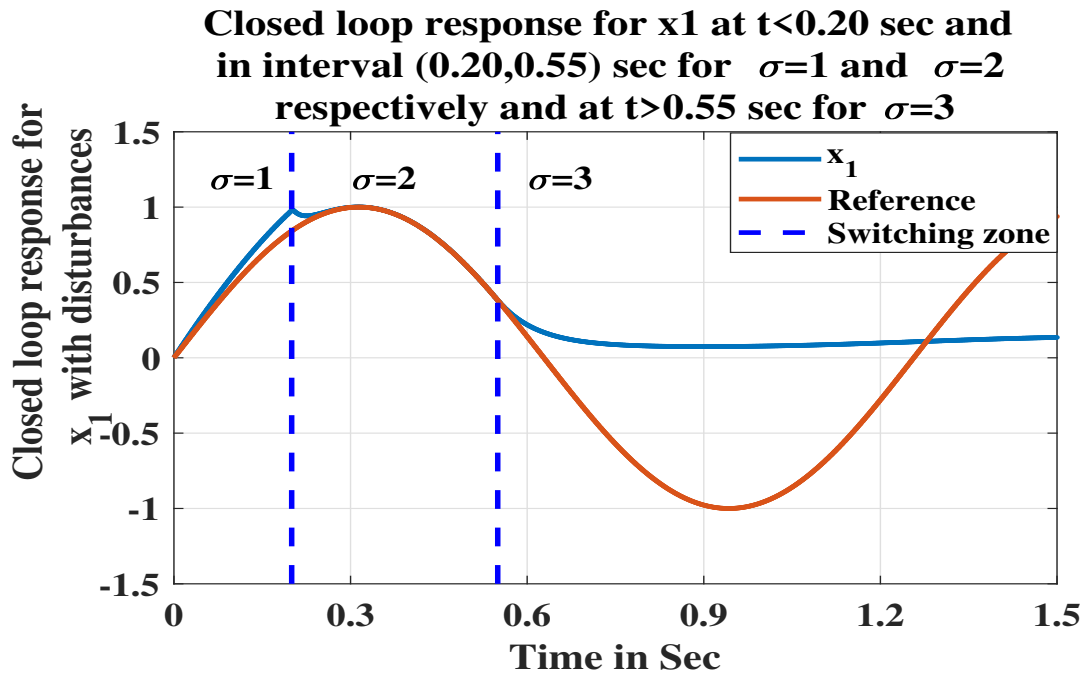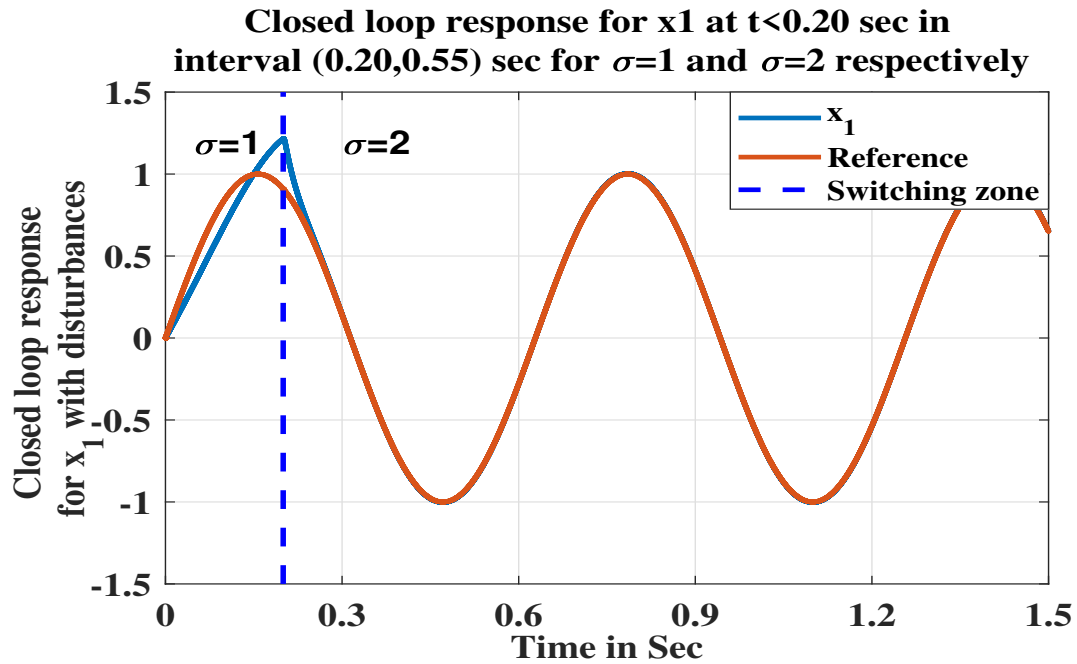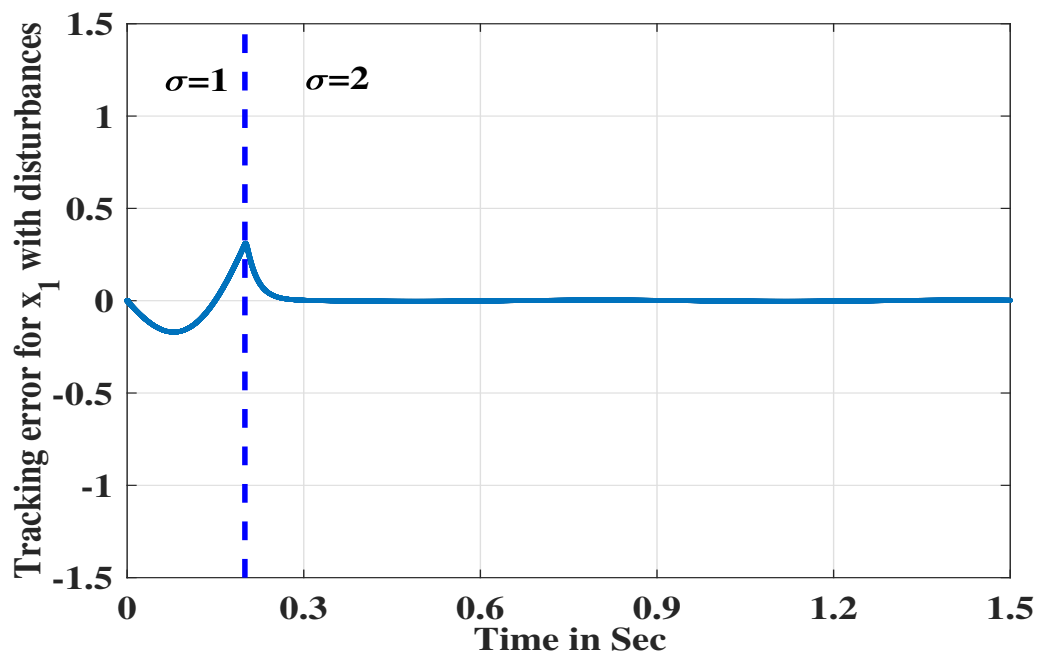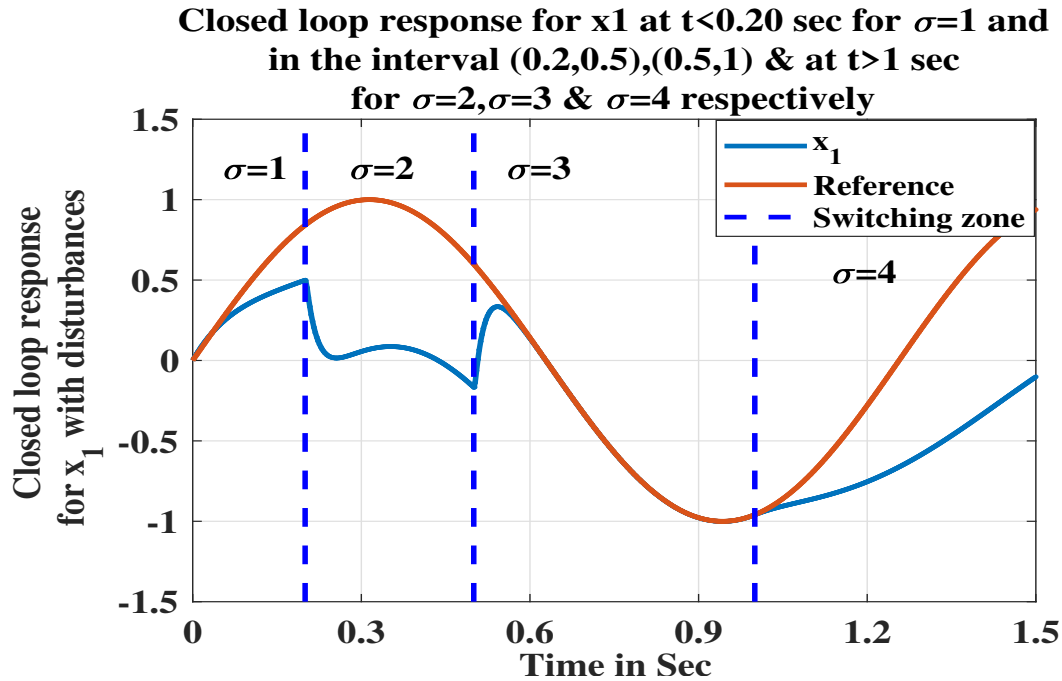

FIGURE 3.15: Closed loop response for Average dwell time not satisfying $\tau_a > \frac{lnl_\mu}{\beta^o}$ and doesn't track the reference signal $sin(5t)$.

Closed loop response for x1 at t<0.20 sec and in interval (0.20,0.50) sec for σ=1 and σ=2 respectively
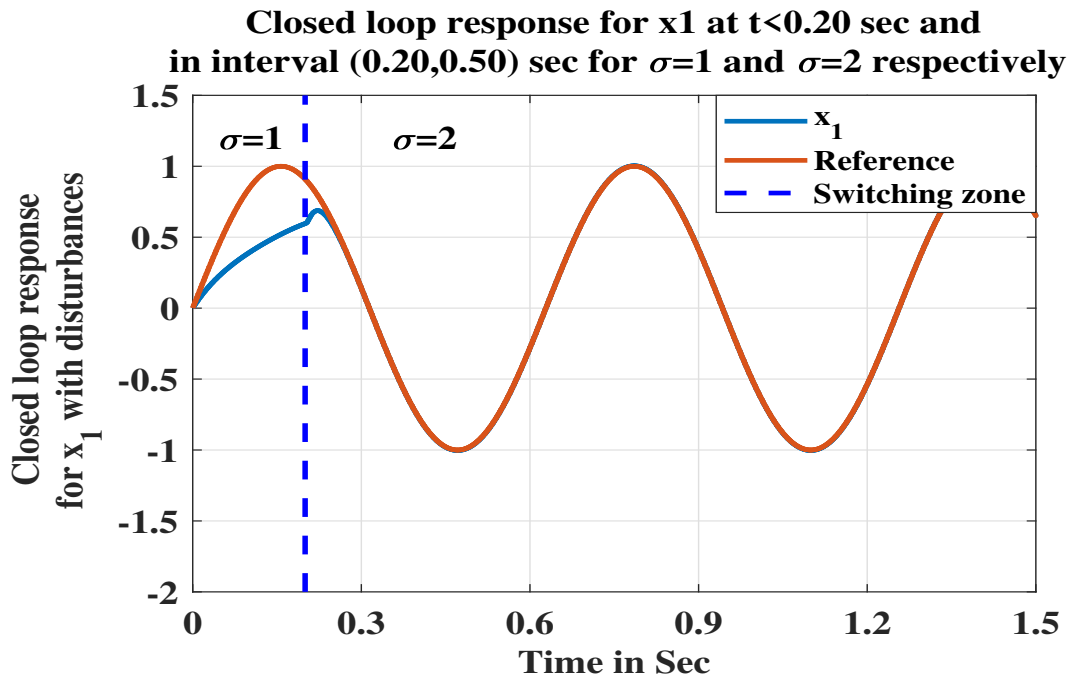
FIGURE 3.16: Closed loop response for x_1 with disturbances and reference $sin(10t)$ for $\sigma = 1, 2$

3.6. Implementation of FB controller on single link manipulator system with actuator dynamics

Closed loop response for x1 at t<0.20 sec and in interval (0.20,0.50) and (0.50,1) sec for σ=1 , σ=2 and σ=3 respectively
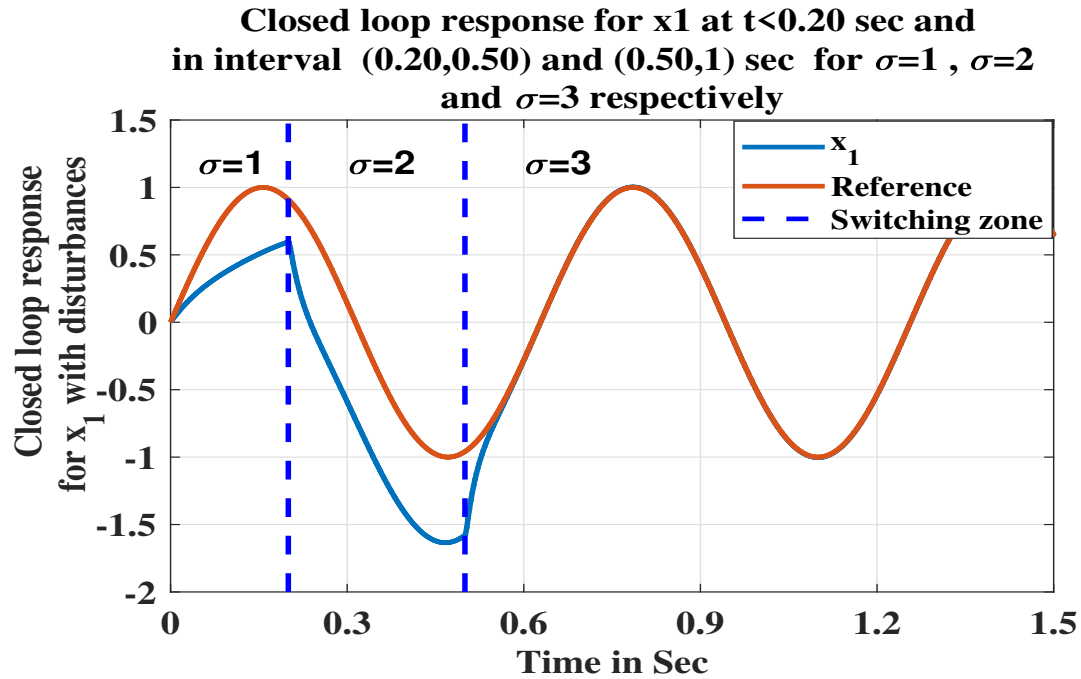
FIGURE 3.17: Closed loop response for x_1 with disturbances and reference $sin(10t)$ for $\sigma = 1, 2, 3$

Closed loop response for x1 at t<0.20 sec for σ=1 and in the interval (0.2,0.5),(0.5,1) & at t>1 sec for σ=2,σ=3 & σ=4 respectively
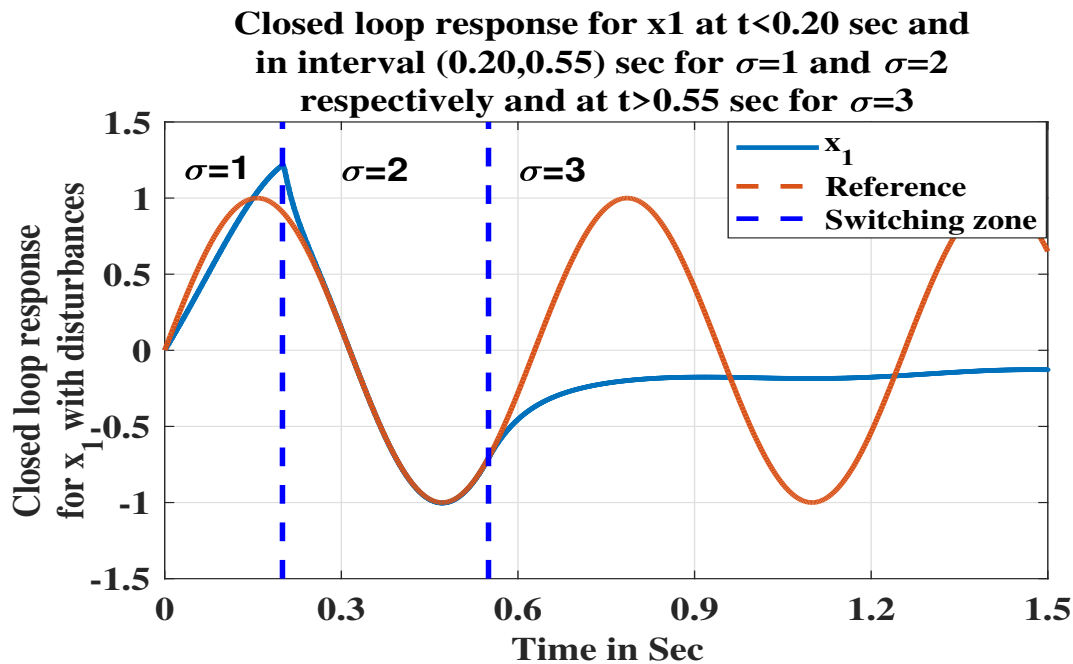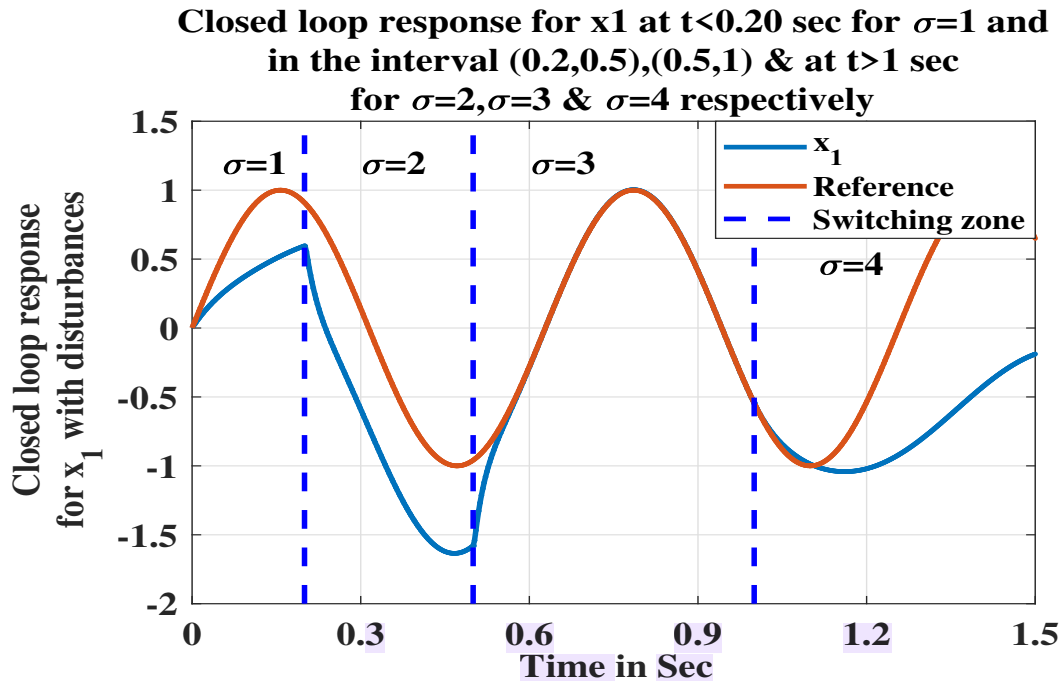

FIGURE 3.18: Closed loop response for Average dwell time not satisfying $\tau_a > \frac{lnl_\mu}{\beta^o}$ and doesn't track the reference signal $sin(10t)$.

*Chapter 3.   Singular perturbation-based filtered backstepping controller for singularly perturbed switched systems*
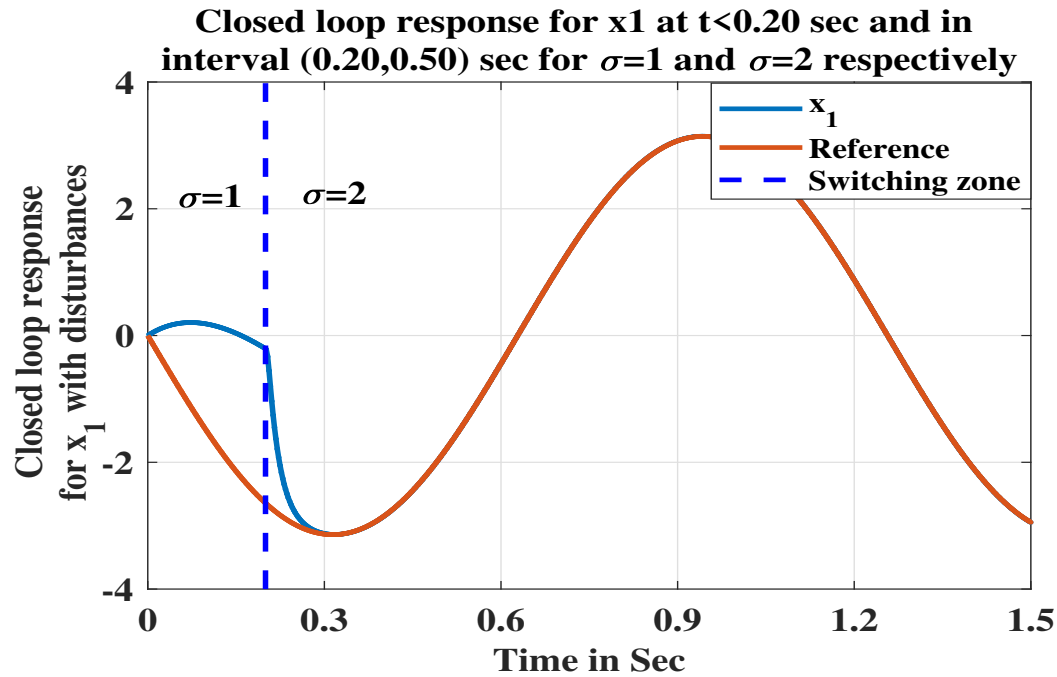
FIGURE 3.19: Closed loop response for x_1 with disturbances and reference $\pi sin(-5t)$ for $\sigma = 1,2$
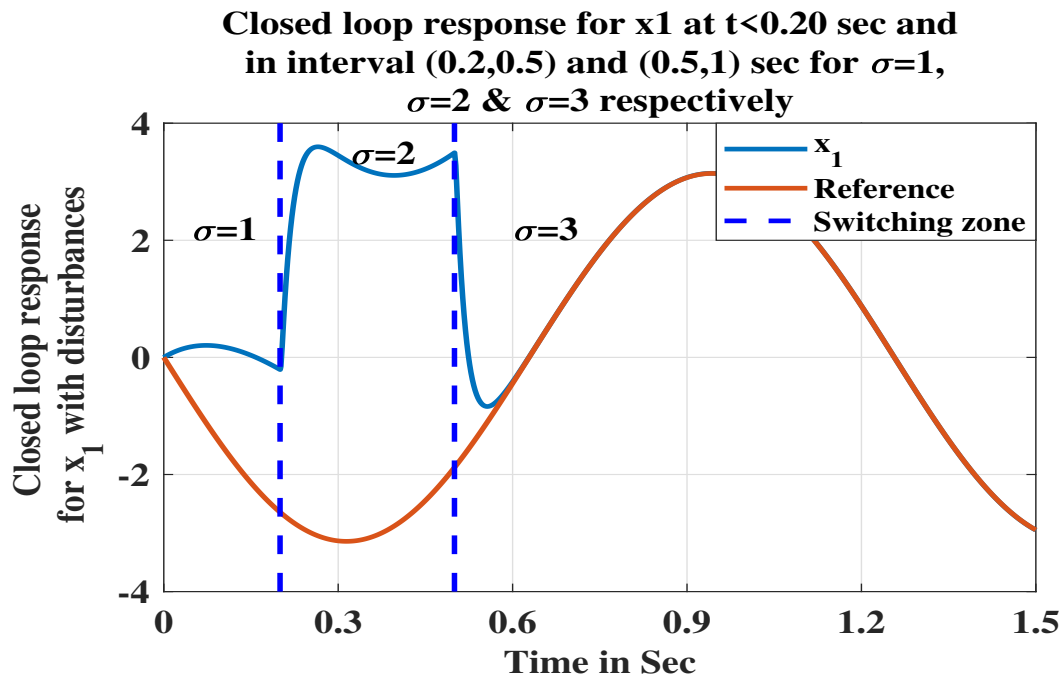
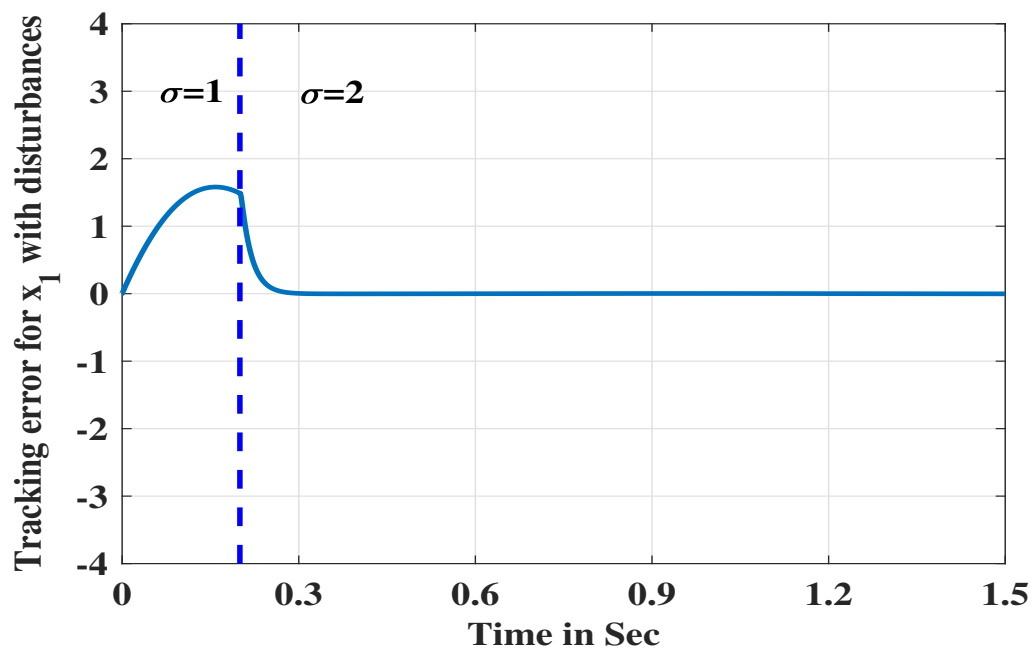FIGURE 3.20: Closed loop response for x_1 with disturbances and reference $\pi sin(-5t)$ for $\sigma = 1,2,3$

**Closed loop response for x1 at t<0.20 sec for σ=1 and
in the interval (0.2,0.5),(0.5,1) & at t>1 sec
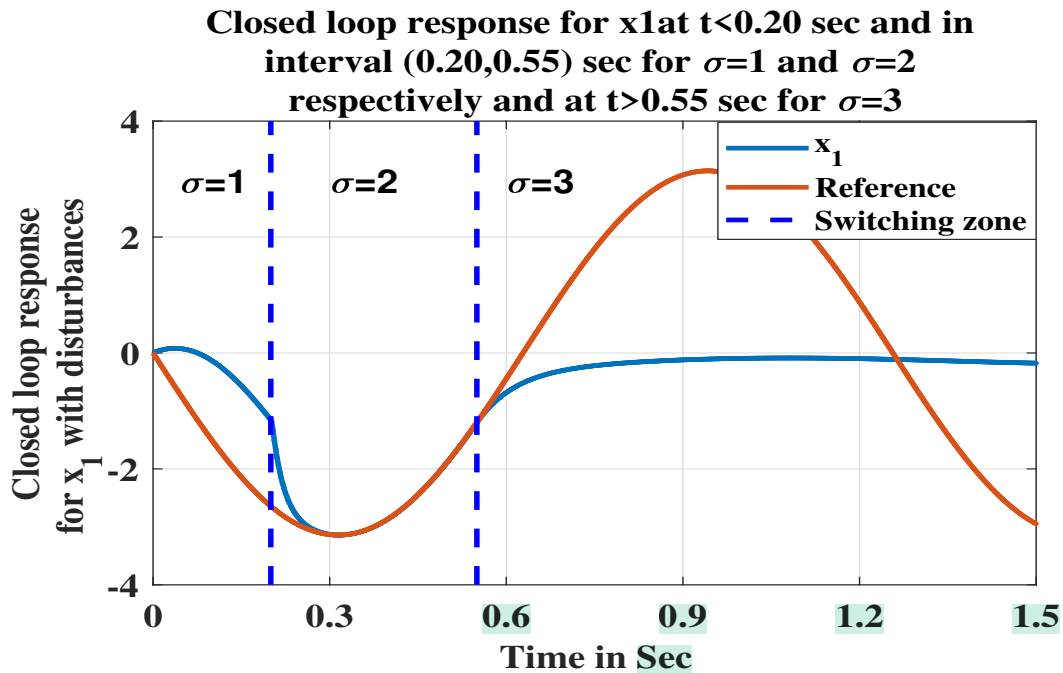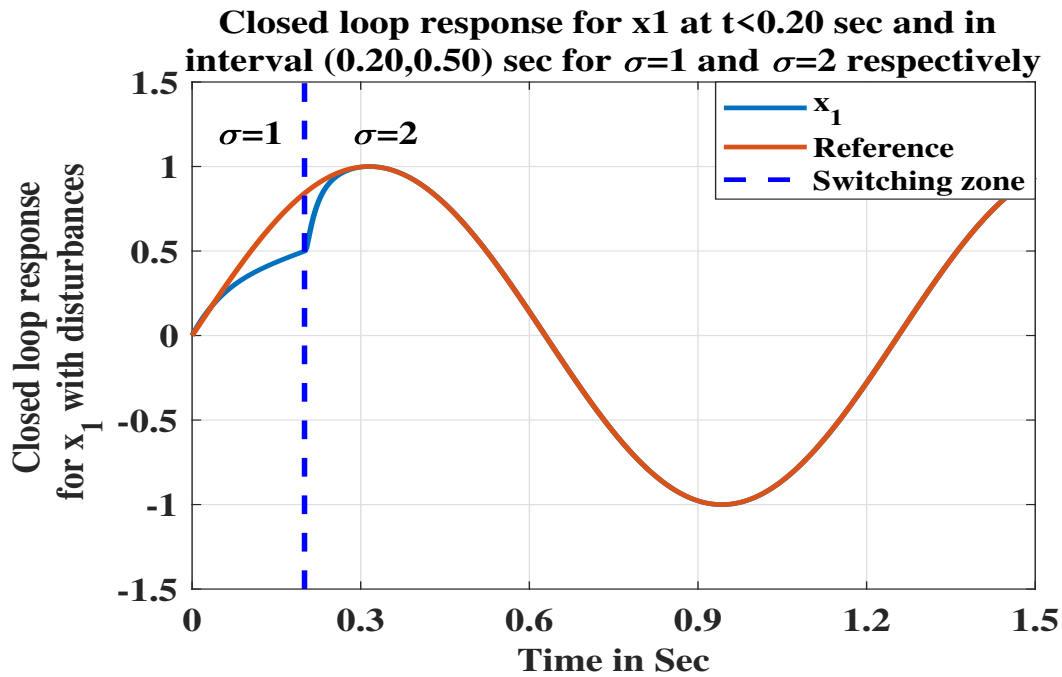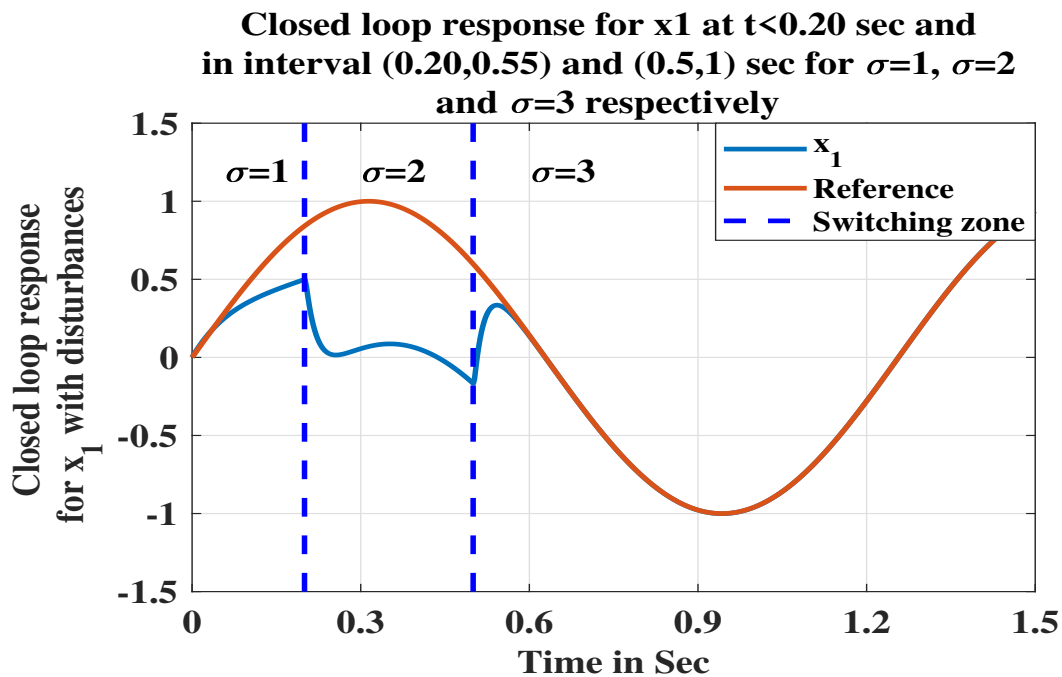for σ=2,σ=3 & σ=4 respectively**
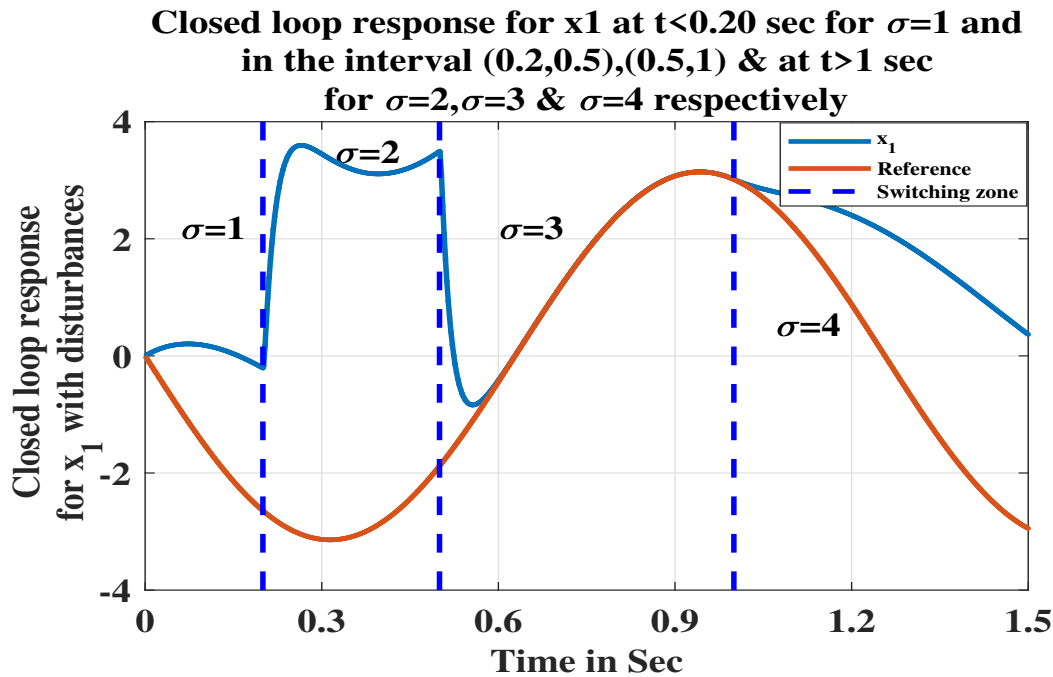
FIGURE 3.21: Closed loop response for Average dwell time not satisfying $\tau_a > \frac{ln l_\mu}{\beta^o}$ and doesn't track the reference signal $\pi sin(-5t)$.

3.7   Concluding remarks

This chapter demonstrates the efficient tracking and stabilization of nonlinear singularly perturbed switched systems by implementing the proposed filtered backstepping control approach utilizing an average dwell time-based Lyapunov criterion. The use of the high-gain filter in conjunction with the disturbance observer successfully tackles the complexities of the system and reduces the uncertainties through the implementation of this proposed singular perturbation technique. The simulation results are validated on a single-link manipulator system with actuator dynamics. This proposed controller exhibits robustness against the dynamics of the switched system, achieves effective trajectory tracking, and ensures stability. The outcomes demonstrate the controller's applicability in real-world higher-order systems with switching dynamics and inherent nonlinearities. Also, the performance of the filtered backstepping technique is better than the standard backstepping technique while switching between different modes in a short period. This implies that the manipulator's

Chapter 3. Singular perturbation-based filtered backstepping controller for singularly perturbed switched systems

movements may grow highly complicated, emphasizing the need to adopt the appropriate control to handle these changes efficiently. To improve control system design and execution, this approach provides helpful guidance for implementing control techniques in other complex systems.

69

Chapter 4

Filtered backstepping controller for singularly perturbed switched systems based on contraction analysis

This chapter was accepted by the Indian Academy of Sciences, Sãdhãna, Springer for publication.

4.1 Background

This chapter focuses on the design of a filtered backstepping controller integrated with a high-gain disturbance observer (HGDO) for singularly perturbed switching systems. Such systems often encounter abrupt mode transitions and external disturbances, posing challenges for stability and performance. The proposed control strategy regulates system dynamics effectively under switching conditions and is validated through implementation on a robotic manipulator. Contraction theory is employed to establish the closed-loop convergence, ensuring robustness within bounded operating ranges [97, 98]. The results demonstrate the capability of the proposed controller to handle switching and disturbances in real-time applications.

Chapter 4. Filtered backstepping controller for singularly perturbed switched systems based on contraction analysis

4.2   Problem Statement

Consider a nonlinear switched system, which described as:

$$
\begin{aligned}
\dot{x}_1 &= f_{1\sigma}(x_1) + g_{1\sigma}(x_1)x_2 + d_{1\sigma} \\
\dot{x}_2 &= f_{2\sigma}(x_1, x_2) + g_{2\sigma}(x_1, x_2)x_3 + d_{2\sigma} \\
&\vdots \\
\dot{x}_n &= f_{n\sigma}(x_1, x_2, x_3, \ldots, x_n) + g_{n\sigma}(x_1, x_2, \ldots, x_n)u_\sigma + d_{n\sigma}
\end{aligned}
\tag{4.1}
$$

Where, $\sigma \in P = \{1, 2, \ldots, N\}$ is a piecewise constant signal with a finite number of values. $u_\sigma \in \mathbb{R}$ is the control input. $d_{i\sigma}$ is unknown disturbances. $f_{i\sigma}(.)$ and $g_{i\sigma}(.)$ are known smooth functions and $g_{i\sigma}(.) \neq 0 \ \forall x \in \mathbb{R}^n$. Hence, for this proposed nonlinear switched system needs to be a control law u by using a filtered backstepping approach. The filtered backstepping approach ensures that the output $x_1(t)$ follows a desired signal $x_d(t)$. The following assumptions are required to maintain stability in the closed-loop system:

Assumption (4.1): The desired signal $x_d(t)$ and its derivatives are continuous and bounded.

Assumption (4.2): The functions $f_{i\sigma}(\bar{x}_i)$ and $g_{i\sigma}(\bar{x}_i)$, $i = 1, 2, 3\ldots n$, along with their derivatives, are continuous up to the second order (C^2).

Assumption (4.3): The disturbances are bounded.

4.3   Filtered Backstepping in the Absence of Disturbances

The contraction theory-based approach is used for developing a filtered backstepping controller for the system (4.1). The design and convergence analysis is performed under the assumption that disturbance terms are absent in

4.3. Filtered Backstepping in the Absence of Disturbances

71

the system dynamics. The proposed control law is:

$$
\begin{aligned}
u_\sigma &= \frac{1}{g_{n\sigma}(x)}\left[-f_{n\sigma}(x) - g_{(n-1)\sigma}(x)z_{n-1} - \chi_{n\sigma}(z_n) + \dot{\alpha}_{nf}\right] \\
z_i &= x_i - \alpha_{if}, (i = 1, 2......n) \\
\alpha_{1f} &= \alpha_1 = x_d(t)
\end{aligned}
\tag{4.2}
$$

where $\chi_{n\sigma}(z_n) = k_{n\sigma}z_n$ are user-defined scalar tuning functions, $i \in 1, 2, 3...n, k_{i\sigma} > 0$. The first order filter α_{if} [75, 76] and expressed as:

$$
\begin{aligned}
\mu\dot{\alpha}_{if} &= -\alpha_{if} + \alpha_{i\sigma} \quad i = 2, \cdots, n \\
\alpha_{i\sigma} &= \frac{1}{g_{(i-1)\sigma}(x)}\left[-f_{(i-1)\sigma}(x_1,..x_{i-1}) - g_{(i-2)\sigma}(x)z_{i-2}\right. \\
&\quad \left. - \chi_{(i-1)\sigma}(z_{i-1}) + \dot{\alpha}_{(i-1)f}\right], g_{0\sigma} = 0 \ i = 2, \cdots, n
\end{aligned}
\tag{4.3}
$$

Here, $\chi_{(i-1)\sigma}$, $i = 1, 2, 3, \ldots, n$, represents a scalar tuning function, and $\mu \in (0, 1)$ denotes the perturbation parameter. The initial condition for (4.3) is set as $\alpha_{if}(0) = \alpha_i(0)$. The closed-loop system can be reformulated as follows by combining (4.2) and (4.3).

$$
\begin{aligned}
\dot{z}_1 &= -\chi_{1\sigma}(z_1) + g_{1\sigma}(x)z_2 + g_{1\sigma}(x)\tilde{\alpha}_{2\sigma} \\
\dot{z}_i &= -g_{(i-1)\sigma}(x)z_{i-1} - \chi_{i\sigma}(z_i) + g_{i\sigma}(x)z_{i+1} + g_{i\sigma}(x)\tilde{\alpha}_{(i+1)\sigma} \\
\dot{z}_n &= -g_{(n-1)\sigma}(x)z_{n-1} - \chi_{n\sigma}(z_n), \ i = 2, \ldots, n-1
\end{aligned}
\tag{4.4}
$$

Here, $\tilde{\alpha}_{if} = \alpha_{if} - \alpha_{i\sigma}$. The closed loop system can be written as:

$$
\begin{aligned}
\dot{z} &= f_\sigma(z, \tilde{\alpha}_f) = f_\sigma(z, \alpha_f, \alpha_\sigma) \tag{4.5} \\
\mu\dot{\alpha}_f &= g_\sigma(\alpha_f, \alpha_\sigma) = -\alpha_f + \alpha_\sigma \tag{4.6}
\end{aligned}
$$

Chapter 4. Filtered backstepping controller for singularly perturbed switched systems based on contraction analysis

where $\alpha_\sigma = [\alpha_{2\sigma}, \alpha_{3\sigma}, \alpha_{4\sigma}...\alpha_{n\sigma}]^T$, $\alpha_f = [\alpha_{2f}, \alpha_{3f}, \alpha_{4f}...\alpha_{nf}]^T$, $\tilde{\alpha}_f = [\tilde{\alpha}_{2f}, \tilde{\alpha}_{3f}, \tilde{\alpha}_{4f}...\tilde{\alpha}_{nf}]^T$ and $f_\sigma(.) = [\bar{f}_{i\sigma}]^T$ with

$$
\begin{aligned}
\bar{f}_{1\sigma}(.) &= -\chi_{1\sigma}(z_1) + g_{1\sigma}(x)z_2 + g_{1\sigma}(x)\tilde{\alpha}_{2\sigma} \\
\bar{f}_{i\sigma}(.) &= -g_{(i-1)\sigma}(x)z_{i-1} - \chi_{i\sigma}(z_i) + g_{i\sigma}(x)z_{i+1} \\
&\quad + g_{i\sigma}(x)\tilde{\alpha}_{(i+1)\sigma}, (i = 2,3...,n-1) \\
\bar{f}_{n\sigma}(.) &= -g_{(n-1)\sigma}(x)z_{n-1} - \chi_{n\sigma}(z_n)
\end{aligned}
\tag{4.7}
$$

The convergence analysis has been discussed in the form of Theorem 4.1:

Theorem 4.1: Assume that the initial conditions are finite and that assumptions (4.1) and (4.2) are satisfied. If a filtered backstepping controller is selected as described in (4.2-4.3), then the reduced slow system in (4.5-4.6) exhibits contraction, and the tracking error will eventually be bounded for all $\mu \in (0,1)$.

Proof: The reduced slow system is derived by setting $\mu = 0$ in the closed-loop dynamics (4.5-4.6). By substituting $\mu = 0$ into equation (4.6), it can be obtained as $\alpha_{if} = \alpha_\sigma$. The reduced slow system can be represented as:

$$
\begin{aligned}
\dot{z}_1 &= -\chi_{1\sigma}(z_{1r}) + g_{1\sigma}(x)z_{2r} \\
\dot{z}_i &= -g_{(i-1)\sigma}(x)z_{(i-1)r} - \chi_{i\sigma}(z_{ir}) + g_{i\sigma}(x)z_{(i+1)r} \\
\dot{z}_n &= -g_{(n-1)\sigma}(x)z_{(n-1)r} - \chi_{n\sigma}(z_{nr}), i = 2,...,(n-1).
\end{aligned}
\tag{4.8}
$$

A Jacobian J to emphasize multivariate changes in a space for the slow system.

$$
J = \begin{bmatrix}
-\frac{\partial \chi_{1\sigma}(z_1)}{\partial z_1} & g_{1\sigma} & 0 & \cdots & 0 & 0 \\
-g_{1\sigma} & -\frac{\partial \chi_{2\sigma}(z_2)}{\partial z_2} & g_{2\sigma} & \cdots & 0 & 0 \\
0 & -g_{2\sigma} & -\frac{\partial \chi_{3\sigma}(z_3)}{\partial z_3} & \cdots & 0 & 0 \\
\vdots & \vdots & \vdots & \ddots & \vdots & \vdots \\
0 & 0 & 0 & \cdots & -\frac{\partial \chi_{(n-1)\sigma}(z_{n-1})}{\partial z_{n-1}} & g_{(n-1)\sigma} \\
0 & 0 & 0 & \cdots & -g_{(n-1)\sigma} & -\frac{\partial \chi_{n\sigma}(z_n)}{\partial z_n}
\end{bmatrix}
$$

Since, $\frac{\partial \chi_{i\sigma}(z_i)}{\partial z_i} > 0$

$$
IJ + J^T I \leq -2Diag\left(\frac{\partial \chi_{1\sigma}(z_1)}{\partial z_1}...\frac{\partial \chi_{n\sigma}(z_n)}{\partial z_n}\right)I
$$

Where $Diag(.)$ denotes a diagonal matrix. The reduced slow system contracts with the identity matrix $M = \Theta^T\Theta = I$. The tuning $\chi_{i\sigma}(z_i)$ determines the

contraction rate. Since $\chi_{i\sigma}(0) = 0$ and the reduced dynamics are autonomous, there will be a unique equilibrium point at $z = 0$ within the contracting region. Consequently, the trajectories of the reduced slow system converge exponentially to zero.

Since the filter parameter μ is not equal to zero. There are specific differences between the virtual control variables α and their filtered counterparts α_f. To verify the boundedness of the system a perturbed system is considered, which is given by:

$$\mu\dot{\alpha}_d = g(\alpha_d, \alpha_\sigma) + \mu Q(z, \alpha_\sigma) \tag{4.9}$$

Here, $Q(z, \alpha_\sigma) = \frac{\partial \alpha_\sigma}{\partial z}\dot{z}$ and α_σ is a particular solution of (4.9). By replacing α_d with α_σ in (4.9), $\mu\dot{\alpha}_\sigma = g(\alpha_\sigma, \alpha_\sigma) + \mu\frac{\partial \alpha_\sigma}{\partial z}\dot{z}$ i.e. $\mu\dot{\alpha}_\sigma = \mu\frac{\partial \alpha_\sigma}{\partial z}\dot{z}$ can be obtained. Also, α_f is a particular solution of (4.9) in the absence of $\mu Q(z, \alpha_\sigma)$. So, Equation (4.9) can be considered as a perturbed form of (4.6) [80]. By exploiting the assumption (4.2) i.e. $f_{i\sigma}(.)$, $g_{i\sigma}(.), \alpha_{i\sigma}$ & their 1st order partial derivative are bounded inside any compact set. So, a positive constant c_1 will exist such that

$$\|Q(z, \alpha_\sigma)\| \leq c_1 \text{ for } (z, \alpha_\sigma) \in (B_z, B_{\alpha_\sigma}) \tag{4.10}$$

In the absence of a bounded perturbation term $Q(z, \alpha_\sigma)$, (4.9) can be written as:

$$\mu\dot{\alpha}_d = g(\alpha_d, \alpha_\sigma) = -\alpha_d + \alpha_\sigma \tag{4.11}$$

The jacobian of (4.11) with respect to α_d is $J_f = \frac{\partial g(.)}{\partial \alpha_d} = -\frac{1}{\mu}$. Thus, the unperturbed dynamics (4.11) exhibit partial contraction in α_d with the identity matrix I and a contraction rate of $\frac{1}{\mu}$. The error bound [49] between (4.6) and (4.9) can be written as:

$$\|\alpha_f(t) - \alpha_\sigma(t)\| \leq \|\alpha_f(0) - \alpha_\sigma(0)\|e^{-\frac{1}{\mu}} + \mu c_1 \tag{4.12}$$

By replacing the root α_σ of the fast subsystem with α_f in (4.5), the following reduced equation can be obtained.

$$\begin{aligned}
\dot{z}_{1r} &= -\chi_{1\sigma}(z_{1r}) + g_{1\sigma}(x)z_{2r} \\
\dot{z}_{ir} &= -g_{(i-1)\sigma}(x)z_{(i-1)r} - \chi_{i\sigma}(z_{ir}) + g_{i\sigma}(x)z_{(i+1)r} \\
\dot{z}_{nr} &= -g_{(n-1)\sigma}(x)z_{(n-1)r} - \chi_{n\sigma}(z_{nr}), \quad i = 2, \ldots, n-1
\end{aligned} \tag{4.13}$$

Chapter 4. Filtered backstepping controller for singularly perturbed switched systems based on contraction analysis

The above equation (4.13) can be written as

$$\dot{z}_r = f(z_r, \alpha_\sigma, \alpha_\sigma) \tag{4.14}$$

Where, $z_r = [z_{ir}]^T$, $i = 1, 2, 3...n$. The Jacobian of (4.14) is the same as (4.8), so (4.14) is also contracting. Equation (4.5) can be represented as (4.15).

$$\dot{z} = f(z, \alpha_\sigma, \alpha_\sigma) + f(z, \alpha_f, \alpha_\sigma) - f(z, \alpha_\sigma, \alpha_\sigma) \tag{4.15}$$

Lets consider $(f(z, \alpha_f, \alpha_\sigma) - f(z, \alpha_\sigma, \alpha_\sigma))$ is perturbation. From assumption (4.2), it is assumed that the functions $f(\cdot), g(\cdot), \alpha_\sigma(\cdot)$, and their partial derivatives with respect to their arguments are continuous and bounded within a compact region. Based on this, it is reasonable to conclude that there exists a positive constant L_1 such that the function $f(\cdot)$ is Lipschitz continuous with respect to its arguments. If we further assume that the function $f(\cdot)$ is Lipschitz continuous in α_f with a constant L_1, equation (4.16) can be derived.

$$\left\| f(z, \alpha_f, \alpha_\sigma) - f(z, \alpha_\sigma, \alpha_\sigma) \right\| \leq L_1 \left\| \alpha_f - \alpha_\sigma \right\| \tag{4.16}$$

Exploiting (4.12) and Lemma A.1 (Appendix A). The following equation can be obtained.

$$\begin{aligned} \|z(t) - z_r(t)\| \leq \ & \left(\|z(0) - z_r(0)\| - \mu \frac{L_1 c_1}{\beta} \right) \\ & \exp(-\beta t) + \frac{L_1 \|\alpha_f(0) - \alpha_\sigma(0)\|}{1 - \mu\beta} \\ & \left(\exp(-\beta t) - \exp\left(\frac{-t}{\mu} \right) \right) + \mu \frac{L_1 c_1}{\beta}. \end{aligned} \tag{4.17}$$

Here, β represents the contraction rate. Since $z_r = 0$ is also a solution to equation (4.14), the norm of $z_r(t)$ satisfies $\|z_r(t) - 0\| = \|z_r(t)\| \leq \|z_r(0)\| \exp(-\beta t)$. Using the triangle inequality, we have $\|z_1(t)\| \leq \|z(t)\| \leq \|z(t) - z_r(t)\| + \|z_r(t)\|$. From

this, it can be concluded that

$$
\begin{aligned}
\|x(t) - x_d(t)\| = \|z_1(t)\| &\leq \|z_r(0)\| \exp(-\beta t) \\
&+ \left(\|z(0) - z_r(0)\| - \mu \frac{L_1 c_1}{\beta} \right) \exp(-\beta t) + \mu \frac{L_1 c_1}{\beta} \\
&+ \frac{L_1 \|\alpha_f(0) - \alpha_\sigma(0)\|}{1 - \mu\beta} \left(\exp(-\beta t) - \exp\left(\frac{-t}{\mu} \right) \right).
\end{aligned}
\tag{4.18}
$$

The Jacobian J of the nominal contracting system depends on the derivatives $\frac{\partial \chi_{i\sigma}(z_i)}{\partial z_i}$ which can be derived as:

$$
IJ + J^T I \leq -2 \operatorname{Diag} \left(\frac{\partial \chi_{1\sigma}(z_1)}{\partial z_1}, \dots, \frac{\partial \chi_{1\sigma}(z_n)}{\partial z_n} \right) I
$$

Exploiting the equation

$$
\left(\dot{\Xi} + \Xi \frac{\partial f}{\partial x} \Xi^{-1} \right) + \left(\dot{\Xi} + \Xi \frac{\partial f}{\partial x} \Xi^{-1} \right)^T \leq -\Delta I
$$

$$
\left(\dot{M} + M \frac{\partial f}{\partial x} + \frac{\partial f^T}{\partial x} M \right) \leq -2\Delta M
$$

As mentioned in the Appendix A, the contraction rate $\beta = \min_{i=1,\dots,n} \frac{\partial \chi_{1\sigma}(z_i)}{\partial z_i}$ can be evaluated. Where, Ξ is a nonsingular matrix called the associated transformation matrix, $M = \Xi^T \Xi$ is called the contraction matrix, and $\Delta \in R^+$ is referred to as the contraction rate.

One straightforward method for selecting the tuning functions is

$$
\chi_{i\sigma}(z_i) = k_{i\sigma} z_i, \quad k_{i\sigma} \in \mathbb{R}^+
$$

In this case, β is determined as

$$
\beta = \min(k_{i\sigma}).
$$

Choosing a very small β can significantly slow down convergence and increase the steady-state error, even for a small μ. In other words, a smaller β demands an exceptionally small μ to achieve a satisfactory system response. The bound

Chapter 4. Filtered backstepping controller for singularly perturbed switched systems based on contraction analysis

established in (4.18) indicates that the transient component of the tracking error is influenced by the contraction rate β, which is determined by the functions $\chi_{i\sigma}(z_i)$. To get a higher β and faster transient response, one could select a larger control gain $k_{i\sigma}$; however, this approach may result in increased control costs. A well-chosen nonlinear tuning function can enhance the transient response and improve the damping characteristics. For example, a tuning function

$$\chi_{i\sigma}(z_i) = \max\left(k_{i1}z_i + k_{i2}z_i^3\right), k_{i1}, k_{i2} \in R^+$$

may result in a faster response and better damping.

A significant portion of the literature on filtered backstepping has focused on analyzing the time-scale behavior and demonstrating semiglobal practical stability for a narrow range of filter parameters [76], [91], [99], [92]. However, Theorem 4.1 demonstrates the ultimate boundedness of the tracking error for all $\mu \in (0,1)$. The relaxation of the magnitude restriction on μ is achieved through the application of contraction theory techniques [49], [47], [100], [101].

4.4 Disturbance Observer

As a contracting observer is exponentially convergent and robust to bounded uncertainties [14, 102], it is advantageous to design a contracting observer. The proposed observer for each $d_{i\sigma}$ is given by:

$$\begin{aligned}
\dot{\eta}_i &= -\lambda\left(\eta_i + kx_i - f_{i\sigma}\left(x_1, x_2, \ldots, x_i\right) - b_{i\sigma}x_{i+1}\right) \\
\dot{\eta}_n &= -\lambda\left(\eta_n + kx_n - f_{n\sigma}\left(x_1, x_2, \ldots, x_n\right) - b_{n\sigma}u\right) \\
\hat{d}_i &= \eta_i + \lambda x_i
\end{aligned} \tag{4.19}$$

where $i \in \{1, 2, \ldots, n-1\}$. $\lambda > 0$ is a scalar positive constant. η_i is an intermediate variable and $\hat{d}_i$ is the estimate of $d_{i\sigma}$ and

By exploiting (4.19), the derivative of the disturbance estimate $(\hat{d}_i)$ can be written as:

$$\dot{\hat{d}}_i = h\left(\hat{d}_i, d_{i\sigma}\right) = -\lambda\left(\hat{d}_i - d_{i\sigma}\right) \tag{4.20}$$

Lets consider a disturbance error $\tilde{d}_i$ which can be written as $\tilde{d}_i = d_{i\sigma} - \hat{d}_{i\sigma}$, and its derivative will be

$$\epsilon\dot{\tilde{d}}_i = -\tilde{d}_i - \epsilon d_{i\sigma} \tag{4.21}$$

where $0 \leq \epsilon = 1/\lambda \leq 1$. The error dynamics in the absence of the perturbation term can be written as:

$$\dot{\tilde{d}}_{io} = -\lambda \tilde{d}_{io} \tag{4.22}$$

The equation (4.22) is contracting with an identity matrix and the contraction rate is λ (Jacobian with respect to d_i is $-\lambda$). From assumption (4.3), we know that the perturbation term $\varepsilon(d_{i\sigma})$ is bounded. The following bound can be derived using Lemma A.1 (Mentioned in Appendix A).

$$\left\|\tilde{d}_i(t) - \tilde{d}_{io}(t)\right\| \leq \left\|\tilde{d}_i(0) - \tilde{d}_{io}(0)\right\| \exp(-\lambda t) + \frac{c_4}{\lambda}$$

It is possible to ensure that the steady-state estimation error is within a narrow neighborhood of origin by choosing λ high. For slowly varying disturbances, the scalar $c_4 = 0$, where $\dot{d}_i \approx 0$ i.e. $\left\|\tilde{d}_{io}(t)\right\| \leq \left\|\tilde{d}_{io}(0)\right\| \exp(-\lambda t)$. Using triangle inequality.

$$\left\|\hat{d}_i - d_{i\sigma}\right\| \leq \left(\left\|\tilde{d}_i(0) - \tilde{d}_{io}(0)\right\| + \left\|\tilde{d}_{io}(0)\right\|\right) \exp(-\lambda t) + \frac{c_4}{\lambda}$$

Thus, in this situation, the disturbance observer precisely estimates the disturbance $\hat{d}_i \to d_{i\sigma}$. In case of slowly varying disturbances for which $\dot{d}_i \approx 0$, the scalar $c_4 = 0$. That is why the disturbance observer exactly estimates $\hat{d}_i \to d_{i\sigma}$.

4.5 Filtered backstepping in the presence of disturbances

In the presence of external disturbances, the filtered backstepping control law can be designed as follows:

$$\begin{aligned} u_\sigma = \frac{1}{g_{n\sigma}(x)}\big[&-f_{n\sigma}(x) - g_{(n-1)\sigma}z_{n-1} - \chi_{n\sigma}(z_n) \\ &+\dot{\alpha}_{nf} - \hat{d}_{n\sigma}\big] \end{aligned} \tag{4.23}$$

Chapter 4. *Filtered backstepping controller for singularly perturbed switched systems based on contraction analysis*

$$z_i = x_i - \alpha_{if}, (i = 1, 2 \ldots \ldots n) \tag{4.24}$$

$$\alpha_{1f} = \alpha_1 = x_d(t) \text{ and for } i \in [2 \ldots n] \tag{4.25}$$

$$\alpha_{i\sigma} = \frac{1}{g_{(i-1)\sigma}} \left[-f_{(i-1)\sigma}(x_1, ..x_{i-1}) - \chi_{(i-1)\sigma}(z_{i-1}) \\ -g_{(i-2)\sigma}z_{i-2} + \dot{\alpha}_{(i-1)f} - \hat{d}_{(i-1)\sigma} \right]. \tag{4.26}$$

By exploiting (4.23) the following equation (4.27) can be obtained as:

$$\dot{z}_1 = -\chi_{1\sigma}(z_1) + g_{1\sigma}z_2 + g_{1\sigma}\tilde{\alpha}_{2\sigma} + \tilde{d}_{1\sigma}$$
$$\dot{z}_i = g_{(i-1)\sigma}z_{i-1} - \chi_{i\sigma}(z_i) + g_{i\sigma}z_{i+1} + g_{i\sigma}\tilde{\alpha}_{(i+1)\sigma}, + \tilde{d}_{i\sigma} \tag{4.27}$$
$$\dot{z}_n = -g_{(n-1)\sigma}z_{n-1} - \chi_{n\sigma}(z_n) + \tilde{d}_{n\sigma}$$

So, in a compact form, the closed-loop dynamics can be written as:

$$\dot{z} = f\left(z, \alpha_f, \alpha_\sigma, \hat{d}_\sigma, d_\sigma\right)$$
$$\mu\dot{\alpha}_f = g\left(\alpha_f, \alpha_\sigma\right) = -\alpha_f + \alpha_\sigma \tag{4.28}$$
$$\varepsilon\dot{\hat{d}} = h(\hat{d}, d_\sigma) = -\hat{d} + d_\sigma$$

where $z = [z_1, z_2, \ldots, z_n]^T, \alpha_f = [\alpha_{2f}, \alpha_{3f}, \ldots, \alpha_{nf}]^T, \alpha_\sigma = [\alpha_{2\sigma}, \alpha_{3\sigma}, \ldots, \alpha_{n\sigma}]^T, \hat{d}_\sigma = [\hat{d}_{1\sigma}, \hat{d}_{2\sigma}, \ldots, \hat{d}_{n\sigma}], d = [d_1, d_2, \ldots, d_n]$ and $\varepsilon = \frac{1}{k} \in (0, 1)$.
The above equation (4.28) is in the perturbed form with three time scales. It can be converted into two time scales by using the ratio $\frac{\varepsilon}{\mu}$. Let's consider a perturbed parameter $\varepsilon < \mu$ so that the observer dynamics are faster than the filter dynamics. Here, $\varepsilon = \kappa\mu$ can be assumed, where the subsystems of (4.28) can be written as:

$$\mu\dot{v} = W(v, \alpha_\sigma, d_\sigma, \kappa) \tag{4.29}$$

where $v = \left[\alpha_f^T, \hat{d}^T\right]^T$ and $W(.) = \left[g^T(.), \frac{1}{\kappa}h^T(.)\right]^T$. Using (4.29), the closed-loop system can be written in two time scales singularly perturbed switched system. Also, the convergence of the trajectories can be obtained by following the same arguments as in the previous section. In a similar way the convergence of the disturbance observer can be concluded as if the initial conditions are finite, and assumptions (4.1-4.3) are true for (4.1). The controller (4.23) and the disturbance observer (4.19) are chosen in such a way that the closed-loop system is uniformly

ultimately bounded (UUB) for all $\mu \in (0,1)$ and the steady-state tracking error is given by:

$$\lim_{t\to\infty} \|x(t) - x_d(t)\| \leq \mu \frac{L_v \left(\max\left(c_1, c_4\right)\right)}{\beta \left\|\max\left(-1, \frac{-1}{\kappa}\right)\right\|} \tag{4.30}$$

where L_v is a Lipschitz constant of the function $W(.)$.

4.6   Mathematical Outcome

The proposed filter backstepping controller with a high-gain disturbance observer is validated on a single-link manipulator [96] to test its performance. The system dynamics are as follows:

$$\begin{aligned} D\ddot{q} + B\dot{q} + N\sin(q) &= \tau \\ M\dot{\tau} + H\tau + K_m\dot{q} &= u \end{aligned} \tag{4.31}$$

The parameters D, B, N, M, H, and K_m are determined by the physical properties of the robot and its actuators, given in Table 4.1 for three different switching signals. The values q and $\dot{q}$ refer to the angular position and angular velocity of the joint, respectively. The torque τ is the force applied to the joint by the actuator motor, and u represents the voltage input supplied to the motor to produce this torque. Let's choose $x_1 = q$, $x_2 = \dot{q}$ and $x_3 = \tau$. The equation (4.31) can be written in a strict feedback form as:

$$\begin{aligned} \dot{x}_1 &= x_2 \\ \dot{x}_2 &= \frac{1}{D}(-N\sin(x_1) - Bx_2) + \frac{1}{D}x_3 \\ \dot{x}_3 &= -\frac{1}{M}(K_m x_2 + Hx_3) + \frac{1}{M}u \end{aligned} \tag{4.32}$$

Chapter 4. Filtered backstepping controller for singularly perturbed switched systems based on contraction analysis

TABLE 4.1: The parameters of the system for different switching signals.

System Parameters	D	B	N	M	H	Km
For $\sigma = 1$	1	8	10	0.01	0.5	100
For $\sigma = 2$	10	150	10	0.01	0.5	10
For $\sigma = 3$	10	1	10	0.01	0.5	100

In [103, 104] it is given that a signal has the average dwell time τ_a if there exists a number N_0 such that $\forall T \geq t \geq 0$:

$$N_\sigma(T - t) \leq N_0 + \frac{T - t}{\tau_a}, \tag{4.33}$$

Here, a reference signal $\pi \sin(-5t)$ has been considered. For $\sigma = 1$, the disturbances are $d_1 = 0.1 \tanh(2t)$ and $d_2 = 0.1 \tanh(2t)$ and for $\sigma = 2, 3$, the disturbances are $d_1 = 0.1 \sin(2t)$ and $d_2 = 0.1 \cos(2t)$ have been added to the system to check the convergence of closed loop trajectories. The systems are switched at $t < 0.20$ sec and in the interval $(0.2, 0.5)$ sec. Despite this, the system is able to follow the reference signal, as shown in Figure. 4.1, and the corresponding error shown in Figure 4.2 which confirms the quick convergence of the controller to zero. Similarly, the same reference signal $\pi \sin(-5t)$ has been considered. This time, the system is switched at $t < 0.20$ sec, in the interval $(0.2, 0.5)$ sec, and at $t > 0.5$ sec. Once again, it can be observed that despite these switches, the system is able to follow the reference signal, as shown in Figure. 4.3, and the corresponding error convergence to zero can be seen in Figure 4.4.

Another reference $\sin(10t)$ has been used. The systems are switched at $t < 0.20$ sec and during the interval $(0.2, 0.5)$ sec. Even with these switches, the system successfully follows the reference, as illustrated in Figure 4.5, and the corresponding error convergence to zero is evident in Figure. 4.6. Similarly, the same reference $\sin(10t)$ is considered, but this time the system is switched at $t < 0.20$ sec, within the interval $(0.2, 0.5)$ sec, and at $t > 0.5$ sec. Once again, it is evident that the system maintains its ability to track the reference, as shown in Figure 4.7, with the corresponding error convergence to zero depicted in Figure

FIGURE 4.1: Closed loop response of x_1 for $\sigma = 1, 2$ for reference signal $\pi sin(-5t)$
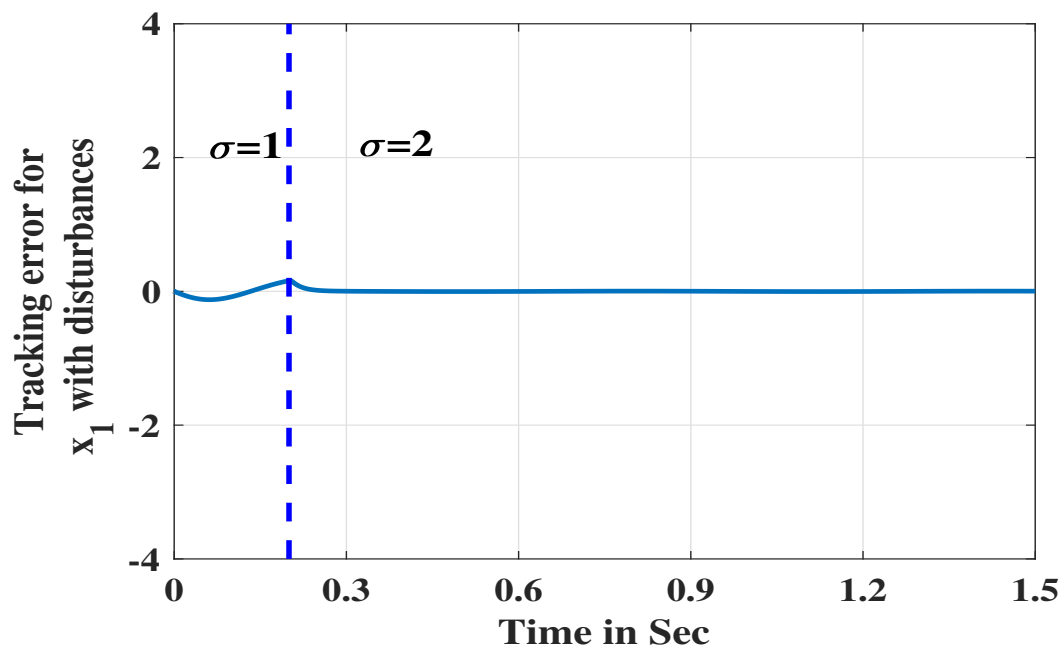
FIGURE 4.2: Error convergence to zero for $\sigma = 1, 2$ for reference signal $\pi sin(-5t)$

Chapter 4. Filtered backstepping controller for singularly perturbed switched systems based on contraction analysis

FIGURE 4.3: Closed loop response of x_1 for $\sigma = 1, 2, 3$ for reference signal $\pi sin(-5t)$
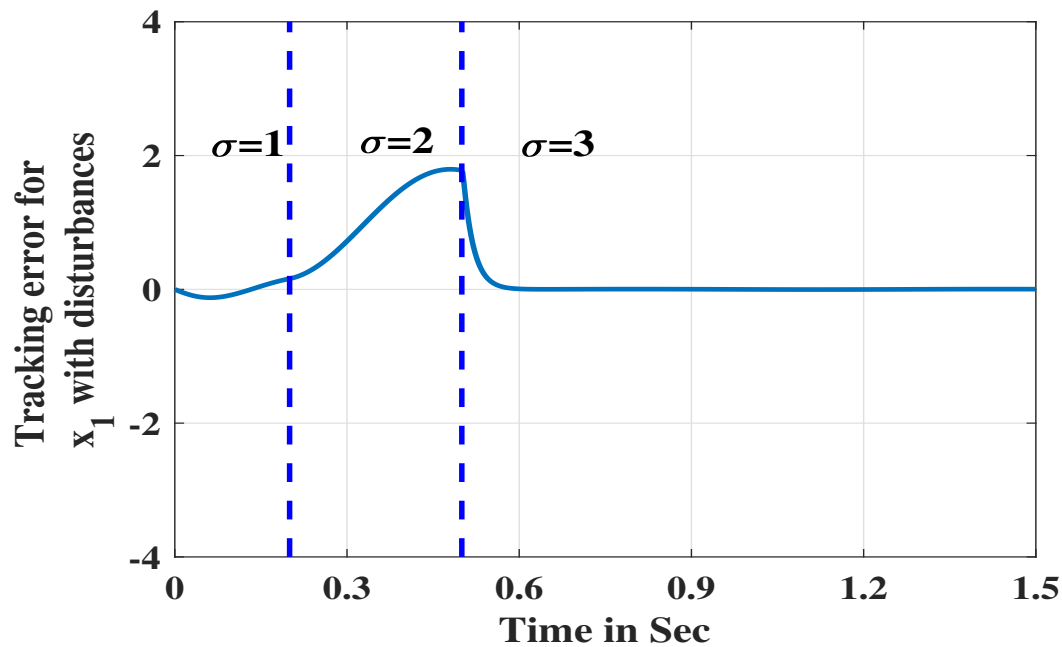
FIGURE 4.4: Error convergence to zero for $\sigma = 1, 2, 3$ for reference signal $\pi sin(-5t)$

Closed loop response for x1 at t<0.20 sec and in the interval (0.2,0.5) sec for $\sigma=1$ and $\sigma=2$ respectively
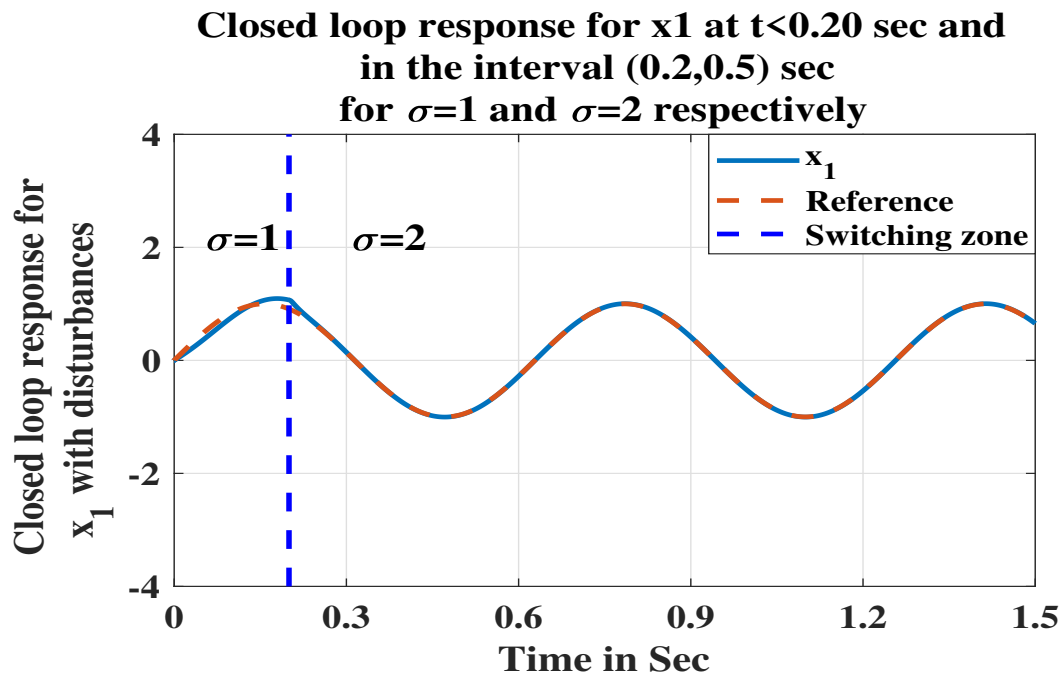
FIGURE 4.5: Closed loop response of x_1 for $\sigma = 1, 2$ for reference signal $\sin(10t)$
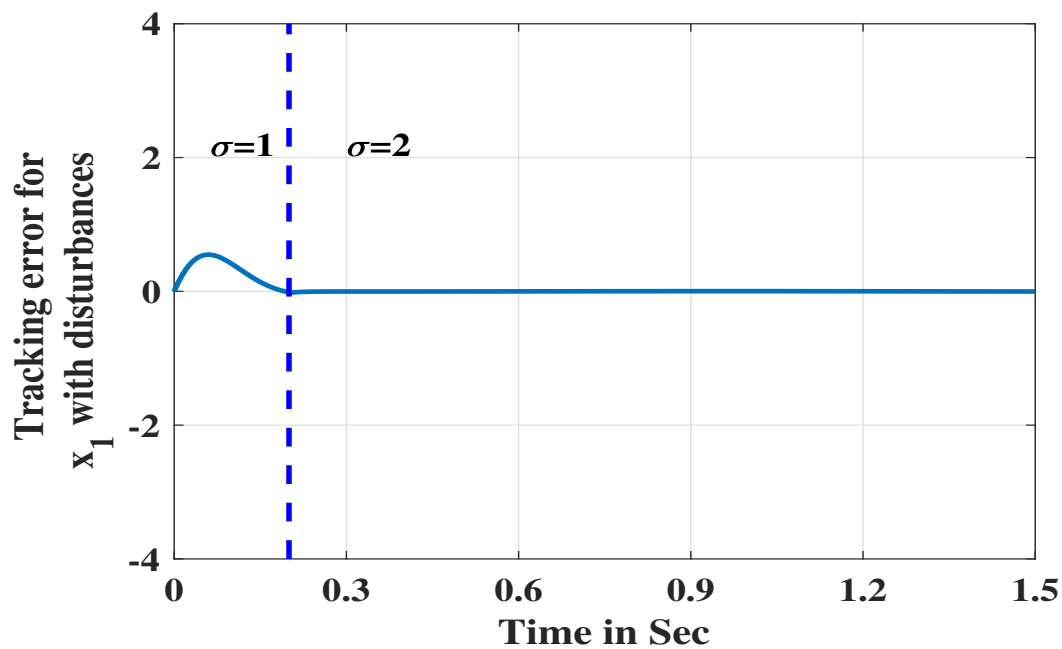
FIGURE 4.6: Error convergence to zero for $\sigma = 1, 2$ for reference signal $\sin(10t)$

Chapter 4. Filtered backstepping controller for singularly perturbed switched systems based on contraction analysis

Closed loop response for x1 at t<0.20 sec and in the interval (0.2,0.5) sec for σ=1 and σ=2 respectively and at t>0.5 sec for σ=3
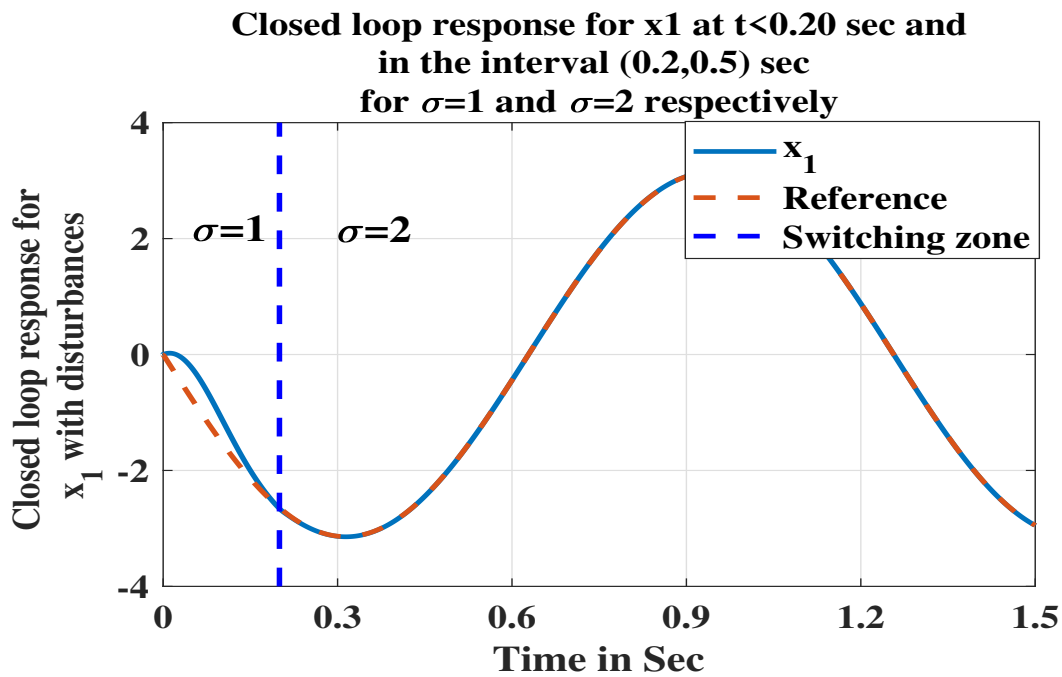

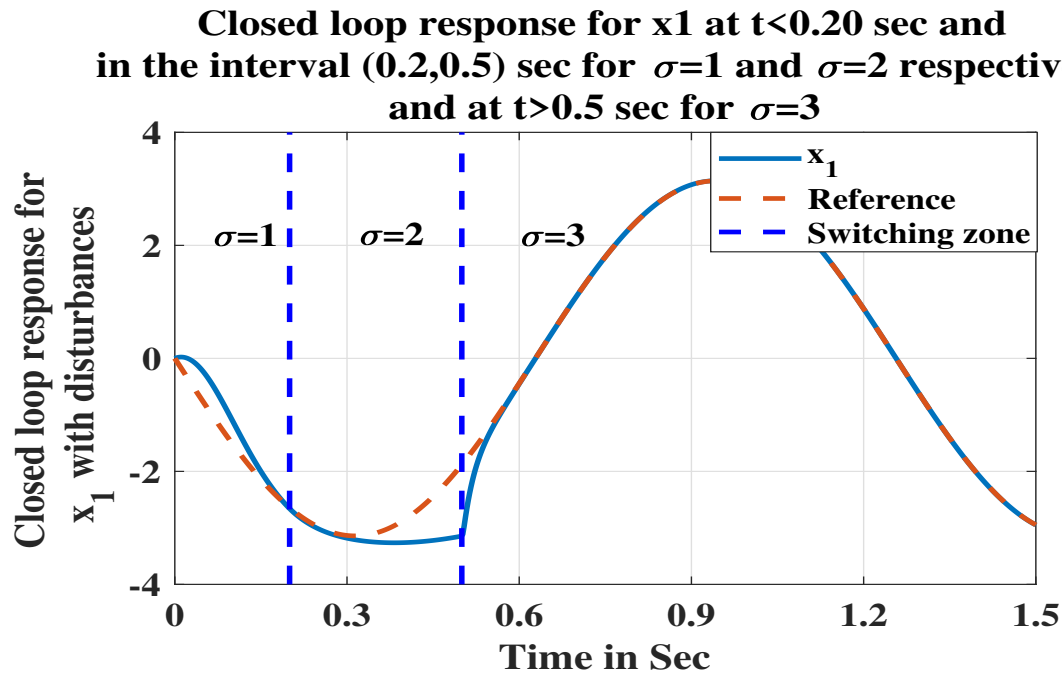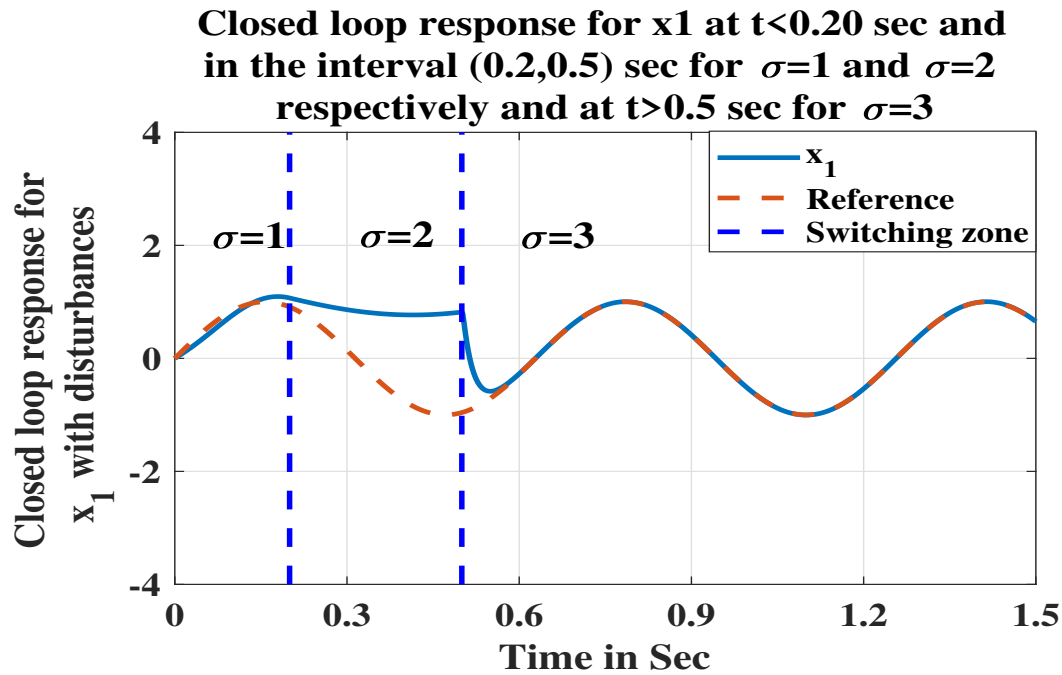FIGURE 4.7: Closed loop response of x_1 for $\sigma = 1,2,3$ for reference signal $\sin(10t)$
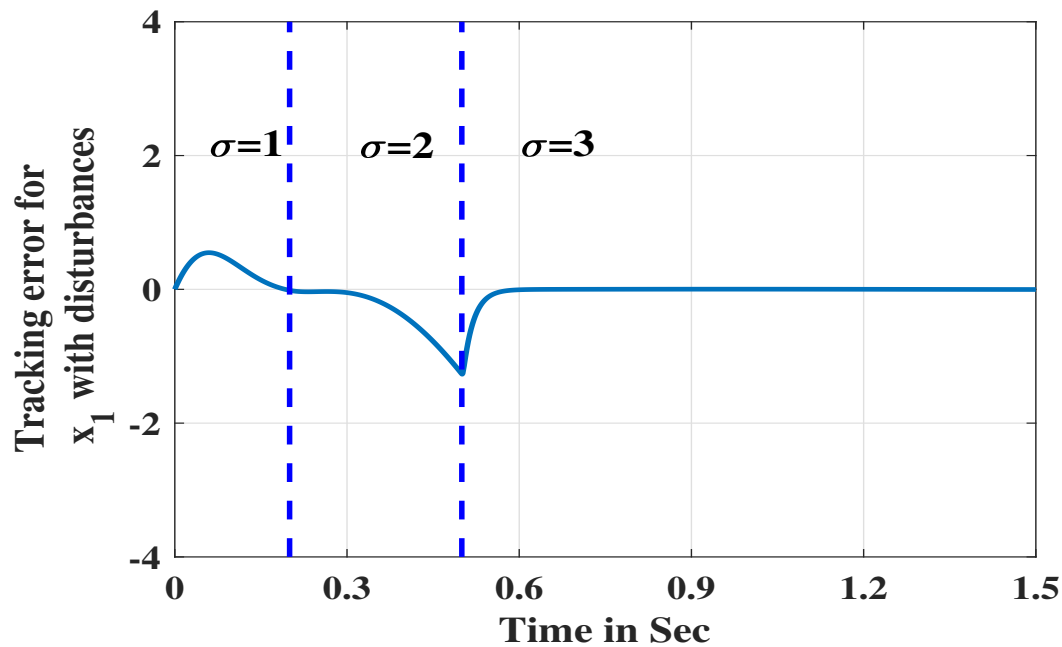
FIGURE 4.8: Error convergence to zero for $\sigma = 1,2,3$ for reference signal $\sin(10t)$

4.8.

All outcomes demonstrate that, despite different switching modes, the system transitions very smoothly, and the trajectories of the closed-loop system exhibit contraction regardless of their initial conditions.

4.7   Concluding remarks

The contraction property of the closed-loop system ensures that the trajectories converge to the reference signal, irrespective of the initial conditions. This behavior is consistently observed across all scenarios, as evidenced by the error convergence to zero. The ability of the system to maintain contraction even during switching, indicating its robustness under disturbances and dynamic changes in the operating conditions. The outcomes validate the claim that the proposed control strategy effectively handles nonlinearity and switching dynamics, providing smooth operation and reliable performance. The demonstrated robustness and adaptability make this approach highly suitable for practical applications where systems operate under changing conditions or require frequent mode transitions.

87

Chapter 5

Neural disturbance observer-based backstepping controller for singularly perturbed switched systems

This chapter has been communicated to the Arabian Journal for Science and Engineering, Springer and revision is submitted.

5.1   Background

This chapter focuses on the control of nonlinear singularly perturbed switched systems (SPSSs) using a filtered backstepping approach. Conventional backstepping methods, though effective, often lead to high computational complexity, particularly in systems with multiple time scales and switching dynamics. To address this challenge, a high-gain filter is incorporated, simplifying the control design while preserving stability and performance. Furthermore, to mitigate the effects of unknown external disturbances, a neural network disturbance observer (NNDO) is employed, exploiting neural networks' approximation capability for real-time disturbance estimation and compensation. The combined strategy enhances robustness, reduces computational effort, and ensures practical applicability. Closed-loop stability during switching is rigorously analyzed using Lyapunov methods under average dwell-time conditions [105]. The proposed methodology is validated on

a single-link robotic manipulator to assess its practical effectiveness and reliability. The simulation results show that the designed controller achieves smooth and accurate trajectory tracking, even in the presence of system uncertainties and external disturbances.

5.2   Problem Statement

A category of nonlinear switched systems can be represented as follows:

$$
\begin{aligned}
\dot{x}_1 &= f_{1\sigma}(x_1) + g_{1\sigma}(x_1)x_2 + \Delta_{1\sigma}(x_1, t) \\
\dot{x}_2 &= f_{2\sigma}(x_1, x_2) + g_{2\sigma}(x_1, x_2)x_3 + \Delta_{2\sigma}(x_1, x_2, t) \\
&\vdots \\
\dot{x}_n &= f_{n\sigma}(x_1, x_2, x_3....x_n) + g_{n\sigma}(x_1, x_2, \ldots, x_n)u_\sigma + \Delta_{n\sigma}(x, t)
\end{aligned}
\tag{5.1}
$$

where $f_{i\sigma}(.), g_{i\sigma}(.)$ are known sufficiently smooth functions, $x = [x_1, x_2, ..., x_n]^T$, $g_{i\sigma}(.) \neq 0 \ \forall x \in R^n$ and $\sigma \in P = [1, 2, \cdots, N]$ is piece-wise constant signal with finite number of values and $u_\sigma \in R$ is the control input. The terms $\Delta_{i\sigma}(.)$ denote uncertain parts of system dynamics.

Assumption 5.1: The desired signal $x_d(t)$ and its derivatives are continuous and bounded. $f_{i\sigma}(.)$, $g_{i\sigma}(.)$ and its partial derivative are continuous upto 2nd order.

Assumption 5.2: The external uncertain parts of the system dynamics $\Delta_{i\sigma}$, $i = 1, 2, 3...n$ are bounded, i.e., there exist unknown positive constants $\bar{\Delta}_{i\sigma} > 0$, such that $\|\Delta_{i\sigma}\| \leq \bar{\Delta}_{i\sigma}$.

5.3   Backstepping without Disturbances

This section presents the design of a filtered backstepping (FB) controller. The method assumes that the system dynamics in equation (5.1) exclude disturbance

5.3. Backstepping without Disturbances

89

terms denoted as $\Delta_{i\sigma}(.)$.

$$
\begin{aligned}
u_\sigma &= \frac{1}{g_{n\sigma}(x)}[-f_{n\sigma}(x) - g_{(n-1)\sigma}(x)z_{n-1} - \lambda_{n\sigma}(z_n) + \dot{\alpha}_{nf}] \\
z_i &= x_i - \alpha_{if}, (i = 1, 2......n) \\
\alpha_{1f} &= \alpha_1 = x_d(t)
\end{aligned}
\tag{5.2}
$$

where $\lambda_{n\sigma}(z_n)$ are user-defined scalar tuning functions, which are chosen as $k_{i\sigma}z_i$, where, $i \in 1, 2, 3...n$, $k_{i\sigma} > 0$. The terms α_{if} are derived using a first-order filter [75, 76]. It can be expressed as:

$$
\begin{aligned}
\mu\dot{\alpha}_{if} &= -\alpha_{if} + \alpha_{i\sigma} \quad i = 2, \cdots, n \\
\alpha_{i\sigma} &= \frac{1}{g_{(i-1)\sigma}(x)}[-f_{(i-1)\sigma}(x_1, ..x_{i-1}) - \lambda_{(i-1)\sigma}(z_{i-1}) \\
&\quad - g_{(i-2)\sigma}(x)z_{i-2} + \dot{\alpha}_{(i-1)f}], g_{0\sigma} = 0 \ i = 2, \cdots, n
\end{aligned}
\tag{5.3}
$$

where $\lambda_{(i-1)\sigma}, i \in 1, 2, 3...n$ is scalar tuning function and $\mu \in (0, 1)$ is called perturbed parameter. $\alpha_{if}(0) = \alpha_i(0)$ has been chosen for (5.3). Equation (5.4) can be obtained using (5.2) and (5.3).

$$
\begin{aligned}
\dot{z}_1 &= -\lambda_{1\sigma}(z_1) + g_{1\sigma}(x)z_2 + g_{1\sigma}(x)\tilde{\alpha}_{2\sigma} \\
\dot{z}_i &= -g_{(i-1)\sigma}(x)z_{i-1} - \lambda_{i\sigma}(z_i) + g_{i\sigma}(x)z_{i+1} + g_{i\sigma}(x)\tilde{\alpha}_{(i+1)\sigma} \\
\dot{z}_n &= -g_{(n-1)\sigma}(x)z_{n-1} - \lambda_{n\sigma}(z_n), \quad i = 2, \ldots, n-1
\end{aligned}
\tag{5.4}
$$

where $\tilde{\alpha}_{if} = \alpha_{if} - \alpha_{i\sigma}$. The overall closed-loop system can be written as

$$
\dot{z} = f_\sigma(z, \tilde{\alpha}_f)
\tag{5.5}
$$

$$
\mu\dot{\alpha}_f = -\alpha_f + \alpha_\sigma
\tag{5.6}
$$

where $\alpha_\sigma = [\alpha_{2\sigma}, \alpha_{3\sigma}, \alpha_{4\sigma}...\alpha_{n\sigma}]^T$, $\alpha_f = [\alpha_{2f}, \alpha_{3f}, \alpha_{4f}...\alpha_{nf}]^T$, $\tilde{\alpha}_f = [\tilde{\alpha}_{2f}, \tilde{\alpha}_{3f}, \tilde{\alpha}_{4f}...\tilde{\alpha}_{nf}]^T$.

Chapter 5. Neural disturbance observer-based backstepping controller for singularly perturbed switched systems

5.4 Closed Loop Stability

It should be noted that the closed loop dynamics (5.5)-(5.6) is a switched nonlinear singularly perturbed system [93]. Replacing α_f in (5.4) with the root of the fast subsystem, α_σ, results in the following reduced slow subsystem:

$$
\begin{aligned}
\dot{z}_1 &= -\lambda_{1\sigma}(z_{1r}) + g_{1\sigma}(x)z_{2r} \\
\dot{z}_i &= -g_{(i-1)\sigma}(x)z_{(i-1)r} - \lambda_{i\sigma}(z_{ir}) + g_{i\sigma}(x)z_{(i+1)r} \\
\dot{z}_n &= -g_{(n-1)\sigma}(x)z_{(n-1)r} - \lambda_{n\sigma}(z_{nr}), i = 2, ..., (n-1).
\end{aligned}
\tag{5.7}
$$

The reduced slow system in compact form can be written as:

$$
\dot{z} = f_\sigma(z)
\tag{5.8}
$$

Consider the fast filter dynamics, when

$$
\mu \to 0 \Rightarrow \alpha_f \to \alpha_\sigma = \alpha_{sm\sigma}
$$

where the slow manifold is represented as ($\alpha_{sm\sigma}$). Define a error variable $y = \alpha_f - \alpha_\sigma$, whose dynamics can be derived as:

$$
\mu\dot{y} = -y - \mu\dot{\alpha}_\sigma.
\tag{5.9}
$$

The fast boundary layer dynamics of (5.9), which are expressed in a stretched timescale $\tau = \frac{t}{\mu}$, can be formulated as follows [93].

$$
\frac{dy}{d\tau} = -y.
\tag{5.10}
$$

5.4.1 Stability of System Between Switching Instants

For a suitable choice of $\lambda_{i\sigma}(z_i) = k_{i\sigma}z_i$ with $k_{i\sigma} > 0 \ \forall\sigma$, the reduced order dynamics (5.7) can be derived to be linear in z, and (5.8) takes the form of

$$
\dot{z} = f_\sigma(z) = \Xi_\sigma z
\tag{5.11}
$$

where

$$
\Xi_\sigma =
\begin{bmatrix}
-k_{1\sigma} & g_{1\sigma}(x) & 0 & \cdots & 0 \\
-g_{1\sigma}(x) & -k_{2\sigma} & g_{2\sigma}(x) & \cdots & 0 \\
\ddots & \ddots & \ddots & \ddots & \ddots \\
0 & \cdots & 0 & g_{(n-1)\sigma}(x) & -k_{n\sigma}
\end{bmatrix}
$$

is a skew-symmetric matrix through the selections of k_i. Exploiting the properties of skew symmetric matrices:

$$
\frac{\Xi_\sigma^T + \Xi_\sigma}{2} =
\begin{bmatrix}
-k_{1\sigma} & 0 & 0 & \cdots & 0 \\
0 & -k_{2\sigma} & 0 & \cdots & 0 \\
\ddots & \ddots & \ddots & \ddots & \ddots \\
0 & \cdots & 0 & 0 & -k_{n\sigma}
\end{bmatrix}.
$$

Hence, there exists a set of symmetric positive definite matrices M_σ, Q_σ such that

$$
M_\sigma \Xi_\sigma + \Xi_\sigma^T M_\sigma \le -Q_\sigma. \tag{5.12}
$$

Let us define a Lyapunov function candidate

$$
V_{r\sigma} = \frac{1}{2} z^T M_\sigma z \tag{5.13}
$$

Then

$$
\underline{m}_\sigma ||z||^2 \le V_{r\sigma} \le \overline{m}_\sigma ||z||^2 \tag{5.14}
$$

where $\underline{m}_\sigma = \lambda_{\min}(M_\sigma), \overline{m}_\sigma = \lambda_{\max}(M_\sigma)$. Using (5.13) yields

$$
\dot{V}_{r\sigma} \le -\beta_\sigma ||z||^2 \le -(\beta_\sigma/\overline{m}_\sigma) V_{r\sigma}, \tag{5.15}
$$

where $\beta_\sigma = \lambda_{\min}(Q_\sigma)$.

Similarly, constructing a Lyapunov function $V_f = \frac{1}{2} y^T y$ and using (5.10), we can show

$$
\dot{V}_f \le -||y||^2 = -2V_f. \tag{5.16}
$$

Chapter 5. Neural disturbance observer-based backstepping controller for singularly perturbed switched systems

Once, the stability of the reduced order system has been established, it can be considered a scalar $(0 < p < 1)$ and set of composite Lyapunov functions

$$V_\sigma = (1-p)V_{r\sigma} + pV_f \tag{5.17}$$

whose derivative along the trajectories of all systems (5.5),(5.9) can be derived as

$$\dot{V}_\sigma(z,y) = (1-p)\frac{\partial V_{r\sigma}}{\partial z}(f_\sigma(z,\tilde{\alpha}_f)) - \frac{p}{\mu}\frac{\partial V_f}{\partial y}y - p\frac{\partial V_f}{\partial y}\dot{\alpha}_\sigma$$

$$\implies \dot{V}_\sigma(z,y) = (1-p)\frac{\partial V_{r\sigma}}{\partial z}(f_\sigma(z)) - \frac{p}{\mu}\frac{\partial V_f}{\partial y}y - p\frac{\partial V_f}{\partial y}\dot{\alpha}_\sigma \tag{5.18}$$

$$+ (1-p)\frac{\partial V_{r\sigma}}{\partial z}\left(f_\sigma(z,\tilde{\alpha}_f) - f_\sigma(z)\right).$$

The last term of (5.18) can be further simplified using the following Lemma 5.1.

Lemma 5.1: There exist positive constants $L_{1\sigma}$ such that

$$\frac{\partial V_{r\sigma}}{\partial z}\left(f_\sigma(z,\tilde{\alpha}_f) - f_\sigma(z)\right) \leq 2L_{1\sigma}||z||||y||. \tag{5.19}$$

Proof: Using Lipschitz inequality:

$$\Rightarrow \frac{\partial V_{r\sigma}}{\partial z}\left(f_\sigma(z,\tilde{\alpha}_f) - f_\sigma(z)\right) \leq \frac{\partial V_{r\sigma}}{\partial z}L_{1\sigma}||\tilde{\alpha}_f||.$$

From the structure of V_r, $||\frac{\partial V_{r\sigma}}{\partial z}|| \leq 2||M_\sigma||||z|| \leq 2\overline{m}_\sigma||z||$. Note that, $\tilde{\alpha} = y$ from the definition of y. Combining these two equations, R.H.S of (5.19) can be evaluated.

Assumption 5.3: There exist positive scalars $L_{2\sigma}, L_{3\sigma} \& L_{31\sigma}$ such that.

$$||\dot{\alpha}_\sigma|| = ||\frac{\partial \alpha_\sigma}{\partial z}\dot{z}|| \leq 2L_{2\sigma}||z|| + L_{3\sigma}||y|| + L_{31\sigma}. \tag{5.20}$$

Assumption 5.3 is standard for singularly perturbed dynamics [93]. It implies the rate of change of the virtual control signal α_σ to be slower than the growth of the weighted combination of z and the fast variable y. Further, many practical systems like robotic manipulators, inverted pendulums, ships, chemical systems,

synchronous machines, etc. satisfy Assumption 5.3 ([93, 94]).
Previously, it is defined that $V_f = \frac{1}{2}y^2y$. So, the value of $\frac{\partial V_f}{\partial y}$ can be evaluated.
Also from the equations (5.15) and (5.19) $\frac{\partial V_{r\sigma}}{\partial z}$ and $\frac{\partial V_{r\sigma}}{\partial z}\left(f_\sigma(z,\tilde{\alpha}_f) - f_\sigma(z)\right)$ can be exploited in equation (5.18) respectively to obtain the following equation (5.21).

$$\dot{V}_\sigma \leq -\beta_\sigma(1-p)||z||^2 - \frac{p}{\mu}||y||^2 + 2pL_{2\sigma}||z||||y||$$
$$+ pL_{3\sigma}||y||^2 + 2(1-p)L_{1\sigma}||z||||y|| + pL_{31\sigma}||y||. \quad (5.21)$$

It can be written in a compact form as:

$$\dot{V}_\sigma = -Z^T S_\sigma Z + pL_{31\sigma}Z \quad (5.22)$$

where $Z = [z,y]^T$ and

$$S_\sigma = \begin{bmatrix} (1-p)\beta_\sigma & -(1-p)L_{1\sigma} - pL_{2\sigma} \\ -(1-p)L_{1\sigma} - pL_{2\sigma} & p(\frac{1}{\mu} - L_{3\sigma}) \end{bmatrix} \quad (5.23)$$

The overall system is asymptotically stable only when S_σ is positive definite [4].
It can be derived that S_σ is positive definite if

$$\mu_\sigma \leq \mu_\sigma^* = \frac{\beta_\sigma}{\beta_\sigma L_{3\sigma} + \frac{1}{p(1-p)}((1-p)L_{1\sigma} + pL_{2\sigma})^2} \quad (5.24)$$

From the properties of M_σ, there exist two positive constants m_l, m_h such that

$$m_l I \leq M_\sigma \leq m_h I.$$

So, one can derive

$$\underline{\alpha}||Z||^2 \leq V_\sigma \leq \bar{\alpha}||Z||^2. \quad (5.25)$$

where

$$\underline{\alpha} = \min(\frac{(1-p)m_l}{2}, \frac{p}{2}), \quad \bar{\alpha} = \max(\frac{(1-p)m_h}{2}, \frac{p}{2}).$$

Hence, it can be concluded that within any two consecutive switching instances, the dynamics of the overall singularly perturbed system is stable, if $\mu_\sigma \leq \mu_\sigma^*$, i.e.

$$\dot{V}_\sigma \leq -\beta_\sigma^o V_\sigma + pL_{31\sigma}||Z|| \quad (5.26)$$

Chapter 5. Neural disturbance observer-based backstepping controller for singularly perturbed switched systems

where $\beta_\sigma^o = \frac{\lambda_{\min}(S_\sigma)}{\lambda_{\max}(S_\sigma)}$.

5.4.2 Lyapunov Function at Switching Instants

Starting with any time stamp $t_i, i \in N$, let the subsystem $\sigma(t_{i+1}^-)$ is active in the time interval $t \in [t_i, t_{i+1})$, and $\sigma(t_{i+1})$ is active when $t \in [t_{i+1}, t_{i+2})$. From (5.25),(5.26), and the structure of the Lyapunov function V_σ, one can derive:

$$V(t_{i+1}) - V(t_{i+1}^-) \leq \frac{\bar{\alpha} - \underline{\alpha}}{\underline{\alpha}} V(t_{i+1}^-)$$

at the switching instant t_{i+1}. Therefore,

$$V(t_{i+1}) \leq l_\mu V(t_{i+1}^-). \tag{5.27}$$

where $l_\mu = \frac{\bar{\alpha}}{\underline{\alpha}} \geq 1$. Consider a time (0, T), where the time of switchings is defined as $t_1, ..., t_{N_\sigma(0,T)}$. For a function

$$R(t) = \exp(\beta_\sigma^o t) V_\sigma, \ \beta^o = \min(\beta_\sigma^o) \forall \sigma \in P$$

it's time derivative in $t \in (t_i, t_{i+1})$ is given by

$$\dot{R}(t) = \beta^o R(t) + \exp(\beta^o t) \dot{V}_\sigma$$

which is non-positive in between two consecutive switching times. Exploiting (5.27), it can be derived that

$$R(T^-) \leq (l_\mu)^{N_\sigma(0,T)} R(t)$$

An average dwell time $\tau_a > 0$ in the interval (0, T) exists if there exists a positive scalar N_o such that

$$N_\sigma(0, T) \leq \frac{T - t}{\tau_a} + N_o \tag{5.28}$$

Using (5.28), it can be obtained

$$\Rightarrow V_{\sigma(T^-)} Z(T) \leq \exp(N_o \ln l_\mu) \exp(\frac{\ln(l_\mu)}{\tau_a} T - \beta_\sigma^o T) V_{\sigma(0)} Z(0).$$

$$\Rightarrow V_{\sigma(T^-)} Z(T) \leq \exp(N_o \ln l_\mu) \exp\left((-\beta^o + \frac{\ln l_\mu}{\tau_a})T\right) V_{\sigma(0)} Z(0)$$

Therefore, the function $V_{\sigma(T^-)} Z(T)$ asymptotically converges to zero, if the average dwell time satisfies

$$\tau_a > \frac{\ln l_\mu}{\beta^o}. \tag{5.29}$$

5.5   Conversion to Singularly Perturbed form

This section discusses control law for the overall closed-loop system with unknown uncertainties.

$$
\begin{aligned}
u_\sigma &= \frac{1}{g_{n\sigma}(x)}[-f_{n\sigma}(x) - g_{(n-1)\sigma}(x)z_{n-1} \\
&\quad - \lambda_{n\sigma}(z_n) + \dot{\alpha}_{nf} - \hat{\Delta}_{n\sigma}] \\
z_i &= x_i - \alpha_{if}, (i = 1, 2 \ldots\ldots n) \\
\alpha_{1f} &= \alpha_{1\sigma} = x_d(t) \text{ and for } i \in [2 \ldots n] \\
\alpha_{i\sigma} &= \frac{1}{g_{(i-1)\sigma}(x)}[-f_{(i-1)\sigma}(x_1, ..x_{i-1}) - \lambda_{(i-1)\sigma}(z_{i-1}) \\
&\quad - g_{(i-2)\sigma}(x)z_{i-2} + \dot{\alpha}_{(i-1)f} - \hat{\Delta}_{(i-1)\sigma}].
\end{aligned}
\tag{5.30}
$$

where the tuning functions are chosen similarly to the case with no disturbances in the system dynamics, i.e. $\lambda_{i\sigma}(z_i) = k_{i\sigma}z_i$. The closed-loop system of (5.1), using the control law (5.30), can be written as:

$$
\begin{aligned}
\dot{z}_1 &= -\lambda_{1\sigma}(z_1) + g_{1\sigma}(x)z_2 + g_{1\sigma}(x)\tilde{\alpha}_{2\sigma} + \tilde{\Delta}_1 \\
\dot{z}_i &= g_{(i-1)\sigma}(x)z_{i-1} - \lambda_{i\sigma}(z_i) \\
&\quad + g_{i\sigma}(x)z_{i+1} + g_{i\sigma}(x)\tilde{\alpha}_{(i+1)\sigma}, +\tilde{\Delta}_i \\
\dot{z}_n &= -g_{(n-1)\sigma}(x)z_{n-1} - \lambda_{n\sigma}(z_n) + \tilde{\Delta}_n.
\end{aligned}
\tag{5.31}
$$

Rewriting (5.31) in a compact form, we can get

$$\dot{z} = f_\sigma(z, \tilde{\alpha}_f, \tilde{\Delta}) \tag{5.32}$$

$$\mu\dot{\tilde{\alpha}}_f = -\tilde{\alpha}_f + \mu\dot{\alpha}_\sigma \tag{5.33}$$

$$\epsilon\dot{\tilde{\Delta}} = h(\hat{\Delta}, \Delta_\sigma) = -\tilde{\Delta} + \epsilon\dot{\Delta}_\sigma \tag{5.34}$$

where $\hat{\Delta} = [\hat{\Delta}_1, \hat{\Delta}_2, \ldots, \hat{\Delta}_n]$, $\tilde{\Delta} = [\tilde{\Delta}_1, \tilde{\Delta}_2, \ldots, \tilde{\Delta}_n]$ $\Delta_\sigma = [\Delta_{1\sigma}\Delta_{2\sigma}, \ldots, \Delta_{n\sigma}]$. The dynamics are transformed into a three-time scale singularly perturbed switched system. It can be rewritten in a two-time scale form using the ratio $\frac{\epsilon}{\mu}$. Without loss of generality, we assume $\epsilon < \mu$, meaning the observer dynamics are faster than the filter dynamics. Let $\epsilon = \kappa\mu$, where κ is less than one. The fast subsystem (5.33), (5.34) can be expressed as:

$$\mu\dot{\tilde{v}} = W_\sigma(\tilde{v}, \dot{v}_\sigma, \kappa) = -\begin{bmatrix} 1 & 0 \\ 0 & \frac{1}{\kappa} \end{bmatrix} \tilde{v} + \mu\dot{v}_\sigma \tag{5.35}$$

where $\tilde{v} = [\tilde{\alpha}_f^T, \tilde{\Delta}^T]^T$, $\dot{v}_\sigma = [\dot{\alpha}_\sigma^T, \dot{\Delta}_\sigma^T]^T$ and $W_\sigma(.) = [g_\sigma^T(.), \frac{1}{\kappa}h_\sigma^T(.)]^T$. Using (5.35), the closed-loop dynamics can be expressed in a two-time scale singularly perturbed form. Therefore, the system's trajectory convergence can be analyzed using the same approach as mentioned in Section 5.4.

5.6   Prerequisites on neural network

The Radial Basis Function Neural Network (RBFNN) is frequently used to simulate nonlinear continuous functions because of its superior function approximation capabilities. In a typical three-layer RBFNN, there are three layers: input, hidden, and output. This structure allows RBFNNs to learn and approximate complex functions effectively.

$$y_k(x, w_k) = \sum_{j=1}^{h} \omega_{kj}\varphi_{kj}(x) \tag{5.36}$$

$$= w_k^T\phi_k(x), k = 1, \ldots, m \tag{5.37}$$

5.6. Prerequisites on neural network

with

$$
w_k = \begin{bmatrix} \omega_{k1} \\ \vdots \\ \omega_{kh} \end{bmatrix}, \phi_k(x) = \begin{bmatrix} \varphi_{k1}(x) \\ \vdots \\ \varphi_{kh}(x) \end{bmatrix}
$$

In an RBFNN, n, h, and m represent the number of neurons in the input, hidden, and output layers, respectively. The network's outputs, denoted as $y_k(x, w_k)$ for $k = 1, \ldots, m$, depend on the input vector x and the adjustable weight parameters ω_{kj}, where $k = 1, \ldots, m$ and $j = 1, \ldots, h$. According to the approximation theorem [106], the activation function $\varphi_j(x)$ in the hidden layer is chosen as a Gaussian function, which is defined as follows:

$$
\varphi_j(x) = \exp \left[-\frac{\|x - \mu_j\|^2}{2\sigma_j^2} \right] \tag{5.38}
$$

$$
= \exp \left[-\frac{(x - \mu_j)^T (x - \mu_j)}{2\sigma_j^2} \right], j = 1, \ldots, h \tag{5.39}
$$

Here, $\mu_j = [\mu_{1j}, \mu_{2j}, \ldots, \mu_{hj}]^T$ represents the center of the receptive field, while σ_j determines the width of the activation function $\varphi_j(x)$. The complete RBFNN can be expressed as:

$$
y(x, \hat{W}) = \begin{bmatrix} f_1(x, w_1) \\ \vdots \\ f_m(x, w_m) \end{bmatrix} = \begin{bmatrix} w_1^T \phi_1(x) \\ \vdots \\ w_m^T \phi_m(x) \end{bmatrix} \tag{5.40}
$$

$$
= \hat{W}^T \Phi(x) \tag{5.41}
$$

where

$$
\hat{W} = \begin{bmatrix} w_1^T \\ w_2^T \\ \vdots \\ w_m^T \end{bmatrix}, \Phi(x) = \begin{bmatrix} \phi_1(x) & 0 & \cdots & 0 \\ 0 & \phi_2(x) & \cdots & 0 \\ \vdots & \vdots & \ddots & \vdots \\ 0 & 0 & \cdots & \phi_m(x) \end{bmatrix}
$$

Chapter 5. Neural disturbance observer-based backstepping controller for singularly perturbed switched systems

In this case, the RBFNN is used to approximate the nonlinear function $\hbar(x)$.

$$\hbar(x) = W^{*\,\mathrm{T}}\Phi(x) + \varepsilon \tag{5.42}$$

Here, W^* represents the ideal weight matrix, and ε is the minimum approximation error.

Lemma 5.2: Let $\hbar(x)$ be a continuous function defined on a compact set Ω. Suppose there is a predefined constraint region $\Omega_W = \{\hat{W} \in \mathbb{R}^{h\times m} \mid \|W\| \leq D_B\}$, where the ideal weight matrix belongs to Ω_W. In this case, the function $\hat{\hbar}(x)$ can approximate $\hbar(x)$ as accurately as possible, i.e.:

$$\sup_{x\in\Omega} |\hbar(x) - \hat{\hbar}(x, \hat{W})| \leq \varepsilon \tag{5.43}$$

Here, $\hat{\hbar}(x)$ represents the RBFNN's estimation of the function $\hbar(x)$. The ideal weight matrix is defined as:

$$W^* = \arg \min_{W\in\Omega_W} \left\{ \sup_{x\in\Omega} |\hbar(x) - \hat{\hbar}(x, \hat{W})| \right\} \tag{5.44}$$

Assumption 5.4: Without loss of generality, we assume that there is a positive constant $D_\varepsilon > 0$ such that the error $|\varepsilon|$ is always bounded by D_ε.

5.6.1   Neural network disturbance observer

The state-space representation, incorporating unknown disturbances and uncertainties, can be expressed using the following equation.

$$\begin{cases} \dot{x}_i = f_{i\sigma}(\bar{x}_i) + g_{i\sigma}(\bar{x}_i)x_{i+1} + \Delta_{i\sigma}(x), \\ i = 1,\ldots,n-1 \\ \dot{x}_n = f_{n\sigma}(\bar{x}_n) + g_{n\sigma}(\bar{x}_n)u + \Delta_{n\sigma}(x) \end{cases} \tag{5.45}$$

Here, $\bar{x}_i = [x_1,\ldots,x_i]^T$ represents the system states. The functions $f_{i\sigma}(\bar{x}_i)$ and $g_{i\sigma}(\bar{x}_i)$ are the known parts of the nonlinear model, while $\Delta_{i\sigma}(x)$ (for $i = 1,\ldots,n$) represents the unknown parts, which include uncertainties and disturbances. To estimate these unknown uncertainties and disturbances $\Delta_{i\sigma}(\bar{x}_i)$, a Neural

Network Disturbance Observer (NNDO) is introduced. The dynamic model of the NNDO is designed as follows:

$$
\begin{cases}
\dot{\varpi}_i = \kappa_i\,(x_i - \varpi_i) + f_{i\sigma}(\bar{x}_i) + \\
\quad g_{i\sigma}(\bar{x}_i)x_{i+1} + \hat{\Delta}_i(x,\hat{W}_i), \\
\qquad\qquad i = 1,\dots,n-1 \\
\qquad\qquad \dot{\varpi}_n = \kappa_n\,(x_n - \varpi_n) + f_{n\sigma}(\bar{x}_n) + \\
\quad g_{n\sigma}(\bar{x}_n)u + \hat{\Delta}_n(x,\hat{W}_n)
\end{cases}
\tag{5.46}
$$

Here, κ_i $(i = 1,\dots,n)$ are positive constants, and $\hat{\Delta}_i(x,\hat{W}_i)$ represents the estimated value of $\Delta_{i\sigma}(x)$ for $i = 1,\dots,n$. Next, we define the auxiliary disturbance observer error variables as:

$$
e_i = x_i - \varpi_i, i = 1,\dots,n \tag{5.47}
$$

Differentiate both sides of Eq. (5.47),

$$
\dot{e}_i = \dot{x}_i - \dot{\varpi}_i = -\kappa_i e_i + \Delta_{i\sigma}(x) - \hat{\Delta}_i\left(x,\hat{W}_i\right) \tag{5.48}
$$
$$
= -\kappa_i e_i + \Delta_{i\sigma}(x) - \hat{W}_i^{\mathrm{T}}\phi_i(x), i = 1,\dots,n \tag{5.49}
$$

Based on Lemma 5.2, the unknown disturbances $\Delta_{i\sigma}(x)$ for $i = 1,\dots,n$ can be expressed as:

$$
\Delta_{i\sigma}(x) = W_i^{*\,\mathrm{T}}\phi_i(x) + \varepsilon_i, i = 1,\dots,n \tag{5.50}
$$

As stated in [107], the neural disturbance observer corresponding to equation (5.45) is formulated as equation (5.46). Furthermore, the adaptive weight parameters of the Radial Basis Function Neural Network (RBFNN) are designed accordingly as

$$
\dot{\hat{W}}_i = \eta_{1i}\left(\phi_i(x)e_i - \eta_{2i}\hat{W}_i\right), i = 1,\dots,n \tag{5.51}
$$

where $\eta_{1i} > 0$ and $\eta_{2i} > 0$ for $i = 1,\dots,n$ are the positive parameters. Then, the weight parameter errors $\tilde{W}_i$ for $i = 1,\dots,n$ and the neural disturbance observer errors e_i remain uniformly ultimately bounded (UUB) within an arbitrarily small region.

5.7 Outcome results

An example of a single-link manipulator system incorporating actuator dynamics has been considered [95, 96]. The system dynamics are given in (5.52).

$$D\ddot{q} + B\dot{q} + N\sin(q) = \tau$$
$$M\dot{\tau} + H\tau + K_m\dot{q} = u \tag{5.52}$$

The model parameters D, B, N, M, H, and K_m are determined by the physical characteristics of both the robot and the actuator. The scalars q and $\dot{q}$ denote the joint's angular position and velocity, respectively. The torque applied at the joint via the motor is represented by τ, while u signifies the control input voltage supplied to the motor to generate the required torque. By choosing,

$$x_1 = q$$
$$x_2 = \dot{q} \tag{5.53}$$
$$x_3 = \tau$$

Equation (5.52) can be written in strict feedback form as

$$\dot{x}_1 = x_2$$
$$\dot{x}_2 = \frac{1}{D}(-N\sin(x_1) - Bx_2) + \frac{1}{D}x_3 \tag{5.54}$$
$$\dot{x}_3 = -\frac{1}{M}(K_m x_2 + Hx_3) + \frac{1}{M}u$$

The objective of the controller is to ensure that the output q follows the desired trajectory $x_d(t)$ while keeping all other signals bounded. The term z_i is defined as $z_i = x_i - \alpha_{if}$, where $i = 1, 2, 3, \ldots, n$, with α_{1f} set as $\alpha_1 = x_d(t)$. Here, the control input u_σ is designed for the switching signals $\sigma = 1, 2, 3, 4$. The system parameter, including D, B, N, M, H, and k_m, corresponding to each switching signal $\sigma = 1, 2, 3, 4$, are given in Table 5.1.

A four time switching mechanism for the reference signals i.e. $\sin(10t)$, $\sin(10t + 20)$ is illustrated in Figures 5.1 to 5.10. Based on different values of $k_{i\sigma}$ and system parameters the value of $\frac{\ln l_\mu}{\beta^o} = 0.48$ sec can be determined. The average dwell time (τ_a) can be computed over the interval 0 to

FIGURE 5.1: Closed loop response for x_1 for reference $\sin(10t)$.

FIGURE 5.2: Tracking error for reference $\sin(10t)$

Chapter 5. Neural disturbance observer-based backstepping controller for singularly perturbed switched systems
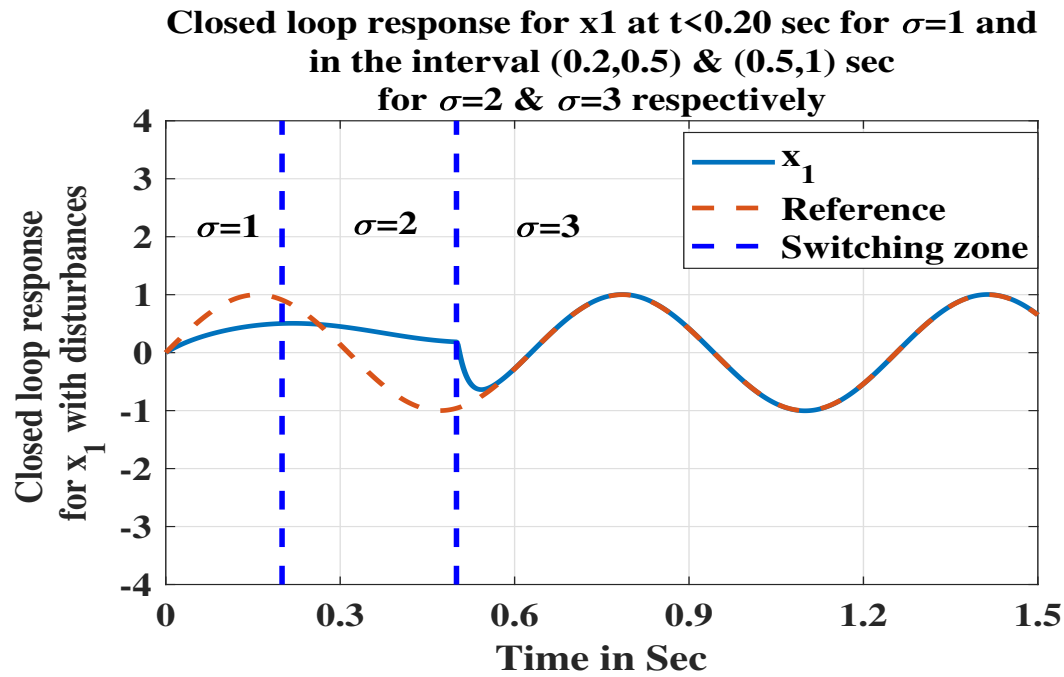
FIGURE 5.3: Closed loop response for x_1 for reference $\sin(10t)$.
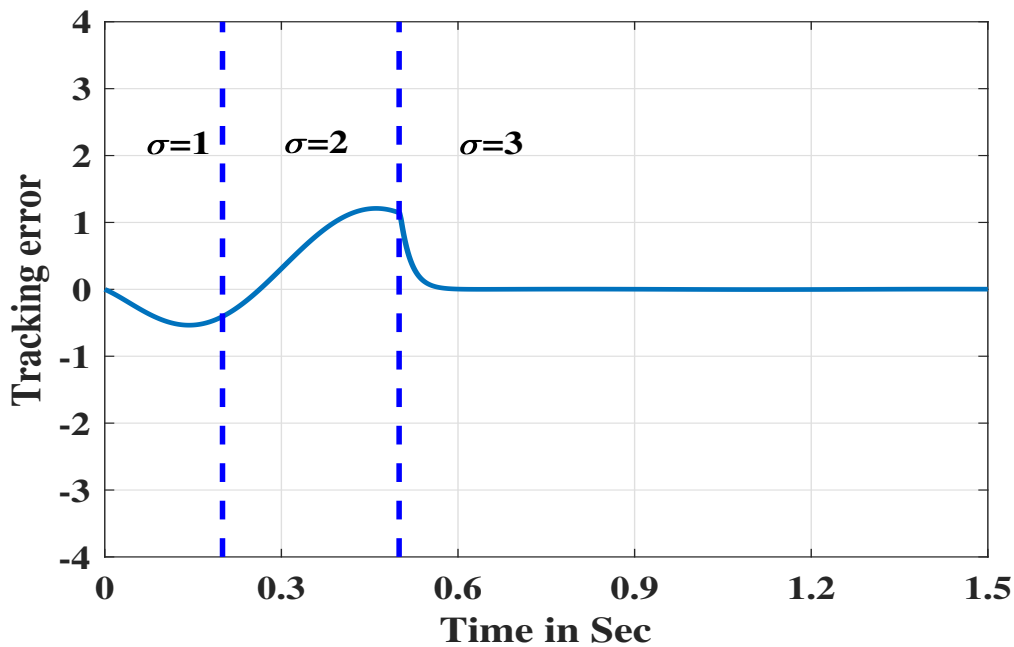
FIGURE 5.4: Tracking error for reference $\sin(10t)$
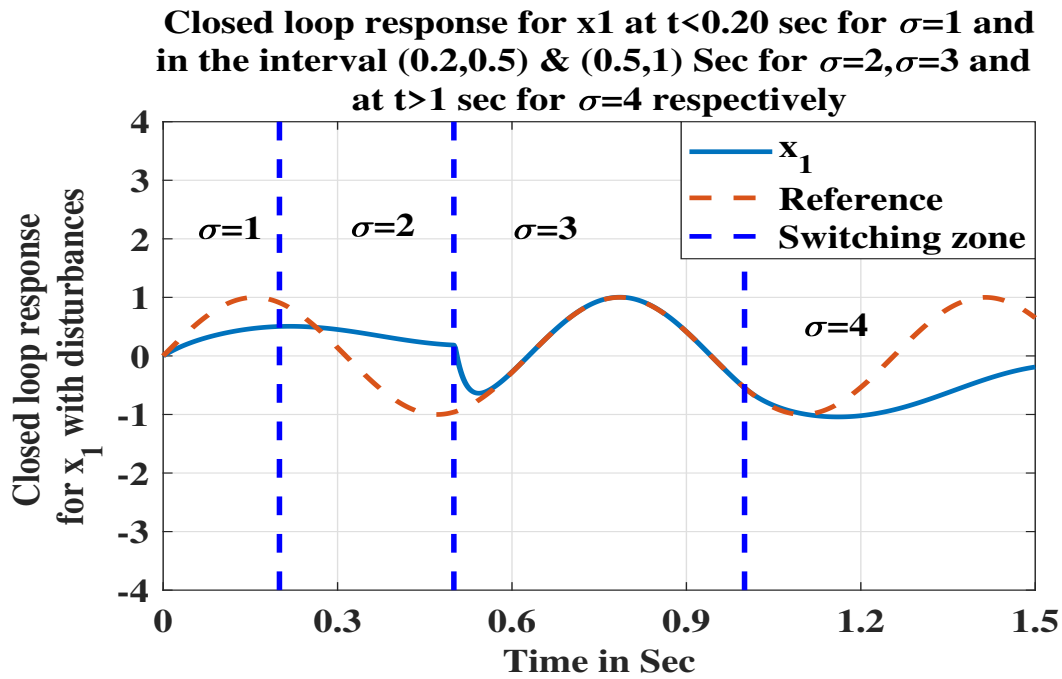
FIGURE 5.5: Closed loop response for $\tau_a \not> \frac{\ln l_\mu}{\beta^o}$ and doesn't track the referemce $sin(10t)$.
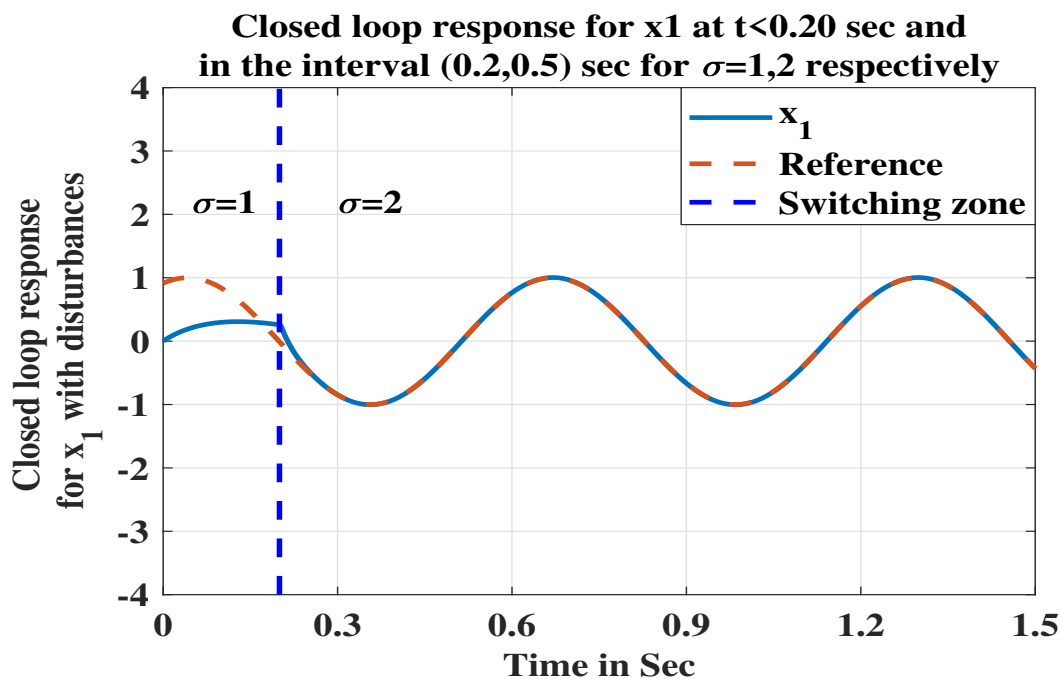
FIGURE 5.6: Closed loop response for x_1 for reference $sin(10t + 20)$.

Chapter 5. Neural disturbance observer-based backstepping controller for singularly perturbed switched systems

FIGURE 5.7: Tracking error for reference $\sin(10t + 20)$
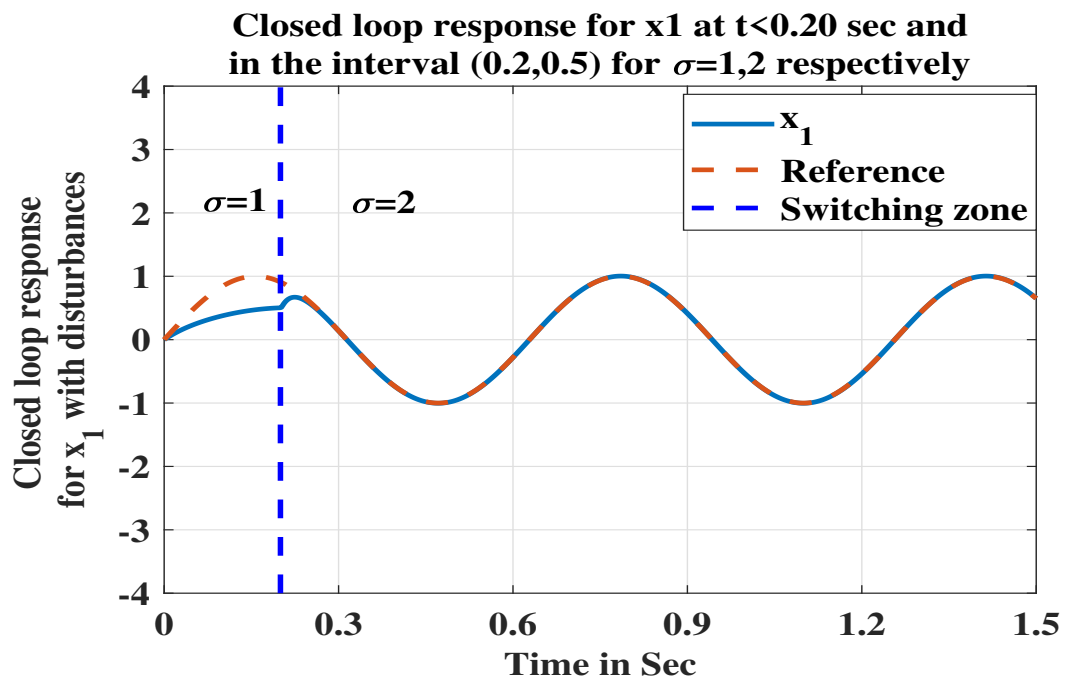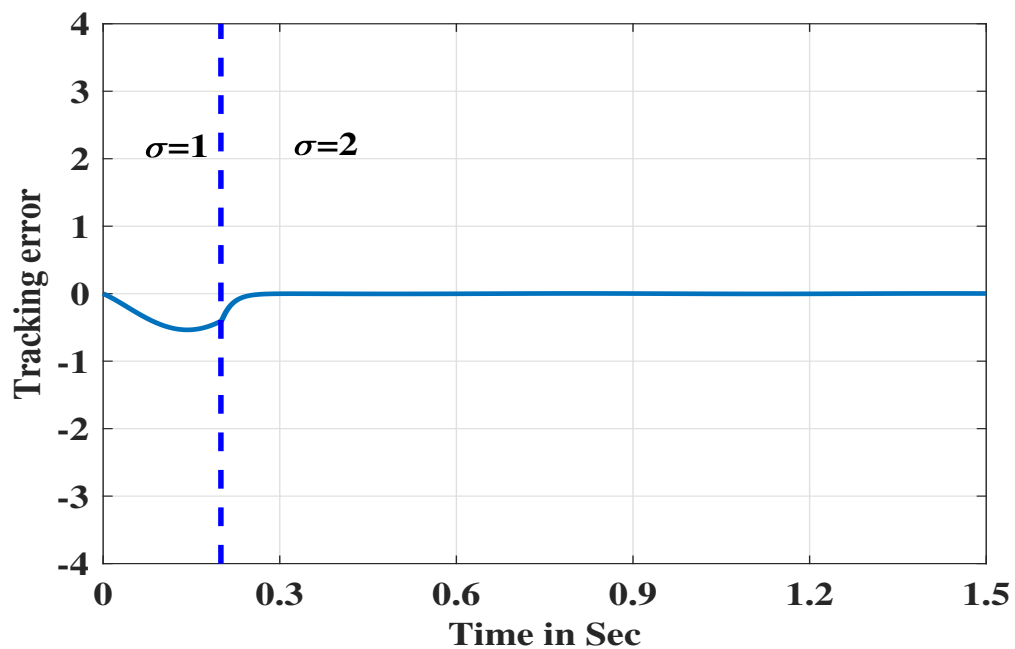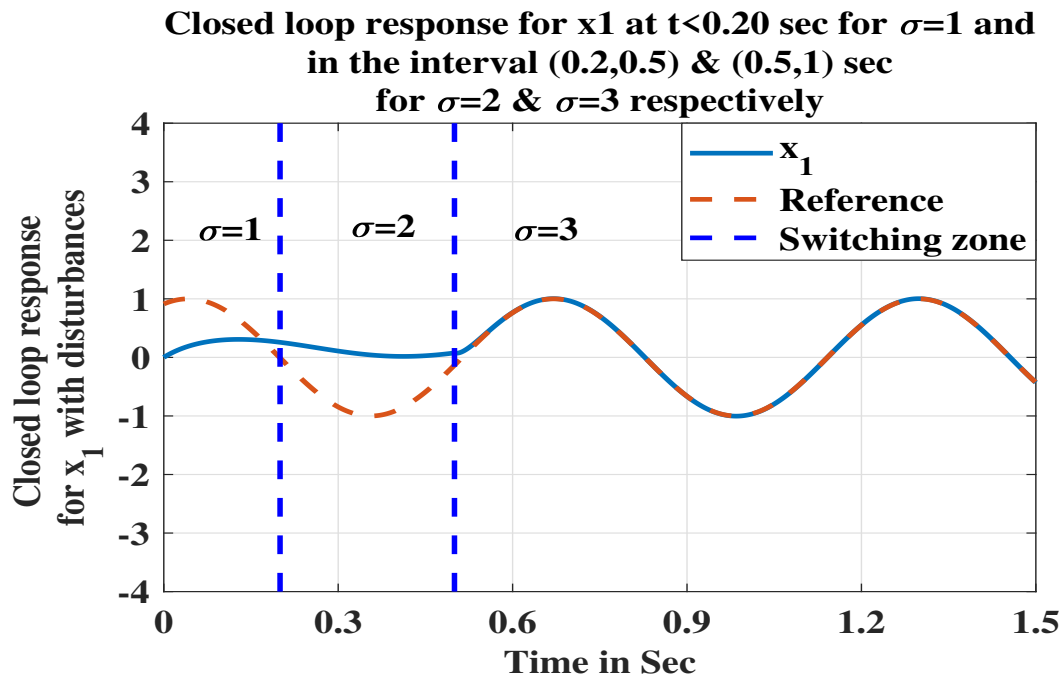
FIGURE 5.8: Closed loop response for x_1 for reference $\sin(10t + 20)$.

FIGURE 5.9: Tracking error for reference $\sin(10t + 20)$

FIGURE 5.10: Closed loop response for $\tau_a \not> \frac{\ln l_\mu}{\beta^o}$ for reference $\sin(10t + 20)$.

Chapter 5. Neural disturbance observer-based backstepping controller for singularly perturbed switched systems

FIGURE 5.11: Closed loop response for x_1 for reference $\sin(10t)$

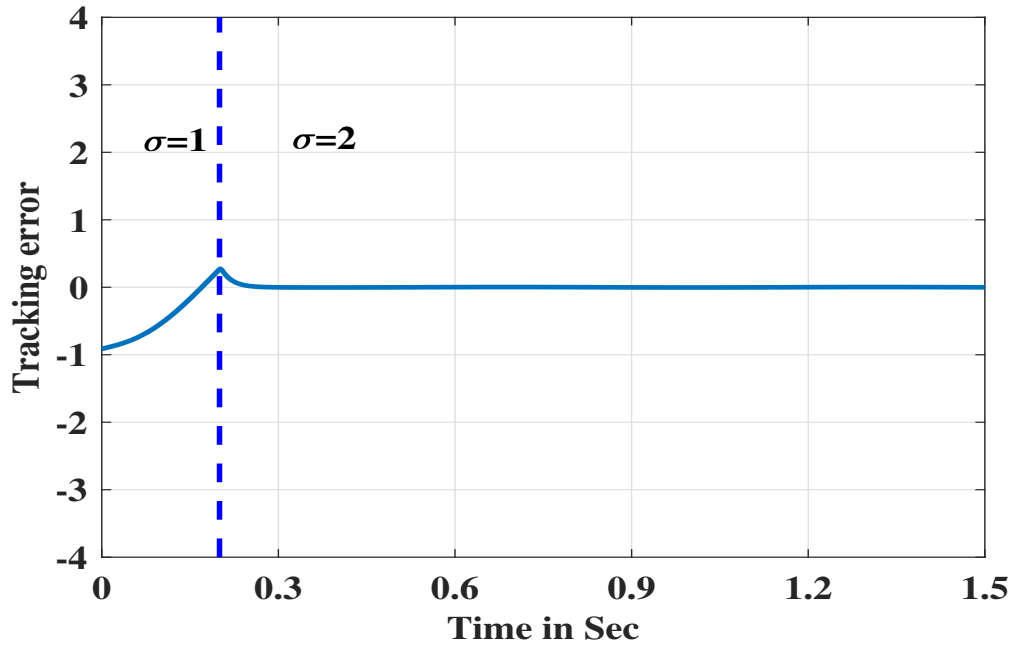FIGURE 5.12: Closed loop response for x_1 for reference $\sin(10t + 20)$
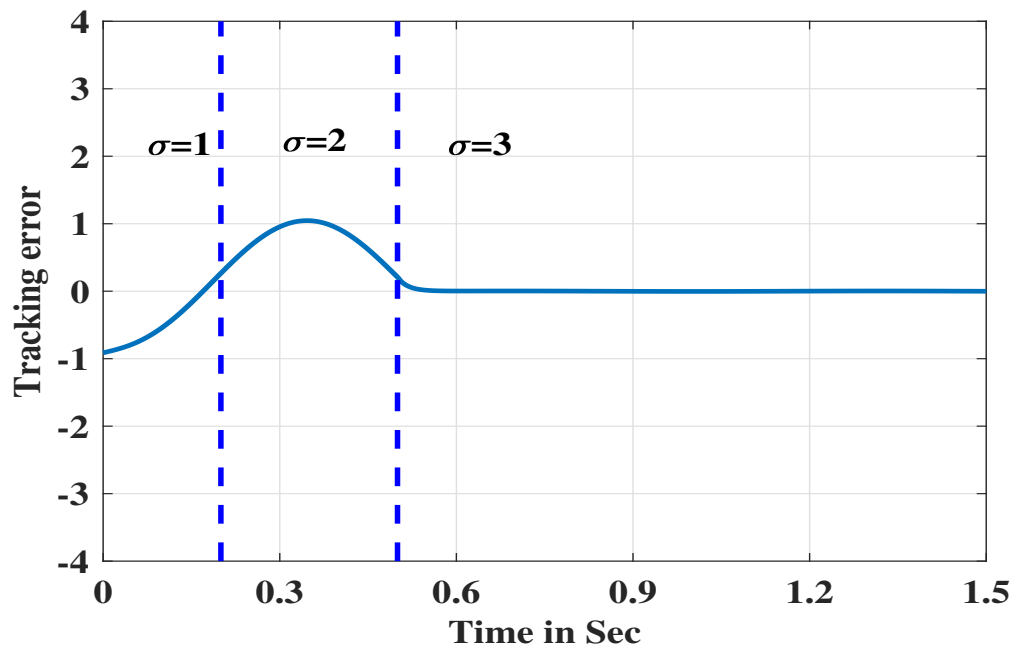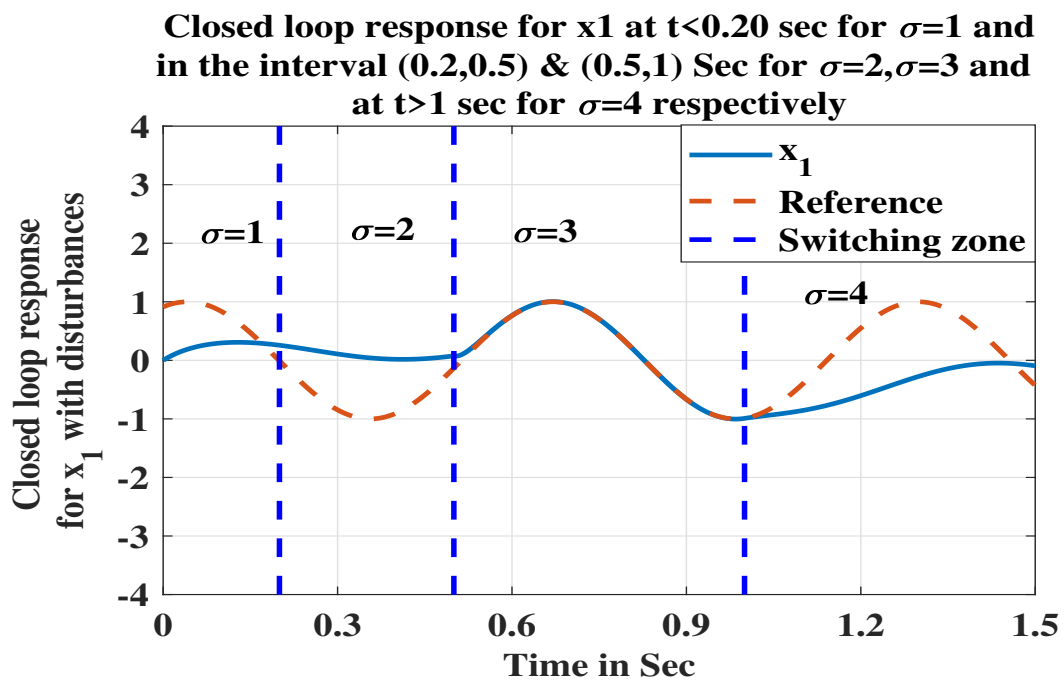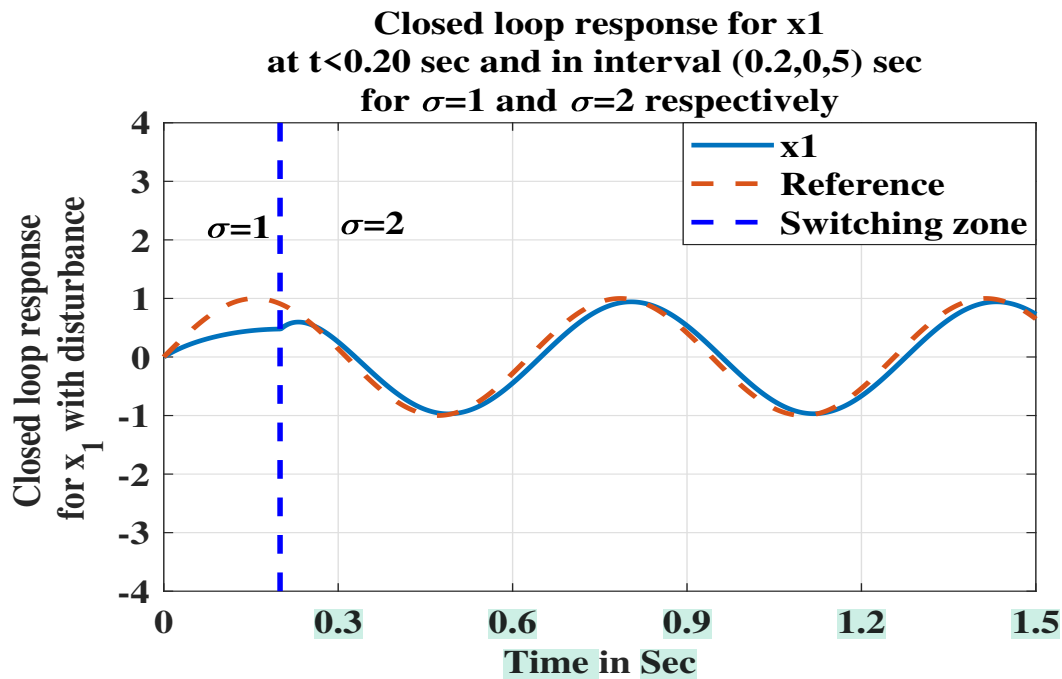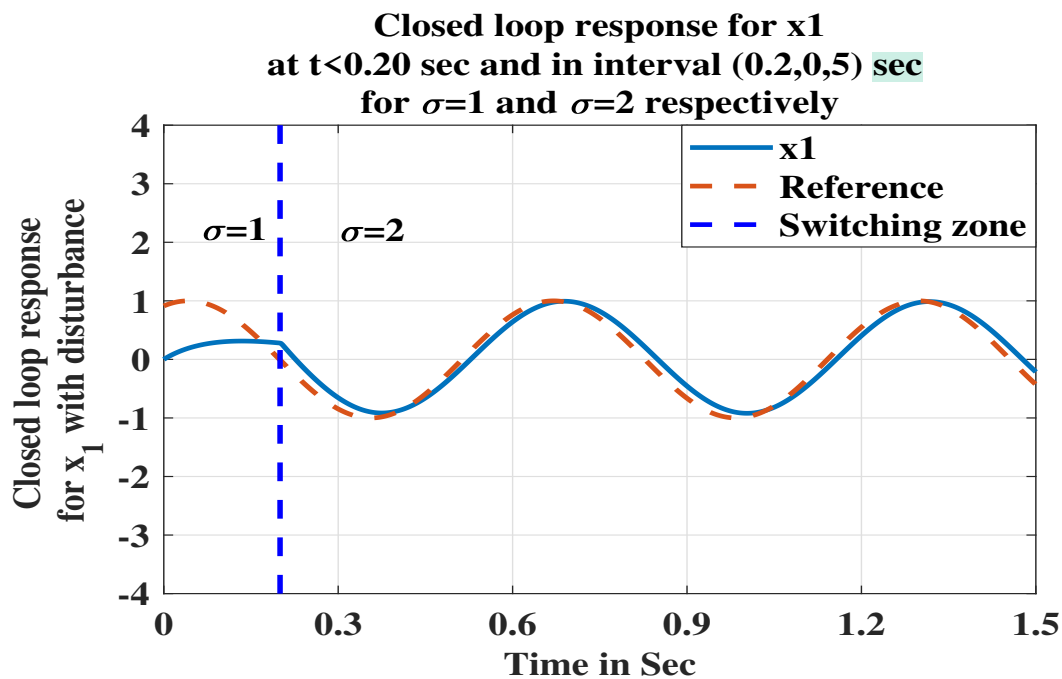
5.7. Outcome results 107

TABLE 5.1: The parameters of the system for different switching signals.

System Parameters	D	B	N	M	H	km
For $\sigma = 1$	1	1	10	0.01	0.5	100
For $\sigma = 2$	10	150	10	0.01	0.5	10
For $\sigma = 3$	10	150	1	0.01	0.5	10
For $\sigma = 4$	10	1	10	0.01	0.5	100

1.5 sec using ($\tau_a = \frac{\text{Time interval}}{\text{No. of switching}}$). For instance, when switching occurs at $\sigma = 1$ for $t < 0.20$ s and at $\sigma = 2$ for the interval 0.2 to 0.55 sec, average dwell time can be calculated as $\tau_a = \frac{1.5}{2} = 0.75$ sec. Here, the disturbances are defined as $\Delta_1 = 0.1 \tanh(2t)$ and $\Delta_2 = 0.1 \tanh(2t)$ for $\sigma = 1$, while for $\sigma = 2, 3, 4$, the disturbances are given by $\Delta_1 = 0.1 \sin(2t)$ and $\Delta_2 = 0.1 \cos(2t)$. The average dwell time for $\sigma = 1$ at $t < 0.20$ sec and for $\sigma = 2$ in the interval 0.20 to 0.50 sec is calculated as $\tau_a = \frac{1.5}{2} = 0.75$ sec. Since this satisfies the condition $\tau_a > \frac{\ln l_\mu}{\beta^o}$ (where $\frac{\ln l_\mu}{\beta^o} = 0.48$ sec), the state x_1 successfully tracks the reference signals, as illustrated in Figures 5.1 and 5.6. The corresponding tracking error is depicted in Figures 5.2 and 5.7.

For $\sigma = 1, 2, 3$, the switching occurs at $t < 0.20$ sec and within the intervals 0.20 to 0.55 sec and 0.50 to 1 sec, respectively. So, the average dwell time will be $\tau_a = \frac{1.5}{3} = 0.50$ sec. Since this satisfies the condition $\tau_a > \frac{\ln l_\mu}{\beta^o}$, the state x_1 successfully tracks the reference signals, as illustrated in Figures 5.3 and 5.8. The corresponding tracking error is presented in Figures 5.4 and 5.9. However, for $\sigma = 1, 2, 3, 4$, where switching occurs at $t < 0.20$ sec and in the intervals 0.20 to 0.50 sec, 0.50 to 1 sec, and $t > 1$ sec, the average dwell time will be $\tau_a = \frac{1.5}{4} = 0.37$ sec. Since this does not satisfy the condition $\tau_a > \frac{\ln l_\mu}{\beta^o}$, the state x_1 fails to track the reference signals. This behavior is depicted in Figures 5.5 and 5.10. The proposed theory of this chapter can be summarized in Theorem 5.1.

Theorem 5.1: Given the singularly perturbed switched system defined by Equation (5.1) and assuming that Assumptions 5.1-5.4 hold, the states of the closed-loop system will asymptotically converge within the bound specified in Equation (5.24) under the switched control law (5.30), provided that the average dwell time condition in inequality (5.29) is satisfied.

Chapter 5. Neural disturbance observer-based backstepping controller for
singularly perturbed switched systems

The control law without switching is presented in reference [80]:

$$u = \frac{1}{g_n(x)}[-f_n(x) - g_{(n-1)}(x)z_{n-1} - \lambda_n(z_n) + \dot{\alpha}_{nf}]$$

$$z_i = x_i - \alpha_{if}, (i = 1, 2......n)$$

$$\alpha_{1f} = \alpha_1 = x_d(t)$$

(5.55)

where $\lambda_i(z_i) = k_i z_i$ are user-defined tuning functions for which $k_i > 0$. The terms α_{if} are obtained through the first order filter [75, 76]. By using this controller the performance of the state x_1 under the switching signal σ for the reference signals $\sin(10t)$ and $\sin(10t + 20)$ is illustrated in Figures 5.11 and 5.12, respectively. It can be observed that the system attempts to follow the reference signal when the switching signal $\sigma = 1, 2$ is applied. However, due to variations in the system's parameters, the state x_1 is unable to accurately track the reference signal x_d. To address this issue, a filtered backstepping controller has been implemented.

5.7.1   The performance of the Controller during four time switching

In four-time switching, the manipulator initially operates in a compressed mode ($\sigma = 1$) for $t < 0.20$ sec. It then transitions to $\sigma = 2$ during the interval 0.20 to 0.50 sec before reverting back to $\sigma = 1$ at $t = 0.5$ sec. Then, the manipulator further changes its configuration to $\sigma = 3$ during the interval 0.50 to 1 sec. Since the switching signals $\sigma = 1, 2, 3$ satisfy the average dwell time condition, the manipulator continues to track the reference signals. This behaviour is illustrated in Figures 5.3 and 5.8. However, the system transitions to $\sigma = 4$ at $t > 1$ sec, at which point the average dwell time condition is no longer met. As a result, the manipulator fails to track the reference signals, as shown in Figures 5.5 and 5.10.

5.8   Concluding remarks

This chapter presents an effective control strategy for nonlinear singularly perturbed switched systems by integrating a neural network-based disturbance observer with a filtered backstepping control approach. The proposed method

5.8. Concluding remarks   109

leverages the average dwell time-based Lyapunov criteria to ensure system stability while mitigating disturbances and uncertainties through adaptive neural network approximation. The high-gain filter, in combination with the disturbance observer, successfully handles the complexities of fast and slow dynamics in the singular perturbation framework. Simulation results, validated on a single-link manipulator system with actuator dynamics, demonstrate the robustness of the proposed controller in trajectory tracking and disturbance rejection. Nevertheless, the methodology also has certain limitations. The reliance on neural network training and adaptation increases computational demand, which may present challenges for real-time implementation on hardware with limited resources. In addition, the controller involves multiple tuning parameters such as neural network learning rates, filter gains, and switching constraints that may require careful adjustment to achieve optimal performance. Furthermore, the stability analysis, while rigorous, assumes ideal conditions that may not fully capture all uncertainties in physical systems. These findings indicate the potential applicability of this control methodology to other complex dynamical systems with switching behaviors, offering a promising direction for future research in intelligent control and adaptive learning-based disturbance compensation.

Chapter 6

Neural backstepping controller for singularly perturbed switched systems

6.1   Background

This chapter addresses the control of singularly perturbed switched systems (SPSSs), which involve fast–slow dynamics and mode transitions, making stability analysis and controller design highly challenging. To handle these complexities, a neural backstepping controller is developed, leveraging the approximation capability of neural networks to manage system uncertainties [108]. A high-gain filter is integrated to reduce computational complexity, while a high-gain disturbance observer (HGDO) is incorporated to suppress unknown external disturbances. The overall strategy enhances robustness and practicality compared to conventional methods. Stability is analyzed under switching conditions, and the effectiveness of the proposed approach is demonstrated through simulations on a single-link manipulator with actuator dynamics.

6.2 System Description

Consider a class of nonlinear systems described as:

$$
\begin{aligned}
\dot{x}_1 &= f_{1\sigma}(x_1) + b_{1\sigma}(x_1)x_2 + \delta_{1\sigma}(x_1, t) \\
\dot{x}_2 &= f_{2\sigma}(x_1, x_2) + b_{2\sigma}(x_1, x_2)x_3 + \delta_{2\sigma}(x_1, x_2, t) \\
&\vdots \\
\dot{x}_n &= f_{n\sigma}(x_1, x_2, x_3....x_n) + b_{n\sigma}(x_1, x_2, \ldots, x_n)u + \delta_{n\sigma}(x, t)
\end{aligned}
\tag{6.1}
$$

where $f_{i\sigma}(.), b_{i\sigma}(.)$ are known sufficiently smooth functions, $x = [x_1, x_2, ..., x_n]^T$, $b_{i\sigma}(.) \neq 0 \; \forall x \in R^n$, $\sigma \in P = [1, 2, \cdots, N]$ is piece-wise constant signal with finite number of values and $u \in R$ is the control input. The terms $\delta_{i\sigma}(.)$ represent uncertainties of systems.

Assumption 6.1: The desired signal i.e. $x_d(t)$ and its derivatives are continuous and have finite bounds.

6.3 Controller Design

The filtered-based control law in the absence of uncertainties is expressed as:

$$
\begin{aligned}
u_\sigma &= \frac{1}{b_{n\sigma}(x)}[-\hat{f}_{n\sigma}(x) - b_{(n-1)\sigma}z_{n-1} - \chi_{n\sigma}(z_n) + \dot{\alpha}_{nf}] \\
z_i &= x_i - \alpha_{if}, (i = 1, 2......n) \\
\alpha_{1f} &= \alpha_1 = x_d(t) = \text{Desired signal}
\end{aligned}
\tag{6.2}
$$

Where, $\hat{f}_i(.)$ is the estimate values of $f(.)$. Assuming that the nonlinear function $f_i(.)$ can be represented by an m-layer neural network with some constant ideal weights W_i for $i = 1, 2, \ldots, m$.

$$
F_i = W_i'\phi_i + \epsilon_i
\tag{6.3}
$$

Where, $||\epsilon_i|| < \epsilon_{iN}$ and ϕ_i is suitable basis function for m NNs. The net reconstruction errors ϵ_i are bounded by known constants $\epsilon_{iN}, i = 1, 2, ...m$. Let us

6.3. Controller Design

113

consider the NN estimation of (6.3) is

$$\hat{F}_i = \hat{W}_i' \phi_i \tag{6.4}$$

Where, $\hat{W}_i$ is the current NN weight estimate. The terms α_{if} are obtained through the first order filter[75, 76] and expressed as:

$$\mu \dot{\alpha}_{if} = -\alpha_{if} + \alpha_{i\sigma} \quad i = 2, \cdots, n$$
$$\alpha_{i\sigma} = \frac{1}{b_{(i-1)\sigma}} [-\hat{f}_{(i-1)\sigma}(x_1, ..x_{i-1}) - \chi_{(i-1)\sigma}(z_{i-1}) \tag{6.5}$$
$$- b_{(i-2)\sigma} z_{i-2} + \dot{\alpha}_{(i-1)f}], b_{0\sigma} = 0 \ i = 2, \cdots, n$$

Here, $\chi_{i\sigma}(z_i) = k_{i\sigma} z_i$ are user-defined tuning functions where $k_{i\sigma} > 0$ and $\mu \in (0,1)$ is called the perturbed parameter. $\alpha_{if}(0) = \alpha_i(0)$ is the initial condition. Utilizing Equations (6.1)-(6.5), the closed-loop system can be rewritten as (6.6).

$$\dot{z}_1 = f_{1\sigma} - \hat{f}_{1\sigma} - \chi_{1\sigma}(z_1) + b_{1\sigma} z_2 + b_{1\sigma} \tilde{\alpha}_{2\sigma}$$
$$\dot{z}_i = f_{i\sigma} - \hat{f}_{i\sigma} + b_{(i-1)\sigma} z_{i-1} - \chi_{i\sigma}(z_i) + b_{i\sigma} z_{i+1} + b_{i\sigma} \tilde{\alpha}_{(i+1)\sigma} \tag{6.6}$$
$$\dot{z}_n = f_{n\sigma} - \hat{f}_{n\sigma} - b_{(n-1)\sigma} z_{n-1} - \chi_{n\sigma}(z_n), \quad i = 2, \ldots, n-1$$

Equation (6.6) can be expressed in a compact form as Equation (6.7), while the filter dynamics are reformulated as Equation (6.8).

$$\dot{z} = \Theta_\sigma(\tilde{f}, z, \tilde{\alpha}_f) \tag{6.7}$$
$$\mu \dot{\alpha}_f = g_\sigma(\alpha_f, \alpha_\sigma) = -\alpha_f + \alpha_\sigma \tag{6.8}$$

where $\tilde{\alpha}_{if} = \alpha_{if} - \alpha_{i\sigma}$, $\alpha_\sigma = [\alpha_{i\sigma}]^T$, $i = 2, .., n$, $\alpha_f = [\alpha_{if}]^T$, $i = 2, .., n$, $\tilde{\alpha}_f = [\tilde{\alpha}_{if}]^T$, $i = 2, .., n$ and $\Theta_\sigma(.) = [\bar{\Theta}_i]^T$ with

$$\bar{\Theta}_1(.) = f_{1\sigma} - \hat{f}_{1\sigma} - \chi_{1\sigma}(z_1) + b_{1\sigma} z_2 + b_{1\sigma} \tilde{\alpha}_{2\sigma}$$
$$\bar{\Theta}_i(.) = f_{i\sigma} - \hat{f}_{i\sigma} + b_{(i-1)\sigma} z_{(i-1)} - \chi_{i\sigma}(z_i) + b_{i\sigma} z_{i+1} +$$
$$b_i \tilde{\alpha}_{(i+1)\sigma}, \tag{6.9}$$
$$\bar{\Theta}_n(.) = f_{n\sigma} - \hat{f}_{n\sigma} - b_{(n-1)\sigma} z_{n-1} - \chi_{n\sigma}(z_n)$$

6.4 Stability of the Closed Loop System

It should be noted that the closed-loop dynamics (6.7)-(6.8) is a nonlinear singularly perturbed system [93]. By substituting ($\mu \to 0$, $\alpha_i = \alpha_\sigma$) the root of the fast subsystem α_i in place of α_f in Equation (6.6), the reduced slow subsystem can be expressed as Equation (6.10).

$$
\begin{aligned}
\dot{z}_1 &= f_{1\sigma} - \hat{f}_{1\sigma} - \chi_{1\sigma}(z_{1r}) + b_1 z_{2r} \\
\dot{z}_i &= f_{i\sigma} - \hat{f}_{i\sigma} - b_{(i-1)} z_{(i-1)r} - \chi_{i\sigma}(z_{ir}) + b_i z_{(i+1)r} \\
\dot{z}_n &= f_{n\sigma} - \hat{f}_{n\sigma} - b_{(n-1)} z_{(n-1)r} - \chi_{n\sigma}(z_{nr}), i = 2, ..., (n-1).
\end{aligned}
\tag{6.10}
$$

By using (6.3) and (6.4), the reduced ordered dynamics can be written as:

$$
\begin{aligned}
\dot{z}_1 &= \tilde{W}_1' \phi_1 - \chi_{1\sigma}(z_1) + b_{1\sigma} z_2 + \epsilon_1 \\
\dot{z}_2 &= \tilde{W}_2' \phi_2 - \chi_{2\sigma}(z_2) - b_1 z_1 + b_{2\sigma} z_3 + \epsilon_2 \\
&\cdots \\
\dot{z}_n &= \tilde{W}_n' \phi_n - \chi_{n\sigma}(z_n) - b_{(n-1)\sigma} z_{(n-1)} + \epsilon_n
\end{aligned}
\tag{6.11}
$$

Where $\tilde{W}_i = W_i - \hat{W}_i$, $i = 1, 2, ... n$. The above equation (6.11) in compact form will be:

$$
\begin{aligned}
\dot{z} &= \Theta_\sigma(\tilde{f}, z) \\
\dot{z} &= \Theta_{1\sigma}(z) + \gamma_2 \\
\dot{z} &= A' z + \gamma_2
\end{aligned}
\tag{6.12}
$$

Where,

$$
A' = \begin{bmatrix}
-k_{1\sigma} & b_{1\sigma} & 0 & \cdots & 0 \\
-b_{1\sigma} & -k_{2\sigma} & b_{2\sigma} & \cdots & 0 \\
\ddots & \ddots & \ddots & \ddots & \ddots \\
0 & \cdots & 0 & b_{(n-1)\sigma} & -k_{n\sigma}
\end{bmatrix}
$$

$\gamma_2 = \tilde{\xi}' \Phi + \epsilon$, $z = [z_1' \; z_2' ... z_n']'$, $\epsilon = [\epsilon_1' \; \epsilon_2' ... \epsilon_n']'$, $\tilde{\xi} = diag\{\tilde{W}_1, \tilde{W}_2 ... \tilde{W}_n\}$, and $\Phi = [\phi_1' \; \phi_2' ... \phi_n']'$.

A' is a stable matrix for $k_{i\sigma} > 0$. Hence, there exists a set of symmetric positive

definite matrices B_σ, Q_σ such that

$$B_\sigma A_\sigma' + A_\sigma'^T B_\sigma \leq -Q_\sigma. \tag{6.13}$$

Assumption 6.2: The ideal weights are bounded by known positive values so that

$$||W_i||_F \leq W_{iM}, i = 1, 2...n.$$

equivalently,

$$||\xi||_F \leq \xi_M$$

Where, $\xi = diag\{W_1, W_2...W_n\}$ and ξ_M is known. $||.||_F$ denotes the Frobenius norm. Under the validity of Assumptions 6.1 and 6.2, also the Theorem mentioned in [109] establishes that the tuning law for the neural network weights can be expressed as:

$$\dot{\hat{W}}_i = \Gamma_i \phi_i z_i^T - k_w \Gamma_i ||z|| \hat{W}_i, \quad i = 1, 2, \ldots, n,$$

where $\Gamma_i = \Gamma_i^T > 0$ $(i = 1, 2, \ldots, n)$ is a positive definite matrix, and k_w is a positive scalar constant. Under this tuning law, both z_i and the neural network weight estimates $\hat{W}_i$ are uniformly ultimately bounded (UUB).

Let us consider a Lyapunov function candidate for reduced order system as

$$V_{r\sigma} = \frac{1}{2} z^T z + \frac{1}{2} tr(\tilde{\xi}^T \Gamma^{-1} \tilde{\xi})$$

The derivative of $V_{r\sigma}$ has been proved negative in [109]. By using norm inequalities and properties of positive definite matrices, it can be obtained that

$$\begin{aligned} &\frac{1}{2}||z||^2 + \frac{1}{2}\lambda_{\min}(\Gamma^{-1})||\tilde{\xi}||_F^2 \leq V_{r\sigma} \leq \frac{1}{2}||z||^2 \\ &+ \frac{1}{2}\lambda_{\max}(\Gamma^{-1})||\tilde{\xi}||_F^2 \end{aligned} \tag{6.14}$$

(or) compactly,

$$\underline{m}_\sigma \left(||z||^2 + ||\tilde{\xi}||_F^2 \right) \leq V_{r\sigma} \leq \overline{m}_\sigma \left(||z||^2 + ||\tilde{\xi}||_F^2 \right) \tag{6.15}$$

Chapter 6. Neural backstepping controller for singularly perturbed switched systems

where

$$\underline{m}_\sigma = \frac{1}{2}\min\{1, \lambda_{\min}(\Gamma^{-1})\}, \quad \overline{m}_\sigma = \frac{1}{2}\max\{1, \lambda_{\max}(\Gamma^{-1})\}.$$

Consider the fast filter dynamics, when

$$\mu \to 0 \Rightarrow g_\sigma(\alpha_f, \alpha_\sigma) \to 0 \Rightarrow \alpha_f \to \alpha_\sigma = \alpha_{sm\sigma}$$

The slow manifold is given by $(\alpha_{sm\sigma})$. Let's define an error variable $y = \alpha_f - \alpha_\sigma$. The dynamics of this error variable can be derived as follows:

$$\mu \dot{y} = -y - \mu \dot{\alpha}_\sigma. \tag{6.16}$$

The fast boundary layer dynamics [93] in the context of stretched timescale $\tau = \frac{t}{\mu}$ can be expressed as:

$$\frac{dy}{d\tau} = -y. \tag{6.17}$$

Similarly, consider a Lyapunov function $V_f = \frac{1}{2}y^T y$ shows

$$\dot{V}_f \le -||y||^2 = -2V_f. \tag{6.18}$$

After confirming the stability of the reduced-order system, a scalar value p within the range $0 < p < 1$ and a set of composite Lyapunov functions can be selected as follows:

$$V_\sigma = (1-p)V_{r\sigma} + pV_f \tag{6.19}$$

whose derivative along the overall system can be derived as

$$\dot{V}_{r\sigma} = (1-p)\frac{\partial V_{r\sigma}}{\partial z}(\Theta_{1\sigma}(\tilde{f}, z)) - \frac{p}{\mu}\frac{\partial V_f}{\partial y}y - p\frac{\partial V_f}{\partial y}\dot{\alpha}_\sigma$$
$$+ (1-p)\frac{\partial V_{r\sigma}}{\partial z}\left(\Theta_{1\sigma}(\tilde{f}, z, \tilde{\alpha}_f) - \Theta_{1\sigma}(\tilde{f}, z)\right). \tag{6.20}$$

Using the following Lemma the last term of (6.20) can be further simplified as .

Lemma 6.1: A positive constant $L_{1\sigma}$ exists such that

$$\frac{\partial V_{r\sigma}}{\partial z}\left(\Theta_{1\sigma}(\tilde{f}, z, \tilde{\alpha}_f) - \Theta_{1\sigma}(\tilde{f}, z)\right) \le 2L_{1\sigma}||z||||y||. \tag{6.21}$$

Proof: Considering the structure of V_r, it follows that $||\frac{\partial V_{r\sigma}}{\partial z}|| \leq 2||z||$. It is important to note that $\tilde{\alpha}$ is equivalent to y as per the definition of y. Utilizing these observations, equation (6.21) can be proved. To ensure the global asymptotic stability of the closed-loop switched system, the subsequent condition must be satisfied.

Assumption 6.3: There exist positive scalars $L_{2\sigma}, L_{3\sigma}, \& L_{4\sigma}$ such that

$$||\dot{\alpha}_\sigma|| = \frac{\partial \alpha_\sigma}{\partial z}\dot{z} \leq 2L_{2\sigma}||z|| + L_{3\sigma}||y|| + L_{4\sigma}. \tag{6.22}$$

Assumption 6.3 is a conventional requirement in the context of singularly perturbed dynamics, as indicated in the reference [93]. This assumption implies that the rate of change in the virtual control signal α_σ should be comparatively slower than the growth of the weighted combination of z and the fast variable y. Moreover, Assumption 6.3 is applicable to various practical systems such as inverted pendulums, robotic manipulators, chemical systems, ships, synchronous machines, and others. Utilizing the given assumptions and the properties of Lyapunov functions, it can be deduced that:

$$\dot{V}_\sigma \leq -(1-p)||z||^2 - \frac{p}{\mu}||y||^2 + 2pL_{2\sigma}||z||||y||$$
$$+ pL_{3\sigma}||y||^2 + 2(1-p)L_{1\sigma}||z||||y|| + pL_{4\sigma}||y|| + (1-p)L_{5\sigma}\gamma_2||z||. \tag{6.23}$$

It can be written in a compact form as:

$$\dot{V}_\sigma \leq -Z^T S_\sigma Z + pL_{4\sigma}||y|| + (1-p)L_{5\sigma}\gamma_2||z|| \tag{6.24}$$

where $Z = [z,y]^T$ and

$$S_\sigma = \begin{bmatrix} (1-p) & -(1-p)L_{1\sigma} - pL_{2\sigma} \\ -(1-p)L_{1\sigma} - pL_{2\sigma} & p(\frac{1}{\mu} - L_{3\sigma}) \end{bmatrix} \tag{6.25}$$

The system achieves asymptotic stability only if S_σ is positive definite. So, we can deduce that S_σ indeed exhibits positive definiteness if

$$\mu_\sigma \leq \mu_\sigma^* = \frac{1}{L_{3\sigma} + \frac{1}{p(1-p)}((1-p)L_{1\sigma} + pL_{2\sigma})^2} \tag{6.26}$$

From the properties of A_σ', there exist two positive constants m_l, m_h such that

$$m_l I \leq A_\sigma' \leq m_h I.$$

So, one can derive

$$\underline{\alpha}||Z||^2 \leq V_\sigma \leq \overline{\alpha}||Z||^2. \tag{6.27}$$

where

$$\underline{\alpha} = \min(\frac{(1-p)m_l}{2}, \frac{p}{2}), \ \overline{\alpha} = \max(\frac{(1-p)m_h}{2}, \frac{p}{2}).$$

Hence, it can be concluded that within any two consecutive switching instances, the dynamics of the overall singularly perturbed system is stable, if $\mu_\sigma \leq \mu_\sigma^*$, i.e.

$$\dot{V}_\sigma \leq -\beta_\sigma^o V_\sigma + pL_{4\sigma}||Z|| + (1-p)L_{5\sigma}\gamma_2||Z|| \tag{6.28}$$

where $\beta_\sigma^o = \frac{\lambda_{\min}(S_\sigma)}{\lambda_{\max}(S_\sigma)}$.

6.5   Robust Filtered Backstepping With Disturbance Observer

In this section, a robust filtered backstepping design is introduced for the uncertain system (6.1) by estimating the unknown parts of the dynamics. The suggested observer for each $\delta_i(.)$ is formulated as follows [96]:

$$\begin{aligned}
\dot{\eta}_i &= -l(\eta_i + lx_i + \hat{f}_{i\sigma}(x_1, x_2, \ldots, x_i) + b_{i\sigma}x_{i+1}) \\
\dot{\eta}_n &= -l(\eta_n + lx_n + \hat{f}_{n\sigma}(x_1, x_2, \ldots, x_n) + b_{n\sigma}u) \\
\hat{\delta}_i(.) &= \eta_i + lx_i \\
\hat{\delta}_n(.) &= \eta_n + lx_n
\end{aligned} \tag{6.29}$$

where the scalar $l > 0$ is a large positive constant, $\hat{\delta}_i(.)$ is the estimate of $\delta_{i\sigma}(.)$, and η_i is an intermediate variable. Using observer (6.29), the dynamics of disturbance estimator ($\hat{\delta}_i$) is given by:

$$\dot{\hat{\delta}}_i = h_{i\sigma}(\hat{\delta}_i, \delta_{i\sigma}) = -l(\hat{\delta}_i - \delta_{i\sigma}). \tag{6.30}$$

Defining a disturbance error variable $\tilde{\delta}_i = \delta_{i\sigma}(.) - \hat{\delta}_i(.)$, the dynamics of estimation error can be written as:

$$\epsilon\dot{\tilde{\delta}}_i(.) = -\tilde{\delta}_i - \epsilon\dot{\delta}_{i\sigma}(.). \tag{6.31}$$

where $0 \le \epsilon = 1/k \le 1$. The boundary layer dynamics resulting from (6.31) can be written as:

$$\frac{d}{d\tau}(\tilde{\delta}_i) = -\tilde{\delta}_i. \tag{6.32}$$

6.5.1   Conversion to Singularly Perturbed form

The disturbance observer-based filtered backstepping control law for the system in Equation (6.1) is given as follows.

$$u_\sigma = \frac{1}{b_{n\sigma}(x)}[-\hat{f}_{n\sigma}(x) - b_{(n-1)\sigma}z_{n-1} - \chi_{n\sigma}(z_n) + \dot{\alpha}_{nf} - \hat{\delta}_{n\sigma}]$$

$$z_i = x_i - \alpha_{if}, (i = 1, 2......n)$$

$$\alpha_{1f} = \alpha_1 = x_d(t) \tag{6.33}$$

$$\alpha_{i\sigma} = \frac{1}{b_{(i-1)\sigma}}[-\hat{f}_{(i-1)\sigma}(x_1,..x_{i-1}) - \chi_{(i-1)\sigma}(z_{i-1})$$

$$- b_{(i-2)\sigma}z_{i-2} + \dot{\alpha}_{(i-1)f} - \hat{\delta}_{(i-1)\sigma}], b_{0\sigma} = 0 \ \ i = 2, \cdots, n$$

$$\mu\dot{\alpha}_{if} = -\alpha_{if} + \alpha_{i\sigma} \ \ \ i = 2, \cdots, n$$

$$\alpha_{i\sigma} = \frac{1}{b_{(i-1)\sigma}}[-\hat{f}_{(i-1)\sigma}(x_1,..x_{i-1}) - \chi_{(i-1)\sigma}(z_{i-1})$$

$$- b_{(i-2)\sigma}z_{i-2} + \dot{\alpha}_{(i-1)f}], b_{0\sigma} = 0 \ \ i = 2, \cdots, n \tag{6.34}$$

where the tuning functions are chosen similar to the case with no disturbances in the system dynamics, i.e. $\chi_{i\sigma}(z_i) = k_{i\sigma}z_i$. The closed-loop system from Equation

Chapter 6. Neural backstepping controller for singularly perturbed switched systems

(6.1), using the control law (6.33), can be written as follows.

$$
\begin{aligned}
\dot{z}_1 &= f_{1\sigma} - \hat{f}_{1\sigma} - \chi_{1\sigma} + b_{1\sigma}z_2 + b_{1\sigma}\tilde{\alpha}_{2\sigma} + \tilde{\delta}_1 \\
\dot{z}_i &= f_{i\sigma} - \hat{f}_{i\sigma} + b_{(i-1)\sigma}z_{i-1} - \chi_{i\sigma}(z_i) + b_{i\sigma}z_{i+1} + \\
&\quad b_{i\sigma}\tilde{\alpha}_{(i+1)\sigma} + \tilde{\delta}_i \\
\dot{z}_n &= f_{n\sigma} - \hat{f}_{n\sigma} - b_{(n-1)\sigma}z_{n-1} - \chi_{n\sigma}(z_n) + \tilde{\delta}_n, \\
i &= 2,\ldots,n-1
\end{aligned}
\tag{6.35}
$$

Rewriting (6.35) in a compact form as:

$$
\dot{z} = \Theta_\sigma(\tilde{f}, z, \tilde{\alpha}_f, \tilde{\delta})
\tag{6.36}
$$

$$
\mu\dot{\tilde{\alpha}}_f = g_\sigma(\alpha_f, \alpha_\sigma) = -\tilde{\alpha}_f + \mu\dot{\alpha}_\sigma
\tag{6.37}
$$

$$
\epsilon\dot{\tilde{\delta}} = h(\hat{\delta}, \delta_\sigma) = -\tilde{\delta} + \epsilon\dot{\delta}_\sigma
\tag{6.38}
$$

where $\hat{\delta} = [\hat{\delta}_1, \hat{\delta}_2, \ldots, \hat{\delta}_n]$, $\tilde{\delta} = [\tilde{\delta}_1, \tilde{\delta}_2, \ldots, \tilde{\delta}_n]$ $\delta_\sigma = [\delta_{1\sigma}\delta_{2\sigma}, \ldots, \delta_{n\sigma}]$. The system dynamics are converted into a three-time-scale singularly perturbed switched system. However, by using the ratio $\frac{\epsilon}{\mu}$, it can be simplified into a two-time-scale form. Let's assume that $\epsilon < \mu$, so that the observer dynamics is faster than the filter dynamics. It can be chosen that $\epsilon = \kappa\mu$, where κ is a small positive constant less than one. The fast subsystem (6.37) and (6.38) can be expressed as follows.

$$
\mu\dot{\tilde{v}} = W_\sigma(\tilde{v}, \dot{v}_\sigma, \kappa) = -
\begin{bmatrix}
1 & 0 \\
0 & \frac{1}{\kappa}
\end{bmatrix}
\tilde{v} + \mu\dot{v}_\sigma
\tag{6.39}
$$

where $\tilde{v} = [\tilde{\alpha}_f^T, \tilde{\delta}^T]^T$, $\dot{v}_\sigma = [\dot{\alpha}_\sigma^T, \dot{\delta}_\sigma^T]^T$ and $W_\sigma(.) = [g_\sigma^T(.), \frac{1}{\kappa}h_\sigma^T(.)]^T$. Using Equation (6.39), the closed-loop dynamics can be written in a two-time-scale singularly perturbed form. Therefore, the system's trajectory convergence can be analyzed using similar arguments from Section 6.4.

6.6   Lyapunov Function at Switching Instants

Consider any time instant t_i, where $i \in \mathbb{N}$. Suppose the subsystem $\sigma(t_{i+1}^-)$ remains active during the time interval $t \in [t_i, t_{i+1})$, while the subsystem $\sigma(t_{i+1})$ becomes

6.6. Lyapunov Function at Switching Instants

121

active for $t \in [t_{i+1}, t_{i+2})$. Based on equations (6.27) and (6.28), along with the structure of the Lyapunov function V_σ, the following relation can be derived:

$$V(t_{i+1}) - V(t_{i+1}^-) \leq \frac{\overline{\alpha} - \underline{\alpha}}{\underline{\alpha}} V(t_{i+1}^-)$$

at the switching instant t_{i+1}. Therefore,

$$V(t_{i+1}) \leq l_\mu V(t_{i+1}^-). \tag{6.40}$$

where $l_\mu = \frac{\overline{\alpha}}{\underline{\alpha}} \geq 1$. Consider a time (0, T), where the time of switchings is defined as $t_1, ..., t_{N_\sigma(0,T)}$. For a function

$$R(t) = \exp(\beta_\sigma^o t) V_\sigma, \ \beta^o = \min(\beta_\sigma^o) \forall \sigma \in P$$

it's time derivative in $t \in (t_i, t_{i+1})$ is given by

$$\dot{R}(t) = \beta^o R(t) + \exp(\beta^o t) \dot{V}_\sigma$$

which is non-positive between two consecutive switching times. Exploiting (6.40), it can be derived that

$$R(T^-) \leq (l_\mu)^{N_\sigma(0,T)} R(t)$$

An average dwell time $\tau_a > 0$ in the interval (0, T) exists if there exists a positive scalar N_o such that

$$N_\sigma(0, T) \leq \frac{T - t}{\tau_a} + N_o \tag{6.41}$$

Using (6.41), it can be obtained

$$\Rightarrow V_{\sigma(T^-)} Z(T) \leq \exp(N_o \ln l_\mu) \exp(\frac{\ln(l_\mu)}{\tau_a} T - \beta_\sigma^o T) V_{\sigma(0)} Z(0).$$

$$\Rightarrow V_{\sigma(T^-)} Z(T) \leq \exp(N_o \ln l_\mu) \exp((-\beta^o + \frac{\ln l_\mu}{\tau_a}) T) V_{\sigma(0)} Z(0)$$

Therefore, the function $V_{\sigma(T^-)} Z(T)$ asymptotically converges to zero if the average dwell time satisfies

$$\tau_a > \frac{\ln l_\mu}{\beta^o}. \tag{6.42}$$

6.7   Result outcomes

The concept of average dwell time (ADT) has been utilized to govern system switching, enabling the observation of tracking of reference signals. A single-link manipulator system with actuator dynamics [95] has been shown in equation (6.43). In this case, $b_{i\sigma}$ (See equation (6.1) for b_σ & f_σ) $(i = 1, 2, \ldots, n)$ is considered to be known.   The conventional backstepping controller design approach assumes that $f_{i\sigma}$ $(i = 1, 2, \ldots, n)$ is linearly parameterizable in terms of unknown system parameters.   In contrast, the proposed controller design utilizes a two-layer neural network to approximate $f_{i\sigma}$ $(i = 1, 2, \ldots, n)$. The proposed neural backstepping can be applied directly. Each of the 2-layer neural networks uses 10 neurons. The sigmoid function is used for ϕ_i. The initial conditions for x_1, x_2, and x_3 are set to 0, 6.28, and 0, respectively. The model-specific parameters D, B, N, M, H, and K_m for each switching signal are given in Table 6.1. The joint's angular position and velocity are represented by the variables q and $\dot{q}$, respectively. The torque supplied to the joint by the motor is denoted by the symbol τ, and the input voltage that is used to drive the motor and produce the necessary torque is represented by the symbol u_σ.

$$D\ddot{q} + B\dot{q} + N\sin(q) = \tau$$
$$M\dot{\tau} + H\tau + K_m\dot{q} = u_\sigma \tag{6.43}$$

Let's consider $x_1 = q$, $x_2 = \dot{q}$, $x_3 = \tau$. Equation (6.43) can be written as

$$\dot{x}_1 = x_2$$
$$\dot{x}_2 = \frac{1}{D}(-N\sin(x_1) - Bx_2) + \frac{1}{D}x_3 \tag{6.44}$$
$$\dot{x}_3 = -\frac{1}{M}(K_m x_2 + Hx_3) + \frac{1}{M}u_\sigma$$

A four-time switching strategy for the reference signal, namely $\sin(20t)$, is demonstrated in Figures 6.1 to 6.5. Here, the uncertainties are defined as $\delta_1 = 0.1\tanh(2t)$ and $\delta_2 = 0.1\tanh(2t)$ for $\sigma = 1$, while for $\sigma = 2, 3, 4$, the uncertainties are given by $\delta_1 = 0.1\sin(2t)$ and $\delta_2 = 0.1\cos(2t)$. By using the values of $k_{i\sigma} > 0$ and other system parameters, the quantity $\frac{\ln l_\mu}{\beta^o} = 0.48$ s can be obtained. The average dwell time (τ_a) is evaluated over the time interval 0 to 1.5 sec using the
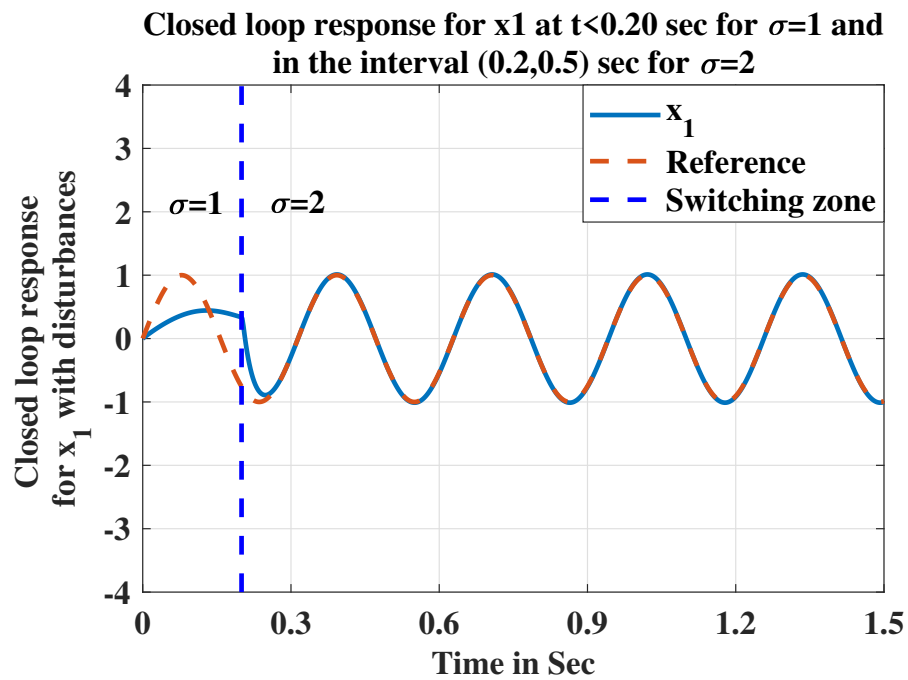
FIGURE 6.1: Closed loop response for x_1 for reference signal $sin(20t)$.

FIGURE 6.2: Tracking error for reference signal $sin(20t)$.

Chapter 6. Neural backstepping controller for singularly perturbed switched systems

FIGURE 6.3: Closed loop response for x_1 for reference signal $sin(20t)$.

FIGURE 6.4: Tracking error for reference signal $sin(20t)$.

Closed loop response for x1 at t<0.20 sec for $\sigma=1$ and in the interval (0.2,0.5) & (0.5,1) sec for $\sigma=2, \sigma=3$ & at t>1 sec $\sigma=4$ respectively

FIGURE 6.5: Closed loop response for $\tau_a \not> \frac{\ln l_\mu}{\beta^o}$ and doesn't track the reference $sin(20t)$.

Closed loop response for x1 at t<0.20 sec and in interval (0.2,0.5) sec for $\sigma=1$ and $\sigma=2$ respectively
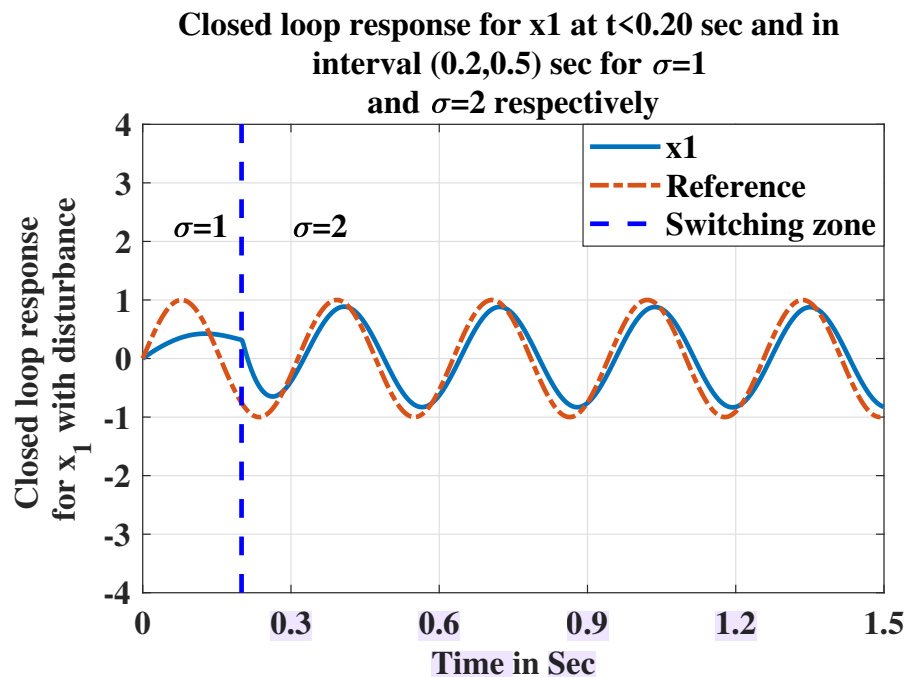
FIGURE 6.6: Closed loop response for x_1 for reference signal $sin(20t)$.
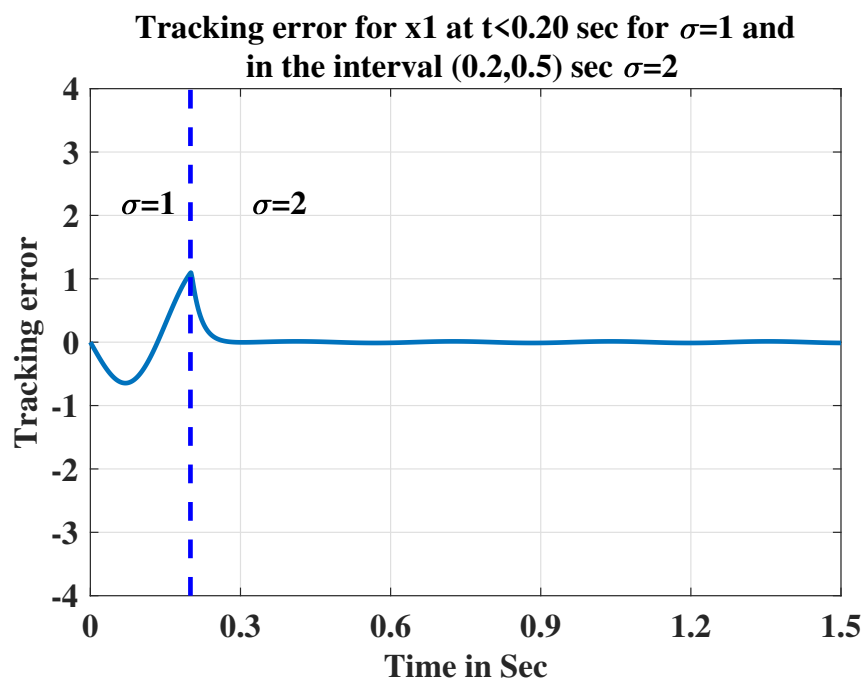
Chapter 6.   Neural backstepping controller for singularly perturbed switched systems

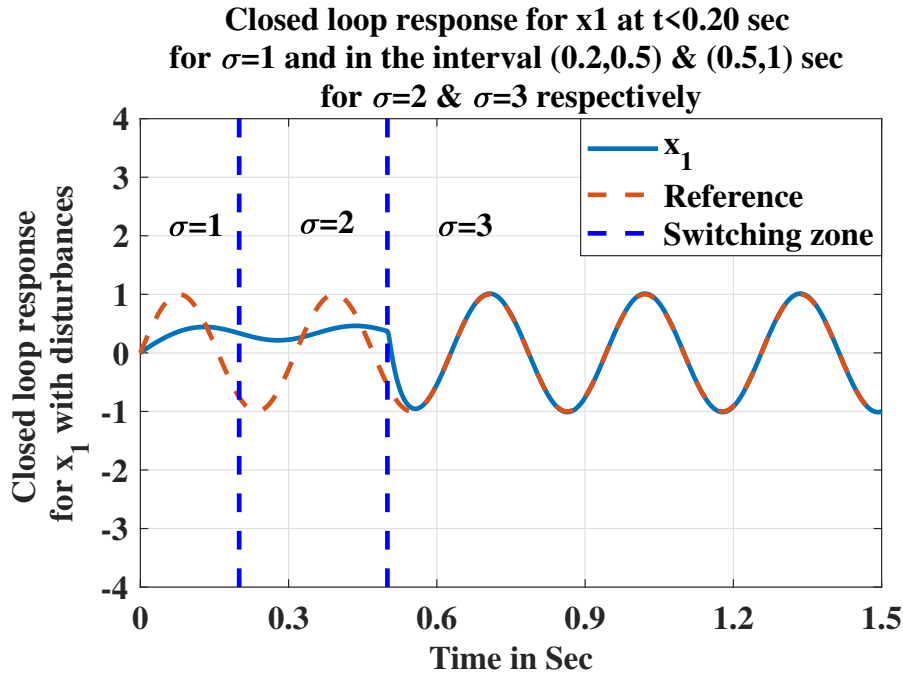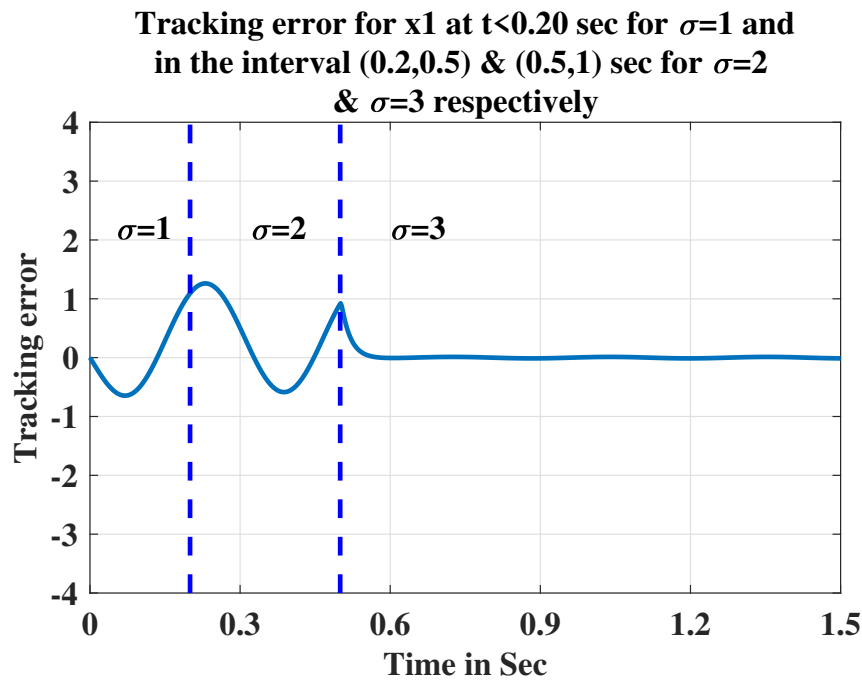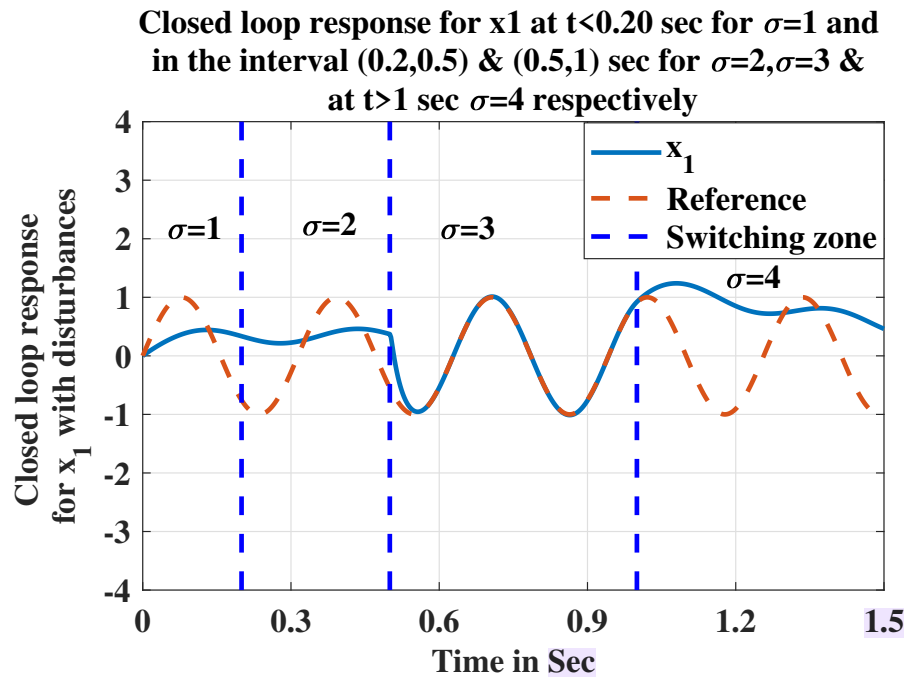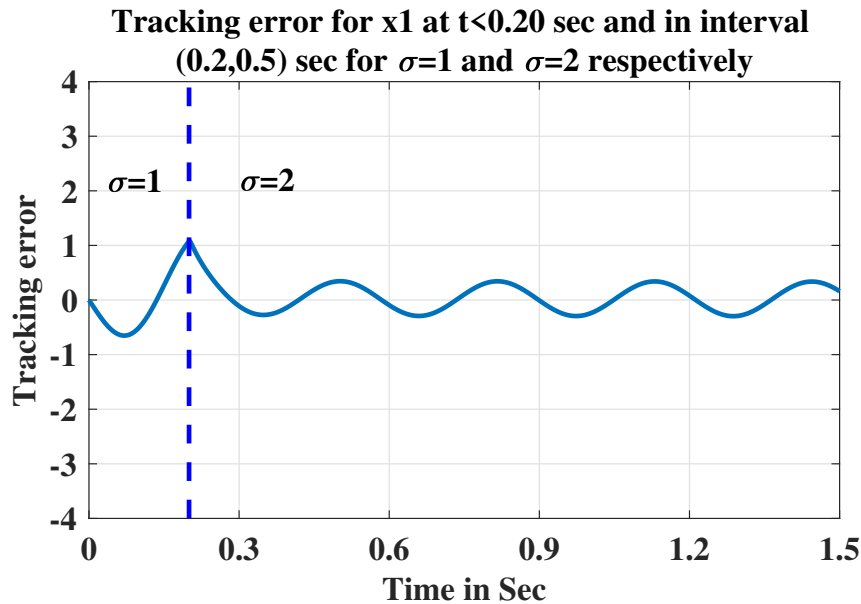FIGURE 6.7: Tracking error for reference signal $sin(20t)$.

formula $\tau_a = \frac{\text{Time interval}}{\text{Number of switchings}}$.   For example, suppose the system changes its parameters during the switching signal $\sigma = 1$ at $t < 0.20$ sec, and again changes its parameters during the switching signal $\sigma = 2$ in the interval 0.20 to 0.55) sec. In that case, the average dwell time is calculated as $\tau_a = \frac{1.5}{2} = 0.75$ sec.   As the condition $\tau_a > \frac{\ln l_\mu}{\beta^o}$ (with $\frac{\ln l_\mu}{\beta^o} = 0.48$ sec) is satisfied, the state x_1 is able to effectively track the reference signal, as shown in Figure 6.1 and the associated tracking error is presented in Figure 6.2.

For $\sigma = 1, 2, 3$, the switching occurs at $t < 0.20$ sec and within the intervals 0.20 to 0.55 sec and 0.50 to 1 sec, respectively. So, the average dwell time will be $\tau_a = \frac{1.5}{3} = 0.50$ sec.   Since this satisfies the condition $\tau_a > \frac{\ln l_\mu}{\beta^o}$, the state x_1 successfully tracks the reference signals, as illustrated in Figure 6.3 and the corresponding tracking error is presented in Figure 6.4.   Similarly, for $\sigma = 1, 2, 3, 4$, where switching occurs at $t < 0.20$ sec and in the intervals 0.20 to 0.50 sec, 0.50 to 1 sec, and at $t > 1$ sec, the average dwell time will be $\tau_a = \frac{1.5}{4} = 0.37$ sec. Since this does not satisfy the condition $\tau_a > \frac{\ln l_\mu}{\beta^o}$, the state x_1 fails to track the reference signal. This behaviour is depicted in Figure 6.5.

TABLE 6.1: The parameters of the system for different switching signals.

System Parameters	D	B	N	M	H	km
For $\sigma = 1$	1	1	10	0.01	0.5	100
For $\sigma = 2$	10	150	10	0.01	0.5	10
For $\sigma = 3$	10	150	1	0.01	0.5	10
For $\sigma = 4$	10	1	10	0.01	0.5	100

The control law without switching is presented in [80]:

$$
\begin{aligned}
u &= \frac{1}{g_n(x)}[-f_n(x) - g_{(n-1)}(x)z_{n-1} - \lambda_n(z_n) + \dot{\alpha}_{nf}] \\
z_i &= x_i - \alpha_{if}, (i = 1, 2......n) \\
\alpha_{1f} &= \alpha_1 = x_d(t)
\end{aligned}
\tag{6.45}
$$

where $\lambda_i(z_i) = k_i z_i$ are user-defined tuning functions for which $k_i > 0$. The terms α_{if} are obtained through the first order filter [75, 76]. By using this controller, the performance of the state x_1 under the switching signal σ for the reference signals $\sin(20t)$ is illustrated in Figure 6.6, and the corresponding error is presented in Figure 6.7, which are not comply with the reference trajectory. To address these challenges, a neural backstepping controller has been proposed and implemented in this chapter. This controller leverages the universal approximation capability of neural networks to estimate the unknown nonlinearities in the system in real-time. By incorporating the neural network with the traditional backstepping design framework, the controller adaptively compensates for uncertainties and ensures improved tracking performance. As a result, the closed-loop system demonstrates enhanced robustness and stability, with the state x_1 achieving better convergence towards the desired signal x_d across different switching scenarios.

6.7.1   The performance of the Controller during during switching

In the four time switching, the manipulator initially operates in a compressed mode ($\sigma = 1$) for $t < 0.20$ sec. It then transitions to $\sigma = 2$ during the interval

Chapter 6. Neural backstepping controller for singularly perturbed switched systems

(0.20,0.50) sec before reverting back to $\sigma = 1$ at $t = 0.5$ sec. Then, the manipulator further changes its configuration to $\sigma = 3$ during the interval (0.50,1) sec. Since the switching signals $\sigma = 1,2,3$ satisfy the average dwell time condition, the manipulator continues to track the reference signals. This behavior is illustrated in Figure 6.3. However, the system transitions to $\sigma = 4$ at $t > 1$ sec, at this point, the average dwell time condition is no longer met. As a result, the manipulator fails to track the reference signals, as shown in Figure 6.5. The proposed theory of this chapter can be summarized in Theorem 6.1.

Theorem 6.1: Consider the singularly perturbed switched system described by Equation (6.1). Assuming that Assumptions 6.1–6.3 hold, the states of the closed-loop system under the switched control law (6.33) will asymptotically converge to the bound given in Equation (6.26), provided that the average dwell time condition specified in Equation (6.42) is satisfied.

6.8   Concluding Remarks

This chapter presented a robust controller design for nonlinear switched systems subjected to disturbances and frequent switching. The proposed controller demonstrated its effectiveness in ensuring accurate tracking of various reference signals under different switching scenarios. Simulation results confirmed that the system maintains stable performance and achieves error convergence to zero despite the presence of disturbances and varying switching intervals. The results illustrate the versatility and reliability of the controller in handling dynamic environments and switching behaviors, making it suitable for practical applications in complex control systems. Future work will explore the extension of this approach to multi-input multi-output (MIMO) systems and its implementation on hardware platforms to validate real-time performance.

129

Chapter 7

Conclusion and Future Work

7.1   Overall Conclusion

This thesis has explored advanced control methodologies for singularly perturbed systems (SPSs), switched nonlinear systems, and singularly perturbed switched systems (SPSSs), each of which presents unique challenges due to multi-time-scale dynamics, switching mechanisms, and external disturbances. The research systematically progressed from theoretical preliminaries to the design and validation of robust controllers, ultimately establishing a comprehensive framework for stabilizing complex nonlinear systems under uncertainty and switching conditions.

- The foundation was laid in Chapter 1, where key mathematical tools such as contraction theory, Lyapunov stability analysis, and average dwell time (ADT) were discussed with the theoretical backbone for the subsequent control strategies.

- Building on this groundwork, the thesis developed and validated several robust control approaches: In Chapter 2, a saturated controller was designed for singularly perturbed systems, incorporating filters and disturbance observers, with contraction theory ensuring stability.   The method was validated on the Twin Rotor MIMO System (TRMS) for pitch angle control.

- In Chapter 3, switched nonlinear systems were studied, and a robust filter backstepping controller with time-scale redesign was proposed. Singular perturbation theory was used to design high-gain filters and disturbance

Chapter 7. Conclusion and Future Work

observers, while ADT-based Lyapunov stability ensured robustness of the resulting three-time-scale closed-loop system. Numerical simulations on a single-link manipulator verified the approach.

- In Chapter 4, singularly perturbed switched systems were addressed with a filtered backstepping controller enhanced by a high-gain disturbance observer (HGDO). Contraction theory was employed to guarantee closed-loop convergence, and implementation on a robotic manipulator highlighted practical feasibility.

- In Chapter 5, robustness was further improved through the integration of a neural network disturbance observer (NNDO), enabling real-time estimation and compensation of unknown disturbances. Lyapunov-based ADT analysis ensured closed-loop stability, and the method was validated on a robotic manipulator.

- In Chapter 6, a neural backstepping controller was proposed for SPSSs, augmented with high-gain filters and a disturbance observer to manage actuator dynamics and external uncertainties. The strategy was successfully demonstrated on a single-link manipulator.

- This Thesis summarizes the findings, highlighting that the proposed controllers effectively enhance stability, robustness, and tracking performance across multiple nonlinear system classes.

- Overall, this thesis has contributed novel control strategies that integrate backstepping, singular perturbation methods, high-gain filters, disturbance observers, and neural networks within a Lyapunov and contraction-theoretic framework. The theoretical analysis, supported with Lemmas and Theorems also validated on nonlinear dynamical systems such as TRMS, robotic manipulator, which confirms the applicability of the proposed designs.

7.2 Future Work

Despite these advances, certain limitations remain, most notably the focus on SISO systems and simulation-based validations.   These open promising directions for future research, including:

- Developing output feedback controllers for singularly perturbed systems with uncertainties and switching, reducing the dependence on full state measurements.

- Extending the proposed methodologies to MIMO systems, thereby broadening their applicability to more complex real-world processes.

- Implementing and testing the controllers on hardware platforms, such as robotic manipulators or aerospace systems, to assess real-time feasibility and performance.

- Incorporating adaptive or learning-based techniques, including neural adaptation and reinforcement learning, to enhance disturbance rejection and adaptability in dynamic environments.

In summary, this thesis has contributed robust and theoretically sound control solutions for SPSs, switched systems, and SPSSs.   By bridging advanced nonlinear control theory with practical implementations, it lays a strong foundation for future advancements in real-time, adaptive, and scalable control of complex dynamical systems.

133

Bibliography

[1] Z. Jiang, J. Hu, Y. Zhao, X. Huang, and H. Li, "A goal-conditioned policy search method with multi-timescale value function tuning," *Robotic Intelligence and Automation*, vol. 44, no. 4, pp. 549–559, 2024.

[2] J. Zhao, C. Yang, W. Gao, L. Zhou, and X. Liu, "Adaptive optimal output regulation of interconnected singularly perturbed systems with application to power systems," *IEEE/CAA Journal of Automatica Sinica*, vol. 11, no. 3, pp. 595–607, 2024.

[3] W. Ren, B. Jiang, and H. Yang, "Fault-tolerant control of singularly perturbed systems with applications to hypersonic vehicles," *IEEE Transactions on Aerospace and Electronic Systems*, vol. 55, no. 6, pp. 3003–3015, 2019.

[4] P. Kokotović, H. K. Khalil, and J. O'reilly, *Singular perturbation methods in control: analysis and design*.   SIAM, 1999.

[5] P. Lorenzetti and G. Weiss, "Almost global stability results for a class of singularly perturbed systems," *IFAC-PapersOnLine*, vol. 56, no. 2, pp. 809–814, 2023.

[6] C. Wang, T. Ma, Z. Bing, A. Knoll, and X. Su, "Dynamic event-triggered sliding mode control of networked switched systems with imperfect transmissions," *International Journal of Robust and Nonlinear Control*, vol. 35, no. 1, pp. 395–416, 2025.

[7] Z. Ding and W. Ren, "Fault-tolerant control for a class of switched nonlinear systems with actuator faults," in *2023 7th International Symposium on Computer Science and Intelligent Control (ISCSIC)*.   IEEE, 2023, pp. 65–69.

Chapter 7. Conclusion and Future Work

[8] H. Yin, B. Jayawardhana, and S. Trenn, "On contraction analysis of switched systems with mixed contracting-noncontracting modes via mode-dependent average dwell time," *IEEE Transactions on Automatic Control*, vol. 68, no. 10, pp. 6409–6416, 2023.

[9] R. F. A. Khan, K. Rsetam, Z. Cao, and Z. Man, "Singular perturbation-based adaptive integral sliding mode control for flexible joint robots," *IEEE Transactions on Industrial Electronics*, vol. 70, no. 10, pp. 10 516–10 525, 2022.

[10] J. Cheng, J. Xu, H. Yan, Z.-G. Wu, and W. Qi, "Neural network-based sliding mode control for semi-markov jumping systems with singular perturbation," *IEEE Transactions on Cybernetics*, 2024.

[11] S. Pritichhanda, S. Maity, and J. She, "A sensorless peak current-mode controlled dc–dc converter: design and robustness analysis using time-scale decomposition," *IEEE Transactions on Circuits and Systems I: Regular Papers*, vol. 70, no. 8, pp. 3387–3398, 2023.

[12] J. Xu, J. Cheng, H. Yan, J. H. Park, and W. Qi, "Dynamic event-triggered control for semi-markov singularly perturbed systems with generally transition rates," *IEEE Transactions on Systems, Man, and Cybernetics: Systems*, vol. 54, no. 1, pp. 225–235, 2023.

[13] J. Cheng, J. Xu, H. Yan, Z. Wu, and W. Qi, "Neural network-based sliding mode control for semi-markov jumping systems with singular perturbation," *IEEE transactions on cybernetics*, pp. 1 – 10, 2024.

[14] W. Lohmiller and J.-J. E. Slotine, "On contraction analysis for non-linear systems," *Automatica*, vol. 34, no. 6, pp. 683–696, 1998.

[15] Y. Chen, G. Tao, and X. Fan, "A contraction theory-based adaptive robust control for the trajectory tracking of a pneumatic cylinder," *IEEE Transactions on Industrial Electronics*, vol. 71, no. 9, pp. 11 408–11 418, 2023.

[16] B. Yi, R. Wang, and I. R. Manchester, "Reduced-order nonlinear observers via contraction analysis and convex optimization," *IEEE Transactions on Automatic Control*, vol. 67, no. 8, pp. 4045–4060, 2021.

[17] S. Singh, B. Landry, A. Majumdar, J.-J. Slotine, and M. Pavone, "Robust feedback motion planning via contraction theory," *The International Journal of Robotics Research*, vol. 42, no. 9, pp. 655–688, 2023.

[18] F. K. Ndow and Z. Aminzare, "Global synchronization analysis of non-diffusively coupled networks through contraction theory," *arXiv preprint arXiv:2307.00030*, 2023.

[19] Q. Yu and N. Wei, "Stability criteria of switched systems with a binary-dependent average dwell time approach," *Journal of Control and Decision*, vol. 11, no. 3, pp. 483–494, 2024.

[20] S. Liu, S. Martínez, and J. Cortés, "Average dwell-time minimization of switched systems via sequential convex programming," *IEEE Control Systems Letters*, vol. 6, pp. 1076–1081, 2021.

[21] D. Liberzon, *Switching in systems and control*.   Springer, 2003, vol. 190.

[22] T. Liu and Z.-P. Jiang, "Singular perturbation: When the perturbation parameter becomes a state-dependent function," *IFAC-PapersOnLine*, vol. 56, no. 1, pp. 294–300, 2023.

[23] Y. Liu, W.-H. Chen, and X. Lu, "Slow state estimation for singularly perturbed systems with discrete measurements," *Science in China Series F: Information Sciences*, vol. 64, p. 129202, 2021. [Online]. Available: https://dblp.uni-trier.de/db/journals/chinaf/chinaf64.html#LiuCL21

[24] P. T. Cardin and M. A. Teixeira, "Geometric singular perturbation theory for systems with symmetry," *Journal of Dynamics and Differential Equations*, pp. 1 – 13, 2020. [Online]. Available: https://link.springer.com/article/10.1007/s10884-020-09855-2

[25] K. B. Gunti and S. K. Movva, "Singular perturbation method applied to power factor correction converter application," *WSEAS Transactions on Systems and Control archive*, vol. 16, pp. 396 – 403, 2021.

[26] H. Hooshmand and M. Fateh, "Voltage control of flexible-joint robot manipulators using singular perturbation technique for model order

Chapter 7. Conclusion and Future Work

reduction," *Journal of Electrical and Computer Engineering Innovations (JECEI)*, vol. 10, no. 1, pp. 123–142, 2022.

[27] T. Sun, X. Zhang, H. Yang, and Y. Pan, "Singular perturbation-based saturated adaptive control for underactuated euler–lagrange systems," *ISA transactions*, vol. 119, pp. 74–80, 2022.

[28] B. Li, L. Yan, and C. Gerada, "The novel singular-perturbation-based adaptive control with σ-modification for cable driven system," in *Actuators*, vol. 10, no. 3.   MDPI, 2021, p. 45.

[29] D. Kim, K. Koh, G.-R. Cho, and L.-Q. Zhang, "A robust impedance controller design for series elastic actuators using the singular perturbation theory," *IEEE/ASME Transactions on Mechatronics*, vol. 25, no. 1, pp. 164–174, 2019.

[30] Y. He, D. Zhu, Y. Liu, and X. Zhang, "Controller design and stability analysis for singularly perturbed hybrid systems with multi-rate sampling," in *2024 36th Chinese Control and Decision Conference (CCDC)*.   IEEE, 2024, pp. 3005–3010.

[31] J. Wang, C. Peng, J. H. Park, H. Shen, and K. Shi, "Reinforcement learning-based near optimization for continuous-time markov jump singularly perturbed systems," *IEEE Transactions on Circuits and Systems II: Express Briefs*, vol. 70, no. 6, pp. 2026–2030, 2023.

[32] A. Visavakitcharoen, W. Assawinchaichote, Y. Shi, and C. Angeli, "Event-triggered fuzzy integral control for a class of nonlinear singularly perturbed systems," *ISA transactions*, vol. 139, pp. 71–85, 2023.

[33] X. Wang, "Robust multiobjective control of singularly perturbed systems using linear matrix inequality," *International Journal of Adaptive Control and Signal Processing*, vol. 36, no. 7, pp. 1746–1758, 2022.

[34] K. Liang, W. He, F. Qian, and G. Chen, "Synchronization control of networked two-timescale dynamic agents: A singular perturbation approach," *IEEE Transactions on Control of Network Systems*, vol. 11, no. 1, pp. 3–17, 2023.

[35] F. Li, W. X. Zheng, and S. Xu, "Finite-time fuzzy control for nonlinear singularly perturbed systems with input constraints," *IEEE Transactions on Fuzzy Systems*, vol. 30, no. 6, pp. 2129–2134, 2021.

[36] C.-T. Chao, D.-H. Chen, and J.-S. Chiou, "Stabilization and the design of switching laws of a class of switched singularly perturbed systems via the composite control," *Mathematics*, vol. 9, no. 14, p. 1664, 2021.

[37] Y. Guo and J. Li, "Asynchronous non-fragile control for persistent dwell-time switched singularly perturbed systems with strict dissipativity," *Journal of the Franklin Institute*, vol. 358, no. 12, pp. 5985–6012, 2021.

[38] Y. Guo, J. Li, and X. Qi, "Fault-tolerant h control for t–s fuzzy persistent dwell-time switched singularly perturbed systems with time-varying delays," *International Journal of Fuzzy Systems*, vol. 24, no. 1, pp. 247–264, 2022.

[39] J. Wang, X. Liu, J. Xia, H. Shen, and J. H. Park, "Quantized interval type-2 fuzzy control for persistent dwell-time switched nonlinear systems with singular perturbations," *IEEE transactions on cybernetics*, vol. 52, no. 7, pp. 6638–6648, 2021.

[40] J. Wang, Z. Huang, Z. Wu, J. Cao, and H. Shen, "Extended dissipative control for singularly perturbed pdt switched systems and its application," *IEEE Transactions on Circuits and Systems I: Regular Papers*, vol. 67, no. 12, pp. 5281–5289, 2020.

[41] L. Ma, J. Xu, and C. Cai, "Weighted h control of singularly perturbed switched systems with mode-dependent average dwell time," *International Journal of Control, Automation and Systems*, vol. 17, no. 10, pp. 2462–2473, 2019.

[42] G. Zong, C. Zhang, W. Qi, C. K. Ahn, and X. Xie, "Finite-time control synthesis for discrete fuzzy switched singularly perturbed systems," *IEEE Transactions on Circuits and Systems II: Express Briefs*, vol. 70, no. 3, pp. 1109–1113, 2022.

[43] L. Ma and C. Cai, "Stability analysis and stabilization synthesis of singularly perturbed switched systems: An average dwell time approach," *Cogent Engineering*, vol. 3, no. 1, p. 1276875, 2016.

[44] Z. Peng, X. Song, S. Song, and D. Zheng, "Spatiotemporal sampled-data fuzzy control for switched singularly perturbed pde systems with average dwell-time switching mechanism," *Journal of the Franklin Institute*, vol. 360, no. 13, pp. 10 365–10 385, 2023.

[45] Q. Wang, L. Zhou, W. Dai, and X. Ma, "H control for t-s fuzzy singularly perturbed switched systems," *Mathematical Problems in Engineering*, vol. 2017, no. 1, p. 2597071, 2017.

[46] H. Shen, X. Hu, X. Wu, S. He, and J. Wang, "Generalized dissipative state estimation of singularly perturbed switched complex dynamic networks with persistent dwell-time mechanism," *IEEE Transactions on Systems, Man, and Cybernetics: Systems*, vol. 52, no. 3, pp. 1795–1806, 2020.

[47] M. M. Rayguru and I. Kar, "Contraction-based stabilisation of nonlinear singularly perturbed systems and application to high gain feedback," *International Journal of Control*, vol. 90, no. 8, pp. 1778–1792, 2017.

[48] P. Lorenzetti, M. Giaccagli, I.-C. Morarescu, and R. Postoyan, "Singularly perturbed k-contractive linear systems," *IEEE Control Systems Letters*, vol. 8, pp. 1144–1149, 2024.

[49] D. Del Vecchio and J.-J. E. Slotine, "A contraction theory approach to singularly perturbed systems," *IEEE Transactions on Automatic Control*, vol. 58, no. 3, pp. 752–757, 2012.

[50] B. S. Dey, U. Banerjee, and I. N. Kar, "Harmonics suppression in a class of switched mechanical system: A contraction theory approach," in *2023 9th International Conference on Control, Decision and Information Technologies (CoDIT)*. IEEE, 2023, pp. 1737–1742.

[51] R. P. De Souza, Z. Kader, and S. Caux, "Stabilization of a class of singularly perturbed switched systems," in *American Control Conference*, 2023.

[52] Q. Yin, H. Zhang, Q. Mu, J. Yang, and Q. Ma, "Multilayer-neural-network observer with compensator and command-filter-based adaptive backstepping tracking control of switched nonlinear systems," *Journal of the Franklin Institute*, vol. 360, no. 4, pp. 2976–3000, 2023.

[53] N. Xu, Y. Chen, A. Xue, H. Wang, and X. Zhao, "Backstepping-based controller design for uncertain switched high-order nonlinear systems via pi compensation," *IEEE Transactions on Systems, Man, and Cybernetics: Systems*, vol. 52, no. 12, pp. 7810–7820, 2022.

[54] Y. Shu and Y. Tong, "Robust neural tracking controller design for a class of discrete-time nonlinear systems under arbitrary switching," *IEEE Access*, vol. 9, pp. 9682–9689, 2021.

[55] J. Wu, H. Lu, and W. Wang, "Adaptive neural optimized control for a class of switched strict-feedback systems with unknown control gains," *Optimal Control Applications and Methods*, vol. 46, no. 3, pp. 1164–1179, 2025.

[56] H. Wang, M. Tong, X. Zhao, B. Niu, and M. Yang, "Predefined-time adaptive neural tracking control of switched nonlinear systems," *IEEE Transactions on Cybernetics*, vol. 53, no. 10, pp. 6538–6548, 2022.

[57] J. Yang, X. Yang, Z. Chen, J. Wang, and X. Zheng, "Event-triggered adaptive gradient descent neural network backstepping control for a class of uncertain nonlinear systems," in *2024 36th Chinese Control and Decision Conference (CCDC)*.   IEEE, 2024, pp. 3530–3534.

[58] T. Chen, D. Cao, J. Yuan, and H. Yang, "Observer-based adaptive neural network backstepping sliding mode control for switched fractional order uncertain nonlinear systems with unmeasured states," *Measurement and Control*, vol. 54, no. 7-8, pp. 1245–1258, 2021.

[59] Z. Wen, Y. Guo, X. Zhang, and C. Lu, "Sliding mode control for mems gyroscopes using modified neural disturbance observer," in *2024 36th Chinese Control and Decision Conference (CCDC)*.   IEEE, 2024, pp. 4605–4610.

Chapter 7. Conclusion and Future Work

[60] L. Manconi, S. A. Emami, and P. Castaldi, "Quadrotor composite learning neural control with disturbance observer against aerodynamic disturbances," *IFAC-PapersOnLine*, vol. 55, no. 22, pp. 13–18, 2022.

[61] T. Li, G. Zhang, T. Zhang, and J. Pan, "Adaptive neural network tracking control of robotic manipulators based on disturbance observer," *Processes*, vol. 12, no. 3, p. 499, 2024.

[62] Z. Yang, Q. Mao, X. Li, and X. Jin, "Neural network disturbance observer-incorporated fault detection scheme for electro-mechanical flight actuators," in *2023 35th Chinese Control and Decision Conference (CCDC)*. IEEE, 2023, pp. 4132–4137.

[63] J. Hu and M. Zheng, "Disturbance observer-based control with adaptive neural network for unknown nonlinear system," *Measurement and Control*, vol. 56, no. 1-2, pp. 287–294, 2023.

[64] N. Wang, J. Zhang, K. Xu, and H. Junzhe, "Robust control of multi degree of freedom robot based on disturbance observer of neural network." *Journal of Engineering Science & Technology Review*, vol. 13, no. 3, 2020.

[65] H. Gao, W. Tang, and R. Fu, "Sliding mode control for hypersonic vehicle based on extreme learning machine neural network disturbance observer," *IEEE Access*, vol. 10, pp. 69 333–69 345, 2022.

[66] Z. Chen, F. Li, D. Luo, J. Wang, and H. Shen, "Stabilization of discrete-time semi-markov jump singularly perturbed systems subject to actuator saturation and partially known semi-markov kernel information," *Journal of the Franklin Institute*, vol. 359, no. 12, pp. 6043–6060, 2022.

[67] Y. Yan, C. Yang, and X. Ma, "Event-triggered observer-based fuzzy control for coal-fired power generation systems based on singularly perturbed theory," *IEEE Access*, vol. 8, pp. 133 283–133 294, 2020.

[68] Q. Meng and Q. Ma, "Observer-based adaptive fuzzy control for singular systems with nonlinear perturbation and actuator saturation," *IEEE Transactions on Artificial Intelligence*, 2024.

[69] M. M. Rayguru, S. Roy, and I. N. Kar, "Time-scale redesign-based saturated controller synthesis for a class of mimo nonlinear systems," *IEEE Transactions on Systems, Man, and Cybernetics: Systems*, vol. 51, no. 8, pp. 4681–4692, 2019.

[70] Y. Lei, Y.-W. Wang, X.-K. Liu, and W. Yang, "Prescribed-time stabilization of singularly perturbed systems," *IEEE/CAA Journal of Automatica Sinica*, vol. 10, no. 2, pp. 569–571, 2023.

[71] M. L. Castaño and X. Tan, "Backstepping-based tracking control of underactuated aquatic robots," *IEEE Transactions on Control Systems Technology*, vol. 31, no. 3, pp. 1179–1195, 2022.

[72] Y. Xie, J. Qiao, X. Yu, and L. Guo, "Dual-disturbance observers-based control for a class of singularly perturbed systems," *IEEE Transactions on Systems, Man, and Cybernetics: Systems*, vol. 52, no. 4, pp. 2423–2434, 2021.

[73] J. Xu, Y. Niu, and P. Shi, "Adaptive multi-input super twisting control for a quadrotor: Singular perturbation approach," *IEEE Transactions on Industrial Electronics*, vol. 71, no. 5, pp. 5195–5204, 2023.

[74] Z. Ma, Z. Wang, Y. Yuan, and T. Hong, "Singular perturbation-based large-signal order reduction of microgrids for stability and accuracy synthesis with control," *IEEE Transactions on Smart Grid*, vol. 15, no. 4, pp. 3361–3374, 2024.

[75] D. Swaroop, J. K. Hedrick, P. P. Yip, and J. C. Gerdes, "Dynamic surface control for a class of nonlinear systems," *IEEE transactions on automatic control*, vol. 45, no. 10, pp. 1893–1899, 2000.

[76] Y. Pan and H. Yu, "Dynamic surface control via singular perturbation analysis," *Automatica*, vol. 57, pp. 29–33, 2015.

[77] G. Russo and M. Di Bernardo, "Contraction theory and master stability function: Linking two approaches to study synchronization of complex networks," *IEEE Transactions on Circuits and Systems II: Express Briefs*, vol. 56, no. 2, pp. 177–181, 2009.

Chapter 7. Conclusion and Future Work

[78] M. M. Rayguru and I. N. Kar, "High gain observer-based saturated controller for feedback linearizable system," *IEEE Transactions on Circuits and Systems II: Express Briefs*, vol. 67, no. 1, pp. 122–126, 2019.

[79] A. Pavlov, A. Pogromsky, N. van de Wouw, and H. Nijmeijer, "Convergent dynamics, a tribute to boris pavlovich demidovich," *Systems & Control Letters*, vol. 52, no. 3-4, pp. 257–261, 2004.

[80] M. Rayguru and I. Kar, "Contraction theory approach to disturbance observer based filtered backstepping design," *Journal of Dynamic Systems, Measurement, and Control*, vol. 141, no. 8, p. 084501, 2019.

[81] S. Zeghlache, L. Benyettou, A. Djerioui, and M. Z. Ghellab, "Twin rotor mimo system experimental validation of robust adaptive fuzzy control against wind effects," *IEEE Systems Journal*, vol. 16, no. 1, pp. 409–419, 2020.

[82] S. K. Valluru, M. Singh, Ayush, and A. Dharavath, "Design and experimental implementation of multi-loop lqr, pid, and lqg controllers for the trajectory tracking control of twin rotor mimo system," in *Intelligent Communication, Control and Devices: Proceedings of ICICCD 2018.* Springer, 2020, pp. 599–608.

[83] R. B. Anderson, J. A. Marshall, A. L'Afflitto, and J. M. Dotterweich, "Model reference adaptive control of switched dynamical systems with applications to aerial robotics," *Journal of Intelligent & Robotic Systems*, vol. 100, no. 3, pp. 1265–1281, 2020.

[84] Y. Chen, Y. Li, and D. J. Braun, "Data-driven iterative optimal control for switched dynamical systems," *IEEE Robotics and Automation Letters*, vol. 8, no. 1, pp. 296–303, 2022.

[85] A. Rahdan and M. Abedi, "Asynchronous time dependent switched model predictive control for nonlinear systems considering feasibility constraints," *International Journal of Robust and Nonlinear Control*, vol. 35, no. 1, pp. 359–394, 2025.

[86] N. Kessler and L. Fagiano, "On the stabilization of forking and cyclic trajectories for nonlinear systems," *IFAC-PapersOnLine*, vol. 56, no. 3, pp. 199–204, 2023.

[87] J. Gallegos, N. Aguila-Camacho, and F. Núñez, "High-gain adaptive control with switching derivation order and its application to a class of multiagent systems," *IEEE Transactions on Systems, Man, and Cybernetics: Systems*, vol. 54, no. 7, pp. 3960–3971, 2024.

[88] S. Yang and X.-D. Li, "Iterative learning consensus control for switched discrete-time multi-agent systems based on the 2-d linear discrete model," *International Journal of Systems Science*, vol. 56, no. 10, pp. 2231–2245, 2025.

[89] D. Swaroop, J. K. Hedrick, P. Yip, and J. C. Gerdes, "Dynamic surface control for a class of nonlinear systems," *IEEE Transactions on Automatic Control*, vol. 41, no. 11, pp. 1671–1677, 1996.

[90] J. A. Farrell and M. M. Polycarpou, *Command-Filtered Backstepping*. Boca Raton, FL: CRC Press, 2009.

[91] J. Wu, J. Huang, Y. Wang, and K. Xing, "Nonlinear disturbance observer-based dynamic surface control for trajectory tracking of pneumatic muscle system," *IEEE Transactions on Control Systems Technology*, vol. 22, no. 2, pp. 440–455, 2013.

[92] D. Won, W. Kim, D. Shin, and C. C. Chung, "High-gain disturbance observer-based backstepping control with output tracking error constraint for electro-hydraulic systems," *IEEE transactions on control systems technology*, vol. 23, no. 2, pp. 787–795, 2014.

[93] H. K. Khalil and J. W. Grizzle, *Nonlinear systems*. Prentice hall Upper Saddle River, NJ, 2002, vol. 3.

[94] A. Narang-Siddarth and J. Valasek, *Nonlinear Time Scale Systems in Standard and Nonstandard Forms: Analysis and Control*. SIAM, 2014.

[95] B. B. Sharma and I. N. Kar, "Contraction theory-based recursive design of stabilising controller for a class of non-linear systems," *IET Control Theory & Applications*, vol. 4, no. 6, pp. 1005–1018, 2010.

[96] D. Prasad, S. K. Valluru, and M. M. Rayguru, "Filter-based saturated controller design for a class of nonlinear singularly perturbed systems," *Sādhanā*, vol. 49, no. 2, p. 184, 2024.

[97] H. Tsukamoto and S.-J. Chung, "Learning-based robust motion planning with guaranteed stability: A contraction theory approach," *IEEE Robotics and Automation Letters*, vol. 6, no. 4, pp. 6164–6171, 2021.

[98] N. Javanmardi, P. Borja, and J. Scherpen, "Contraction-based tracking control of electromechanical systems," *arXiv preprint arXiv:2311.06684*, 2023.

[99] B. Xu, "Robust adaptive neural control of flexible hypersonic flight vehicle with dead-zone input nonlinearity," *Nonlinear Dynamics*, vol. 80, no. 4, pp. 1509–1520, 2015.

[100] M. Rayguru and I. Kar, "A singular perturbation approach to saturated controller design with application to bounded stabilization of wing rock phenomenon," *Nonlinear Dynamics*, vol. 93, no. 4, pp. 2263–2272, 2018.

[101] M. M. Rayguru and I. N. Kar, "Contraction based stabilization of approximate feedback linearizable systems," in *2015 European Control Conference (ECC)*.   IEEE, 2015, pp. 587–592.

[102] J. Jouffroy and J. Lottin, "On the use of contraction theory for the design of nonlinear observers for ocean vehicles," in *Proceedings of the 2002 American Control Conference (IEEE Cat. No. CH37301)*, vol. 4.   IEEE, 2002, pp. 2647–2652.

[103] J. P. Hespanha and A. S. Morse, "Stability of switched systems with average dwell-time," *Proceedings of the 38th IEEE Conference on Decision and Control*, vol. 3, pp. 2655–2660, 1999.

[104] G. Zhai, B. Hu, K. Yasuda, and A. N. Michel, "Stability analysis of switched systems with stable and unstable subsystems: an average dwell time approach," *International Journal of Systems Science*, vol. 32, no. 8, pp. 1055–1061, 2001.

[105] M. Della Rossa and A. Tanwani, "Converse lyapunov results for stability of switched systems with average dwell-time," *ESAIM: Control, Optimisation and Calculus of Variations*, vol. 31, p. 15, 2025.

[106] J. Park and I. W. Sandberg, "Universal approximation using radial-basis-function networks," *Neural Computation*, vol. 3, no. 2, pp. 246–257, 1991.

[107] J. Peng, S. Ding, and R. Dubay, "Adaptive composite neural network disturbance observer-based dynamic surface control for electrically driven robotic manipulators," *Neural Computing and Applications*, vol. 33, no. 11, pp. 6197–6211, 2021.

[108] M. H. Rezaei, M. Ghaseminezhad, and M. Kabiri, "Control of uncertain non-affine nonlinear systems using neural networks subject to input saturation with unknown control direction," *Journal of Vibration and Control*, vol. 31, no. 17-18, pp. 3647–3660, 2025.

[109] C. Kwan and F. L. Lewis, "Robust backstepping control of induction motors using neural networks," *IEEE Transactions on Neural Networks*, vol. 11, no. 5, pp. 1178–1187, 2000.

[110] E. M. Aylward, P. A. Parrilo, and J.-J. E. Slotine, "Stability and robustness analysis of nonlinear systems via contraction metrics and sos programming," *Automatica*, vol. 44, no. 8, pp. 2163–2170, 2008.

147

Appendix A

Contraction Theory

A system of the form $\dot{f} = f(x,t)$ is considered contracting if all trajectories that begin within a certain region of the state space converge to one another [110]. A region in the state space is defined as a contraction region if the system dynamics satisfy any of the following inequalities.

$$\left(\dot{\Xi} + \Xi \frac{\partial f}{\partial x} \Xi^{-1}\right) + \left(\dot{\Xi} + \Xi \frac{\partial f}{\partial x} \Xi^{-1}\right)^T \leq -\Delta I,$$

$$(\dot{M} + M \frac{\partial f}{\partial x} + \frac{\partial f^T}{\partial x} M) \leq -2\Delta M$$

The inequality describes a contraction condition, where $\Delta \in \mathbb{R}^+$ represents the contraction rate. Here, Ξ is a nonsingular matrix known as the associated transformation matrix, and $M = \Xi^T \Xi$ is referred to as the contraction metric.

Lemma A.1: Consider a system represented in its perturbed form as:

$$\dot{x}_p = f(x_p, t) + d(x_p, w, t),$$

where w is an external parameter, and the disturbance satisfies $||d(x_p, w, t)|| \leq d_0$, with $d_0 \in \mathbb{R}^+$. Assume the nominal system, given by $\dot{x} = f(x,t)$, is contracting with a transformation matrix Θ and a contraction rate λ. The deviation between the trajectories of the perturbed system and the nominal system can then be bounded as:

$$||x_p(t) - x(t)|| \leq \gamma ||x_p(0) - x(0)|| \exp(-\lambda t) + \frac{\gamma d_0}{\lambda},$$

148

Appendix A. Contraction Theory

where γ denotes the supremum of the condition number of Θ, and $\exp(.)$ represents the standard exponential function.

List of Publications from Research Work

Papers in Referred Journals

[1] **Dipak Prasad**, Sudarshan K. Valluru, and Madan Mohan Rayguru. Filter based saturated controller design for a class of nonlinear singularly perturbed systems. *Sādhanā*, 49(2):184, 2024 (SCIE indexed).

[2] **Dipak Prasad**, Sudarshan K. Valluru, and M. M. Rayguru. Singular perturbation-based robust controller for a class of nonlinear systems. *International Journal of Control*, 98(7):1688–1703, 2025 (SCIE indexed).

[3] **Dipak Prasad** and Sudarshan K. Valluru. Filtered backstepping controller for nonlinear singularly perturbed switched systems based on contraction analysis. *Sādhanā*, 2025 (SCIE indexed) (Accepted).

[4] **Dipak Prasad** and Sudarshan K. Valluru. Neural disturbance observer-based backstepping controller for singularly perturbed switched systems. *Arabian Journal for Science and Engineering*, 2025 (SCIE indexed) (Revision submitted).

[5] **Dipak Prasad** and Sudarshan K. Valluru. Singular perturbation-based neural backstepping control for a class of nonlinear singularly perturbed switched systems. *International Journal of Adaptive Control and Signal Processing*, 2025 (SCIE indexed) (Communicated).

150

International Conference Proceedings

[1] **Dipak Prasad**, Sudarshan K. Valluru, and Madan Mohan Rayguru. Filter based saturated controller for a class of nonlinear singularly perturbed system. In *2024 Control Instrumentation System Conference (CISCON)*, pages 1–5, 2024. doi: 10.1109/CISCON62171.2024.10696189.

[2] **Dipak Prasad**, Sudarshan K. Valluru, and Madan Mohan Rayguru. Filtered and standard backstepping controllers for singularly perturbed switched systems. In *2024 IEEE 21st India Council International Conference (INDICON)*, pages 1–5, 2024. doi: 10.1109/INDICON63790.2024.10958251.